

**Functional evaluation of *RAMOSA2* cis-regulatory regions from
different grass species for shaping inflorescence architecture in barley**

Dissertation

zur Erlangung des

Doktorgrades der Agrarwissenschaften (Dr. agr.)

der

Naturwissenschaftlichen Fakultät III
Agrar- und Ernährungswissenschaften,
Geowissenschaften und Informatik

der Martin-Luther-Universität Halle-Wittenberg

vorgelegt von

Herrn M.Sc. Omar Fathy Helmy Heliel

geb. am: 01.02.1983 in Giza, Egypt

Verteidigt am 20.03.2023 in Halle (Saale)
Gutachter: Prof. Dr. T. Schnurbusch und Prof. Dr. R. Waugh

Acknowledgments

First and foremost, I would like to praise Allah the Almighty, the Most Gracious, and the Most Merciful, for His blessing to me during my study and the strength in completing this thesis.

I gratefully acknowledge the Ministry of Higher Education and scientific research of the Arab Republic of Egypt for financially supporting me for the first two years of my study, and for the opportunity to start my doctorate in Germany. This opportunity increased my knowledge, allowed me to learn new techniques and skills, and improved my career.

I sincerely thank Dr. Britt Leps for her time, support, and help during my stay in Germany.

I want to thank my friend Dr. Mohamed Nadi from the desert research center in Egypt for his generous support and for taking care of all issues related to me in Egypt.

I sincerely thank my supervisor, Prof. Dr. Thorsten Schnurbusch, for allowing me to join his research group. And for his scientific guidance, support, and motivation that helped me to complete this work. My special thanks to Dr. Ravi Koppolu and Dr. Goetz Hensel for their collaborative efforts, fruitful scientific discussions, and advice.

I am grateful for the collaboration with Dr. Twan Rutten and Dr. Jozefus Schippers for their help and support. And I thank my colleague, Dr. Yongyu Huang, for his helpful scientific discussion.

Finally, I sincerely thank the technical staff and all PBP members.

Contents

1.0. Introduction	1
1.1. Barley	2
1.1.2. Taxonomy	3
1.1.3. Barley life cycle	4
1.2. Inflorescence architecture development in grasses	7
1.2.1. Development of inflorescence meristem (IM) in grasses	7
1.2.2. Spike architecture development	9
1.3. Regulation of RAMOSA pathway in inflorescence architecture of maize	15
1.4. Regulation of COMPOSITUM pathway in inflorescence architecture of barley	16
1.5. The function of LBD transcription factors	18
1.5. Functional Genomics	19
1.5.1. Reverse genetics approaches to study gene function	20
1.6. Cis-regulatory elements and regulation of gene expression	26
1.6.1. Enhancers and Silencer	28
1.6.2. Insulators	30
1.7. Aims and underlying working hypotheses of the present thesis	31
1.7.2. The major objectives of the present study are:	32
1.8. Data contributions	33
2.0. Materials and Methods	35
2.1. Plant materials and growth conditions	35
2.2. Fluorescence Microscopy	35
2.3. Molecular analysis	36
2.3.1. Genomic DNA extraction	36
2.3.2. Polymerase chain reaction (PCR) conditions	37
2.3.3. Purification of PCR products	38
2.3.4. Sequencing	38
2.3.5. Southern Blotting	38
2.3.6. RNA extraction	39
2.3.7. Synthesis of cDNA	40
2.3.8. Real-time PCR analysis	41

2.4. Transgenic constructs generation and barley transformation.....	42
2.4.1. Generation of complementation constructs.....	42
2.4.2. Promoter activity localization constructs	43
2.4.3. RGEN design and vector construction	44
2.5. Protein-protein interactions study	45
2.5.1. Yeast two-hybrid assay.....	45
2.5.2. Construction of prey clones	45
2.5.3 Preparation of yeast-competent cells	46
2.5.4 Yeast co-transformation.....	47
2.6. Basic cloning methods	48
2.6.1. Colony PCR	48
2.6.2. Isolation of plasmid DNA	48
2.6.2. DNA gel extraction	49
2.6.3. Digestion of plasmid DNA.....	49
2.6.4. DNA ligation.....	49
2.6.4. Preparation of bacteria glycerol stocks.....	49
2.6.5. Transformation of <i>E-coli</i> competent cells.....	50
2.6.6. Transformation of Agrobacteria competent cells.....	50
3.0 Results	51
3.1 Complementation into BW-NIL(<i>mull.a</i>) background	52
3.1.1 Identification of promoter regions, putative transcription factor binding sites, and cis-motif analysis.....	52
3.1.2. The two-rowed wild-type condition was partially restored in <i>vsr4</i> mutant complemented with a native gene and parts of the endogenous barley promoter sequence ..	56
3.1.3. Restoration of wild-type two-rowed condition in transgenic plant complemented with <i>HvRA2</i> CDS driven by <i>RA2</i> promoter from wheat	58
3.1.4. The two-rowed condition was partially achieved in transgenic plant complemented with <i>SbRA2</i> CDS driven by <i>RA2</i> sorghum promoter.....	60
3.1.5. There is no clear relation between copy number and spike phenotype and gene expression in the transgenic plants.....	61
3.2. Constitutive overexpression of <i>RA2</i> studies.....	64

3.2.1 Constitutive overexpression of <i>AetRA2</i> CDS in wheat (cultivar Bobwhite) affects plant morphology	64
3.3. Promoter activity localization	65
3.3.1. Temporal gene expression pattern for GFP was not achieved under the cloned <i>RAMOSA2</i> promoters from barley, sorghum, and wheat	65
3.3.2. No clear difference between the amount of expression of the <i>GFP</i> driven by different promoters	67
3.4. Knockout of <i>HvRA2</i> in barley Golden Promise cultivar mediated by RNA-guided endonuclease (RGEN) approach.	68
3.4.1 Targeted mutagenesis of <i>HvRA2</i> induced by RGEN in the T0 generation	68
3.4.2. Analysis of targeted mutagenesis of <i>HvRA2</i> in the T1 generation	72
3.4.3. Validation of <i>HvRA2</i> knockout by qRT-PCR	76
3.4.4. Putative off-target analysis for homozygous <i>HvRA2</i> mutants	77
3.5. Complementation of <i>HvRA2</i> RGEN <i>KOs</i> with promoter swapped <i>RA2</i> transgene cassettes	79
3.5.1. Phenotypic analysis of the super transformed <i>HvRA2</i> Golden Promise <i>KOs</i> with <i>HvRA2</i> CDS driven by different <i>RA2</i> promoters from sorghum, barley, and wheat	80
3.5.2. Expression analysis of the <i>HvRA2</i> in Transgenic plants	84
3.5.3. Transgenic plants showed a negative effect on the entire plants' elongation	87
3.5.4 Complementation lines with <i>HvRA2</i> tagged with GFP display varied GFP expression patterns between different transgenic lines.	92
3.6. Possible interaction between <i>HvRA2</i> and other genes related to spike development	93
4.0. Discussion	98
4.1. Identification of <i>cis</i> -motifs and promoter's analysis	98
4.2. Promoter activity localization	100
4.3. No clear difference between the amount of expression of the GFP driven by different <i>RA2</i> promoters	102
4.4. Complementation of <i>RA2</i> fused with different promoters into BW-NIL(<i>mull.a</i>) background	102
4.5. Complementation of <i>RA2</i> fused with different promoters into RGEN <i>ra2 mutant</i> (Golden Promise background)	104
4.5.1. Barley <i>RA2</i> fused with regulatory regions from different species showed partly near-complete recovery of wild-type inflorescence architecture	104

4.5.2. <i>HvRA2</i> transgene recovers normal inflorescence architectures in <i>ra2</i> mutants independent of the <i>HvRA2</i> dosage.	106
4.5.3. The constitutive <i>HvRA2</i> expression with higher dosage is negatively associated with plant height.....	107
4.6. Knockout of <i>HvRA2</i> in barley cultivar Golden Promise mediated by RNA-guided endonuclease (RGEN) approach	108
4.6.1. The <i>hvra2</i> RGEN knock-out mutant lost its spikelet determinacy and identity.	110
4.7. Possible interaction between <i>HvRA2</i> and other genes related to spike development	112
5.0. Outlook.....	114
6.0. Summary	116
7.0. Zusammenfassung	117
8.0. References.....	119
9.0. Appendix.....	155
10.0. Eidesstattliche Erklärung	166

List of Figures

Figure 1.1.3.1: Barley life cycle: vegetative, reproductive, and grain-filling phases.....	4
Figure 1.1.3.2: Spikelet developmental phases of Barley.....	6
Figure 1.2.1 Schematics of meristem differentiation between rice, maize, barley, and wheat.....	9
Figure 1.2.2 Barley row-types	10
Figure: 1.2.3. Spike morphology of different row-type loci.....	13
Figure 1.3.1. Model for inflorescence branching regulation in barley and maize.	17
Figure 1.6.1: Schematic representation for promoter elements in plant.....	27
Figure 1.6.2 proposed models for the function of enhancers.....	29
Figure 3.1.1 mVISTA plots of RA2 promoter sequence alignments.....	53
Figure 3.1.2. Frequency of the distribution of the putative TFBSs in <i>RAMOSA2</i> promoter	54
Figure 3.1.3. Motif analysis of RA 2 Promoters sequences	55
Figure 3.1.4. Schematic representation of complementation construct with modified sorghum promoter.....	56
Figure 3.1.2.1. Schematic representation of complementation construct; Expression cassette of <i>HvRA2</i> driven by <i>HvRA2</i> promoter.	57
Figure 3.1.3.1. Schematic representation of complementation construct with RA2 Regulatory element from wheat	59
Figure 3.1.3.2. Spike Phenotypes of T2 generation barley pAetRA2:: <i>HvRA2</i> CDS:: <i>Aet3'</i> UTR transformants.	59

Figure 3.1.3.3 Effect of <i>HvRA2</i> expression driven by Wheat regulatory elements on plant height	60
Figure 3.1.4.1. Spike Phenotypes of T2 generation of transformed barley plants with sorghum cassette.....	61
Figure 3.1.5.1 Expression analysis of <i>HvRA2</i> in T2 transgenic lines.....	64
Figure 3.2.1.1 Constitutive over-expression of transgenic wheat plants.....	65
Figure 3.3.1.1. GFP fluorescence in spikes of transgenic plants	66
Figure 2.3.2.1 The expression level of GFP driven by different promoters	67
Figure 3.4.1.1: Schematic of <i>HvRA2</i> gene structure and Cas9/gRNA target motif.....	69
Figure 3.4.1.2: Schematic representation of the RGEN T-DNA in binary vector.....	69
Figure 3.4.1.1.1. The phenotype of T0 <i>ra2</i> mutant created by RGEN approach.....	71
Figure 3.4.1.1.2 Mutation types in primary transgenic plants.	71
Figure 3.4.2.1: segregation pattern from T0 to T1.....	73
Figure 3.4.3.1. Expression analysis of <i>VRS1</i> in <i>ra2</i> RGEN knockout mutants.....	77
Figure 3.4.4.1 Putative off-target analysis for <i>HvRA2</i> mutant plants.....	78
Figure 3.4.4.2 Sequence analysis of potential off-targets in T1 plants homozygous knockout mutants.....	78
Figure 3.5.1: Schematic representation of the T-DNA constructs used for barley transformation.....	79
Figure 3.5.1.1.1 The phenotype of T1 super transformed plant	81
Figure 2.5.1.1.2. Complementation degree across different lines transformed with different constructs	82
Figure 3.5.1.2.1. Schematic representation of line selection for T2 and T3	83
Figure 3.5.1.2.2. The phenotype of T2 & T3 super transformed plants	84
Figure 3.5.1.1.3. Degree of complementation across different T2 lines.....	84
Figure 3.5.2.1.1 Expression analyses of <i>HvRA2</i> in T3 transgenic lines.....	85
Figure 3.5.2.2.1 Analysis of RA2 promoter activity in rice protoplasts.....	87
Figure 3.5.3.1. Effect of <i>HvRA2</i> transgene expression on the number of tiller and spike node number.....	88
Figure 3.5.3.2. Effect of <i>HvRA2</i> transgene expression on the number of additional structures... ..	89
Figure 2.5.3.3. Effect of <i>HvRA2</i> transgene expression on the spike length.....	90
Figure 3.5.3.4. Effect of <i>HvRA2</i> expression on the plant height.....	91
Figure 3.5.4.1 Schematic representation of the T-DNA constructs used for barley complementation constructs tagged with <i>GFP</i>	92
Figure 3.5.4.2. GFP fluorescence in the spike of transgenic plants with GFP fused in frame with <i>HvRA2</i> at the C-terminal end.....	93
Figure 3.6.1: Targeted yeast two-hybrid assay for <i>HvRA2</i> with different potential interaction partners.....	96
Figure 4.6. 1. Spike phenotypes of <i>HvRA2</i> RGEN knock out	112

List of Tables

Table 3.4.1.1.1: summary of the analysis of putative <i>ra2</i> mutant plants in T0 generation.	70
Table 3.4.2.1.1: Overview of the selection of the Transgene free homozygous mutant.	75
Table 3.6.1 Selected genes for Targeted yeast two-hybrid assay with HvRA2.....	97

List of Abbreviations

AD	Activation Domain
AF	Additional Floret
AG	AGAMOUS
AGI	AGAMOUS second intron enhancer
ANOVA	Analysis of Variance
AP	Awn Primordium
AP2	APETALA2
ARF	Auxin Response Factor
<i>AetRA2</i>	<i>Aegilops tauschii</i> RAMOSA2
BD	Binding Domain
BIFC	Bimolecular Fluorescence Complementation
BM	Branch Meristem
BOP1	BLADE-ON-PETIOLE1
BR	Brassinosteroid
BTB	Broad-complex, tramtrack, and bric-à-brac
BW-NIL	Bowman Near Isogenic Line
BX1	Benzoxazinless1
°C	Celsius
cm	centimeter
CDNA	Complementary DNA
CDS	Coding Sequence
COM1	COMPOSITUM1
COM2	COMPOSITUM2
CRISPR	Clustered Regularly Interspaced Short Palindromic Repeats
CS	Central Spikelet
CSs	Central Spikelets
CT	Cycle Threshold
CUL4	Uculme4
CYC	CYCLOIDEA
DAP-seq	DNA Affinity Purification sequencing

DEP1	Dense and Erect Panicle
DEPC	Diethyl Pyrocarbonate
DIG	Digoxigenin
DMSO	Dimethyl sulfoxide
DNA	De-oxyribo Nucleic Acid
DOF	DNA-binding with One Finger
DPE	Downstream Promoter Elements
DTT	Dithiothreitol
EDTA	Ethylenediaminetetraacetic acid
EMS	Ethyl Methyl Sulfonate
ERF	Ethylene Responsive Element
EST	Expressed Sequence Tag
FIMO	Find Individual Motif Occurrences
FLUC	Firefly Luciferase
FLZ	FCS-Like Zinc finger
FM	Floret Meristems
FZP	FRIZZLE PANICLE
GFP	Green Fluorescent Protein
GP	Glume Primordium
gRNA	guide RNA
GT1	GRASSY TILLERS1
<i>HvRA2</i>	<i>Hordeum vulgare RAMOSA2</i>
HPT	Hygromycin Phosphotransferase
HST	Hydroxycinnamoyl coenzyme A-quininate transferase
HTX	Hatiexi
IDA	INFLORESCENCE DEFICIENT IN ABSCISSION
IM	Inflorescence Meristem
INDEL	Insertion Deletion
INR	Initiator element
	Leibniz Institute of Plant Genetics and Crop Plant
IPK	Research
KO	knockout
LB	Lysogeny broth
LB, RB	Left and Right Border sequence of the T-DNA
LBD	LOB Domain
LBM	Long Branch Meristem
LS	Lateral Spikelet
LSs	Lateral Spikelets
LOB	Lateral Organ Boundary
LSM	Laser Scanning Microscopes
MEME	Multiple EM for Motif Elicitation

MW	Molecular Weight
μ l	Microlitre
μ m	Micrometre
mm	Millimetre
mRNA	messenger RNA
miRNA	micro RNA
ORF	Open Reading Frame
PAM	Protospacer Adjacent Motif
P-value	Probability value
PBM	Primary Branch Meristems
PCR	Polymerase Chain Reaction
RA2	RAMOSA2
RGEN	RNA-Guided Endonuclease
RNA	Ribonucleic Acid
rpm	rotation per minute
RT	Room Temperature
RT-qPCR	Reverse Transcriptase quantitative PCR
SAM	Shoot Apical Meristem
SBMs	Secondary Branch Meristem
<i>SbRA2</i>	<i>Sorghum bicolor</i> RAMOSA2
SD	Standard Deviation
SDS	Sodium Dodecyl Sulfate
ShBMs	Short Branch Meristems
SM	Spikelet Meristem
SNP	Single Nucleotide Polymorphism
SPM	Spikelet Pair Meristem
SSC	Saline Sodium Citrate
SSPE	Sodium Chloride-Sodium Phosphate-EDTA
T1	Transgenic filial generation 1
T2	Transgenic filial generation 2
TAE	Tris Acetat EDTA
TALEN	Transcription activator-like effector Nuclease
TF	Transcription Factor
TFBS	Transcription Factor Binding Sites
TILLING	Targeting Induced Local Lesions IN Genomes
TM	Triple Mound
TPP	Trehalose-6-phosphate phosphatase
TPP4	Trehalose 6-Phosphate Phosphatase 4
TPS1	Trehalose-6-phosphate synthase 1
TSM	Triple Spikelet Meristem
TSS	Transcriptional Start Site

UTR	UnTranslated Region
WT	Wild Type
Y2H	Yeast 2-Hybrid
YPDA	Yeast Peptone Dextrose Adenine
ZFN	Zinc-Finger Nucleases

1.0. Introduction

The Poaceae family (known as grasses) is one of the most important plant families, as it includes many economically important crops, such as barley (*Hordeum vulgare* L.), wheat (*Triticum aestivum* L.), maize (*Zea mays* L.), sorghum (*Sorghum bicolor* L.), and rice (*Oryza sativa* L.), all of which provide about 70% of food for human (P. J. Brown et al., 2006; Sakuma & Schnurbusch, 2019). Furthermore, one of the essential traits of this family is the inflorescence architecture that directly affects yield production.

Grass species display widely divergent and complex inflorescence architectures, starting with the branchless form of inflorescences, such as the spike of barley and wheat, to severely branched inflorescence structures like the panicle of the sorghum and rice. The barley spike is composed of three spikelets per rachis node arranged on two opposite sides in an alternating manner along the central axis called the rachis, and each of these spikelets produces only one floret. However, in wheat, the spike is composed of one spikelet per rachis node and each spikelet produces multiple florets attached to a structure called rachilla that extends from the rachis (Forster et al., 2007; Koppolu & Schnurbusch, 2019). In barley, there is a predetermined program to produce a specific number of spikelets and florets per rachis node; however, there are some mutants that can produce more than three spikelets per rachis node or more than one floret per spikelet, which will directly affect yield production (Forster et al., 2007; Sakuma et al., 2011)

In contrast, in branched inflorescences of sorghum or rice, the spikelets are produced after multiple rounds of branching, the inflorescence meristem starts with producing several primary branches,

and then the primary branch produces a secondary branch, then the final branches carry either single spikelets, or several paired spikelets (Witt Hmon et al., 2014).

The variation of the inflorescence architecture among grass species provides an excellent system for studying inflorescence development. This inflorescence morphology variation will help us understand the molecular regulation of inflorescence developments, subsequently manipulating floral architecture and increasing crop yields.

1.1. Barley

Barley (*Hordeum vulgare* L.), is one of the most important crops all over the world and is considered to be the fourth most important cereal crop worldwide after corn, rice, and wheat (Fischbeck, 2003; Verstegen et al., 2014). It's a major grass family crop grown in a temperate climate and one of the first cultivated grains in history thousands of years ago (Badr et al., 2000; Kilian et al., 2009).

Due to its adaptation to various environmental conditions, barley shows spring and winter growth habits and can grow in diverse environmental conditions, ranging from growth in high temperatures to very low temperatures. Thus, it is more widely adopted than most other cereals (Nevo et al., 1992; Wahbi, 1989).

Barley is widely used for different purposes; it was initially used as a source of human food and animal feed. But now it's mainly used for animal feed and in the production of beverages (Bothmer et al., 2003). Baik and Ullrich, (2008) reported that barley in ancient times was recognized as a source of high energy, for example, the Roman gladiators were eating barley to give them the power they needed.

Barley is considered to be rich in β -glucan (Quinde et al., 2004), which is very important for human health, especially for cardiovascular health and diabetes, because β -glucans play a role in controlling blood cholesterol levels and glycemic index (Baik & Ullrich, 2008; Pins & Kaur, 2006). For that reason, it is very important to incorporate barley into various food products for its potential health benefits, and more efforts are needed to develop new processes for using barley in the human diet.

1.1.2. Taxonomy

Barley belongs to the Triticeae tribe in the grass family Poaceae (Bothmer et al., 2003). Barley has a genome size of around 5 Gbps (Mascher et al., 2021; Sakkour et al., 2022; The International Barley Genome Sequencing Consortium, 2012), with a high degree of biological diversity. It comprised 32 species with different degrees of polyploidy. The commonly cultivated barley is diploid ($2n = 2x = 14$), whereas other species are tetraploid ($2n = 4x = 28$) or hexaploid ($2n = 6x = 42$), autopolyploidy is also found in two species, *H. bulbosum*, and *H. brevisubulatum*, and most of the polyploids are segmental allopolyploids (Komatsuda et al., 1998; von Bothmer & Jacobsen, 1986).

Barley is self-fertile that increases the chance of mutation to be transmitted to the next generation. Furthermore, due to its genetic diversity and availability of the genome sequence (Mascher et al., 2021; Sakkour et al., 2022; The International Barley Genome Sequencing Consortium, 2012), and the self-fertilization system with its diploid genome, makes barley an ideal model system for studying cereal genetics.

1.1.3. Barley life cycle

Barley is an annual grass plant that belongs to the monocotyledonous angiosperms, reaching 60 to 100 cm in height (Briggs, 1978). The life cycle of barley can be divided into three major phases: vegetative, reproductive, and grain filling (Figure 1.1.3.1) (Sreenivasulu & Schnurbusch, 2012), each of these phases has its unique structure; the vegetative phase begins at germination, followed by leaf initiation characterized by early formation of tillers and leaves (Kirby and Appleyard 1987).

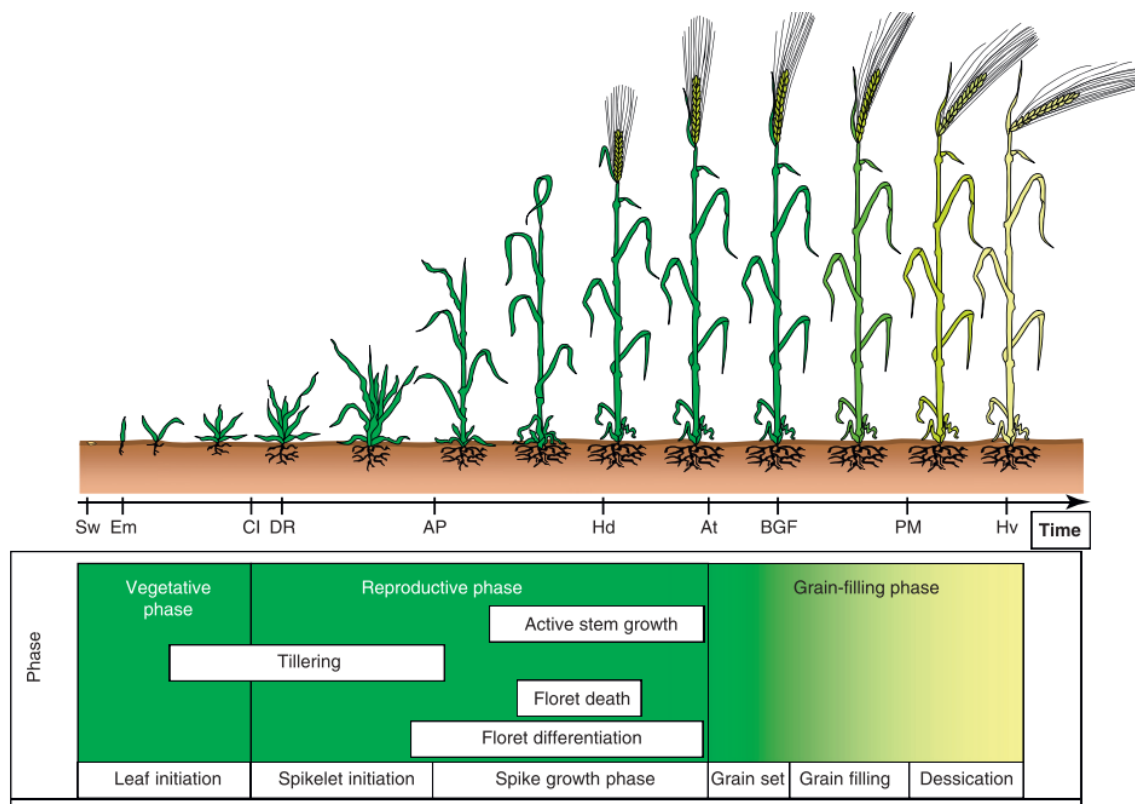


Figure 1.1.3.1: Barley life cycle: vegetative, reproductive, and grain filling phases. according to (Sreenivasulu & Schnurbusch, 2012).

During the vegetative phase, the plant develops tillers, whereas the reproductive phase starts afterward with spikelet/floret initiation starting from collar initiation and reaching the end of the reproductive phase by the anthesis stage (Kirby & Appleyard, 1987). The reproductive phase is

divided into two sub-phases: the early-reproductive phase and late reproductive phase, the early reproductive phase starts by floret initiation to Awn Primordium (AP) stage, and the late-reproductive phase starts from AP to anthesis stage (Kirby & Appleyard, 1987). During the early reproductive stage, there are several distinctive phases of spikelet initiation and differentiation, which start with a double ridge followed by a triple mound, glume primordium, lemma primordium, stamen primordium, and finally awn primordium stage (Figure 1.3.1.2) (Kirby & Appleyard, 1987).

The transition of the vegetative shoot apical meristem to an inflorescence meristem occurs with the start of collar initiation. Followed by the double ridge stage which contains two ridges; leaf ridge (the lower ridge that fails to develop) and spikelets ridge (upper ridge). The upper spikelet ridge specifies the TSM (triple spikelet meristem), which will develop the triple mound stage by forming two lateral meristems and one central spikelet meristem (Kirby & Appleyard, 1987). Each spikelet meristem will develop a single floret meristem; at the base of each spikelet meristem, the glume primordium will be developed, known as the glume primordium stage. Then the lemma primordia develop next to the glume primordia at the base of each floret meristem (FM). The FM will continue developing stamen primordia and awn primordia to form the final shape of the floret organs (Kirby & Appleyard, 1987). The late-reproductive phase, which starts by awn Primordium (AP) stage, comprises three distinctive phases awn tipping, followed by heading, and anther extrusion. The anther development occurs between the AP stage and awn tipping (Kirby & Appleyard, 1987). The development of the anther passes through three different phases, which include the white, green, and yellow-anther stages. The white color of the anther distinguishes the white-anther stage, then the style and stigma start to be developed from the carpel. Afterward, the anther turns to green color, which is known as the green anther stage, at this stage the style appears.

When the anther is matured, it becomes yellow, and the stigma becomes ready to receive pollen (Kirby & Appleyard, 1987). The last phase, grain filling, begins after pollination and starts the accumulation of dry matter to reach maturity, the duration of each phase will be dependent on genotype, geographic area, and environmental factors (Kirby & Appleyard, 1987; Kitchen & Rasmusson, 1983).

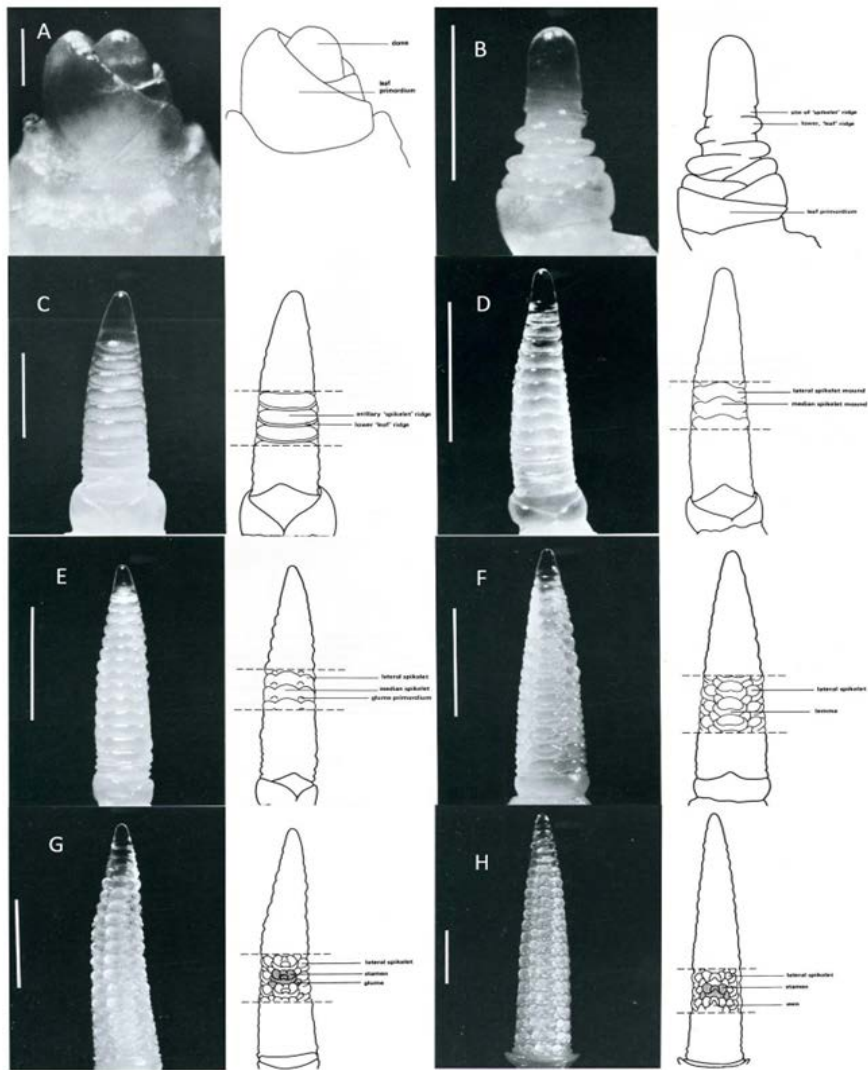


Figure1.3.1.2: Spikelet developmental phases of Barley. A, B) vegetative stage, C) double ridge, D) triple mound, E) glume, F) lemma, G) stamen, and H) awn primordium stages-the figure adopted from(Kirby & Appleyard, 1987).

1.2. Inflorescence architecture development in grasses

1.2 .1. Development of inflorescence meristem (IM) in grasses

The variation of inflorescence architecture depends upon the development of the inflorescence meristem (IM) and its fate (Koppolu & Schnurbusch, 2019). This variation is temporally controlled by two activities: the maintenance of meristem identity for developing new lateral organs and the determinacy of meristems during flower formation (Bommert & Whipple, 2018; C. Wang et al., 2021). The shoot apical meristem (SAM) will be developed into the inflorescence meristem (IM). The IM produces groups of meristematic cells and depending on the species, these cells will be developed into either branch meristems (BMs) or directly into spikelet meristems (SMs). The BMs will be developed into spikelet meristem (SMs) that produce two bracts known as glumes, followed by one or more floret meristem (FMs) in each spikelet (C. Wang et al., 2021).

The developmental variation during the transitioning process from SAM into an FM leads to the diversity of inflorescence architecture among closely related species. Such as the branchless spike of barley and wheat, the highly branched panicle of rice or sorghum, to the moderately branched raceme of maize (Kellogg, 2007; Koppolu & Schnurbusch, 2019; C. Wang et al., 2021; Yuan et al., 2020; C. Zhu et al., 2018). In barley, the TSM will differentiate into three spikelets, one central and two laterals. Based on the lateral spikelet (LS) fertility, spike-types in barley can be differentiated into two-rowed, where the LSs are sterile but central spikelets (CSs) are fertile, and six-rowed barleys when all the three spikelets are fertile (Figure1.21) (Koppolu & Schnurbusch, 2019; C. Wang et al., 2021). In wheat, the IM differentiates into a double ridge that includes a lower leaf ridge and an upper spikelet ridge. The wheat spikelet ridge differentiates into an SM that forms several FMs on the indeterminate rachilla (Figure1.2.1)(Sakuma & Schnurbusch, 2019).

In barley, however, the rachilla stops its meristematic activity after producing one floret with highly reduced internode elongation (Figure 1.2.1) (Forster et al., 2007).

In the panicle of rice, the IM initially produces several primary branch meristems (PBMs) afterward, the PBMs initiate secondary branch meristems (SBMs), and both PBMs and SBMs generate SMs and FMs, in their flanks and terminate in an SM (Figure 1.2.1) (Bommert et al., 2005). Maize has two types of inflorescence architectures that represent an indeterminate type of inflorescence: the male inflorescence (i.e. tassel) and the female inflorescence (i.e. ear) (D. Zhang & Yuan, 2014). The tassel IM of maize initially develops several indeterminate lateral long branch meristems (LBMs) at the base of the main axis of the tassel, followed by the formation of several short branch meristems (ShBMs), also known as spikelet pair meristems (SPMs) at the axis of LBMs in a distichous pattern. After producing LBMs at the base, the IM shift to produce SPMs instead of LBMs at the main axis of the tassel. Finally, the SPMs generate a pair of SMs at their flanks, and the ear inflorescence follows a similar pattern to that of the tassel, except that it does not develop LBM (Figure 1.2.1)(Koppolu & Schnurbusch, 2019; C. Wang et al., 2021).

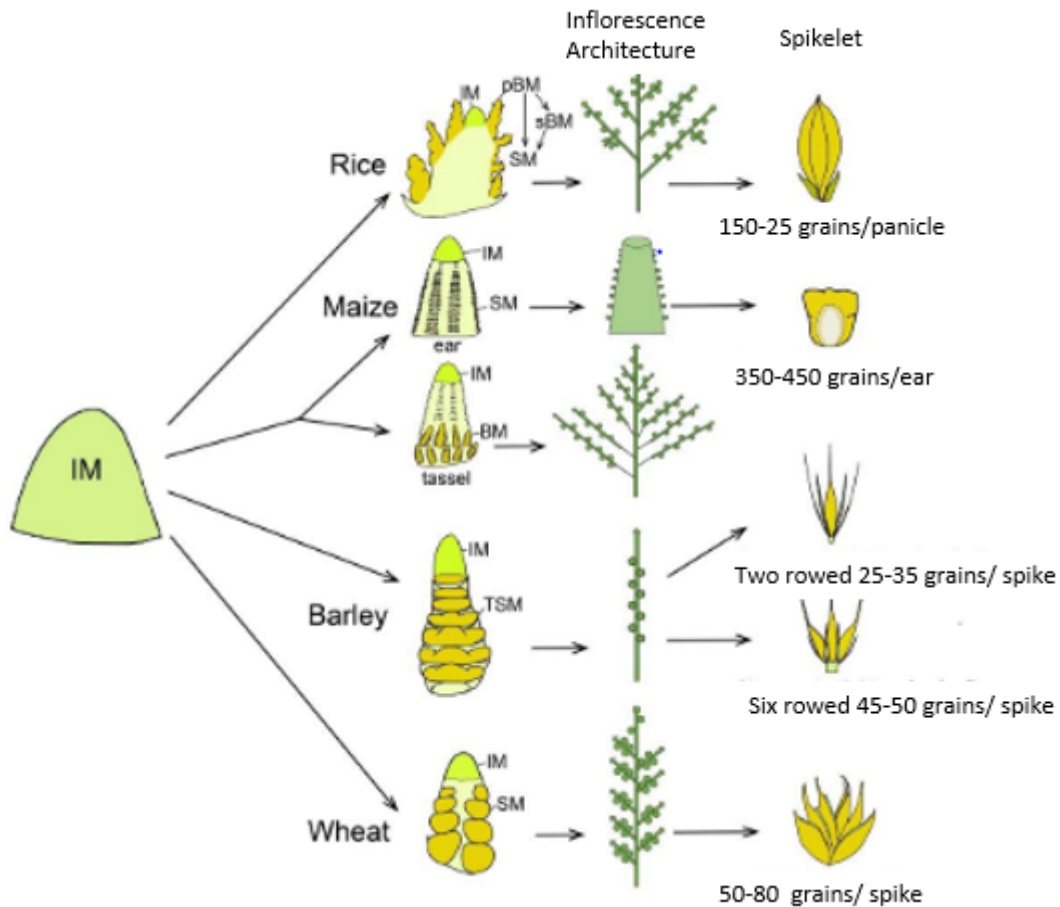


Figure 1.2.1 Schematics of meristem differentiation between rice, maize, barley, and wheat according to (C. Wang et al., 2021)

1.2.2. Spike architecture development

1.2.2.1. Genetic regulation of spike row-type in barley

The barley spike possesses a triple spikelet meristem, which differentiates into three spikelets, one CS, and two LSs, which shows a unique pattern of spikelet development. This arrangement gives the barley spike identity known as “row-type,” a two-rowed or six-rowed state (Cockram et al., 2010; Forster et al., 2007). within the two-rowed and six-rowed types, there are other three types known as deficiens-barley, intermedium-spike barley, and labile barley (Figure1.2.2). The deficiens barley is a two-rowed barley type with extremely reduced LSs (Sakuma et al., 2017). At

the same time, the labile barleys could have the LS developed or absent, fertile or sterile even within one spike of the same genotype. In contrast, the intermedium-spike barley has a fully fertile central spikelet, but the two lateral spikelets could be fertile or rarely fertile for setting small grains(Youssef et al., 2012, 2020)



Figure 1.2.2: Barley row-types (Youssef, 2015)

The barley row type identity is regulated by different genetic loci, such as *Six-rowed spike1(VRS1)*, *VRS2*, *VRS3*, *VRS4*, *intermedium-spike c (int-c)(VRS5)*, and *labile* (Pourkheirandish & Komatsuda, 2007; Youssef et al., 2012, 2020), each one of these loci displays unique spike phenotypes (Figure 1.2.3) (Koppolu et al., 2013). The development of six-rowed spikes in cultivated barleys is largely controlled by a single gene, *Six-rowed spike 1 (VRS1)*, a homeodomain-leucine zipper class I transcription factor, which is a negative regulator of LS fertility, providing the two-rowed condition in its functional state, and in the nonfunctional state,

it promotes lateral spikelet fertility resulting in a complete six-rowed phenotype (Komatsuda et al., 2007). The LS fertility is also conditioned by a modifier gene called *Intermedium spike-c* also known as *VRS5* (ortholog of maize *TEOSINTE BRANCHED 1*) (Ramsay et al., 2011). Loss of function mutation at *int-c* locus promotes LS fertility and an increased number of tillers. Up to ten independent *intermedium-spike* loci distributed across the barley genome modify the degree of lateral spikelet fertility in two-rowed barleys (Lundqvist & Lundqvist, 1988). Alleles at the *int-c* locus play a role in lateral spikelets fertility with consideration for the allelic constitution at *vrs1*; the *int-c.b* allele is generally found in two-rowed barleys (*Vrs1.b*) and inhibits anther development in lateral spikelets, while *int-c.b* produces smaller lateral spikelets in six-rowed barley (*vrs1.a*) (Lundqvist & Lundqvist, 1988; Youssef et al., 2017). The *Int-c.a* allele is present in six-rowed barley (*vrs1.a*), but its presence in two-rowed barley can produce partially fertile lateral spikelets, which results in an intermediate phenotype between two- and six-rowed barley termed *intermedium-spike* phenotype (Ramsay et al., 2011). Recent studies for *VRS5* at the protein level show that *VRS5* potentially interacts with different protein sets, including COMPOSITUM1 (COM1), one of the essential regulatory genes for inflorescence architecture in the grasses (de Souza Moraes et al., 2022).

The *VRS2* encodes a *SHORT INTERNODES (SHI)* transcriptional regulator that maintains hormonal homeostasis during inflorescence development thereby promoting regular spikelet patterning. Spikelet patterning in the mutant of *vrs2* is modulated due to hormonal disruptions, resulting in a distinctive spike architecture. The spike of *vrs2* mutant develops supernumerary spikelets at its base and occasionally enlarged and fertile LSs at the center of the spike. At the same time, it forms sterile LSs at its tip (Youssef, et al., 2017).

The *VRS4* regulates the barley row-type pathway by exerting transcriptional control over *VRS1* (Koppolu et al., 2013), the *vrs4* mutant shows complete fertility of CSs and LSs. In a wild-type condition, *VRS4* most likely transcriptionally activates *VRS1*, promoting the two-rowed condition. However, when *vrs4* is mutated, the transcription of *VRS1* (a negative regulator of LS fertility) is lowered resulting in the six-rowed condition (Koppolu et al., 2013). In addition to lateral spikelet fertility, *vrs4* mutants show indeterminate triple spikelet meristems (TSMs), which in turn produce additional spikelets and florets; therefore, *VRS4* is considered to be one of the genetic regulators of the determinate nature of TSM identity in *Hordeum* species (Koppolu et al., 2013).

The *labile* locus causes irregular spikelet fertility and displays a variable number of fertile spikelets at each rachis node, varying from absent to present fertile spikelets at the same spike; therefore, it can control the floret development as well as row-type in barley (Youssef et al., 2012, 2020).

The *VRS3* alleles show different levels of LS fertility within the same spike displaying two-rowed at the base of the spike, and the rest of the spike appeared to be six-rowed with complete lateral spikelet fertility. The RNA sequence data indicated that *VRS3* is a histone lysine demethylase with a conserved zinc finger C and N domain, controlling lateral spikelet fertility together with *VRS4* and *Int-c* by exerting their transcriptional activation over *VRS1* (Bull et al., 2017; van Esse et al., 2017; Zwirek et al., 2019).

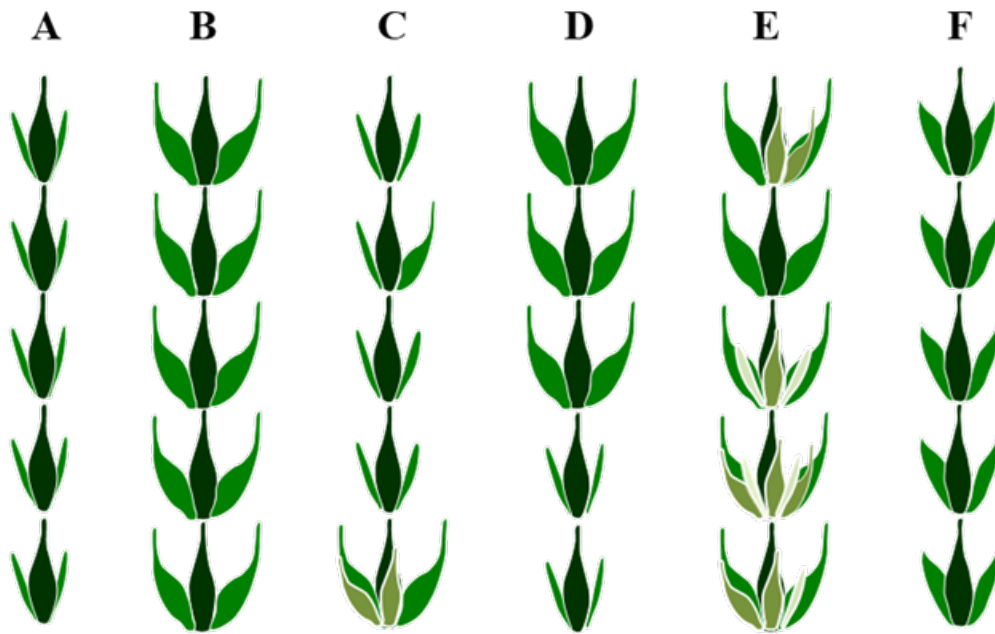


Figure: 1.2.3. Spike morphology of different row-type loci (Koppolu et al., 2013) (A) Two-rowed spike (*Vrs1*) (B) Six-rowed spike1 (*vrs1*). (C) Six-rowed spike2 (*vrs2*) (D) Six-rowed spike3 (*vrs3*). (E) Six-rowed spike4 (*vrs4*). (F) *Intermedium-spike C* (*int-c*).

1.2.2.2. Genetic regulation of spike Branching

The inflorescences of grasses have a variety of inflorescence architectures. Such as highly branched panicles of rice and sorghum, or moderately branched, like tassels of Maize to branchless spikes of wheat and barley (Koppolu & Schnurbusch, 2019; McKim et al., 2018; Perreta et al., 2009; D. Zhang & Yuan, 2014). This variation of inflorescence architecture is controlled by several genes and gene regulatory networks (Koppolu & Schnurbusch, 2019; C. Wang et al., 2021). Forward genetic approaches have been used to study this variation in phenotype by identifying a group of mutants that show non-canonical inflorescence branching (Franckowiak & Lundqvist, 2012). For example, the *loss-of-function* mutation in barley mutants (*com*), including *com1* (5HL), and *com2* (2HS), resulted in a branching spike phenotype. The branching spike phenotype in these mutants develops branching spike-like structures, supernumerary spikelets, and extra florets. The

wild-type form of *com1* and *com2* suppresses the branching phenotype by specifying SM identity and determinacy in all spikelets (Franckowiak & Lundqvist, 2012; Poursarebani et al., 2015, 2020). *COM2* encodes for an APETALA2/ETHYLENE RESPONSE FACTOR (*AP2-ERF*) transcriptional regulator, orthologous to the tetraploid wheat (*branched head (bh')*), (wheat FRIZZY PANICLE (*WFZP*))(O. Dobrovolskaya et al., 2015; O. B. Dobrovolskaya et al., 2017; D. Du et al., 2021; Y. Li, Li, et al., 2021; Poursarebani et al., 2015), rice FRIZZY PANICLE/BRANCHED FLORETLESS 1 (*FZP/BFL1*) (Komatsu et al., 2003), maize BRANCHED SILKLESS 1 (*BD1*) (Chuck et al., 2002). Loss of function mutations in any of these genes promotes inflorescence branching phenotype, indicating a conserved function of these genes across different species.

Shang et al.,(2020) and Poursarebani et al.,(2020) have identified the grass-specific CYC/TB1-type TCP transcription factor as the gene responsible for *COM1* locus. *COM1* is controlling inflorescence branching via specifying meristem identity. The *com1* mutants display an abnormal branching phenotype similar to *com2* (Poursarebani et al., 2020; Shang et al., 2020). The *COM1* is involved in cell wall development, and hormone signaling, which controls spikelet meristem determinacy and boundary formation via boundary signaling (Poursarebani et al., 2020). The qRT-PCR analysis indicated that *COM1* is one of the downstream targets of *VRS4*, among other cell wall-related genes. *COM1* and *COM2* work downstream of *VRS4* to confer meristem identity, but *COM1* is partially independent of *COM2*(Poursarebani et al., 2020).

This data suggests possible crosstalk between *COM genes and VRS4* in maintaining spikelet meristem identity (Koppolu et al., 2013; Poursarebani et al., 2015, 2020).

The proliferation of additional spikelets and florets in barley *vrs4* mutants indicates that *Vrs4* controls spike branching (Koppolu et al., 2013, 2022). The *VRS4* is an ortholog of the maize *RAMOSA2* (*RA2*) which encodes for the lateral organ boundaries (*LOB*) domain transcription factor (Bortiri et al., 2006; Koppolu et al., 2013). In maize, *RA2* (*ZmRA2*) had been implicated as the main regulator of the *RAMOSA* pathway (Bortiri et al., 2006). Mutation in *RAMOSA* genes produces a highly branched inflorescence with various degrees of branches. indicates a potential role for *RA2* in regulating inflorescence branching (Gallavotti et al., 2010; Satoh-nagasawa et al., 2006; Vollbrecht et al., 2005).

Insertional mutagenesis in the barley *miRNA172* that controls *AP2*-related transcriptional regulators (Patil et al., 2019) leads to an abnormal branching spike phenotype observed in *Ds-miR172* barley mutants. The *Ds-miR172* mutants display an abnormal spikelet development, where the glumes convert partially to florets in apical regions of spikes. Whereas at the base, due to indeterminacy of the TSM, it produces multiple branching organs in place of a single spikelet (Brown & Bregitzer, 2011).

Branching is also seen in another type of sterile barley mutant called *rattail* (*rtt*) spike mutant, which displays a severe branching of immature spikelets; the spikelets of this mutant are entirely sterile and do not produce grains (Lundqvist et al., 1997).

1.3. Regulation of RAMOSA pathway in inflorescence architecture of maize

The inflorescence branch formation and *RAMOSA* pathway in maize are controlled and regulated by the collective action of *RAMOSA* genes (Figure 1.3.1) (Koppolu & Schnurbusch, 2019). These genes include *RA1* (C2H2 ZINC FINGER transcription factor), *RA2* (LBD transcription factor),

trehalose-6-phosphate phosphatase genes (*RA3*, *TPP4*), and *REL2* (*RAMOSA1 ENHANCER LOCUS2*) (Claeys et al., 2019; Gallavotti et al., 2010; Satoh-nagasawa et al., 2006; Vollbrecht et al., 2005). *RA2* and *RA3* transcriptionally control the *RA1-REL2* complex, which regulates inflorescence branch outgrowth and spikelet pair meristem (SPM) identity and determinacy in tassel and ear inflorescences of maize (Gallavotti et al., 2010). Loss of function mutants in any *RAMOSA* pathway genes shows highly branched inflorescence due to impaired SPM identity (Bortiri et al., 2006; Vollbrecht et al., 2005).

The Trehalose 6-Phosphate Phosphatase 4 (*TPP4*) has been identified as an *RA3* enhancer associated with inflorescence development in the maize and is redundant for *RA3* (Claeys et al., 2019). The Analysis of an allelic series for *TPP* has shown that the enzymatic activity of *TPP* is not linked to its signaling ability. As a catalytically inactive *RA3* can complement a *ra3* mutant. Indicating that non-enzymatic function is responsible for its role in meristem determinacy (Claeys et al., 2019). A recent study on Maize trehalose-6-phosphate phosphatase identified *GRASSY TILLERS1* (*GT1*) as additional regulators in meristem determinacy by interaction with *RA3* to regulate both meristem determinacy in inflorescences and carpel suppression in flowers (Klein et al., 2022).

1.4. Regulation of COMPOSITUM pathway in inflorescence architecture of barley

The regulation of inflorescence branching through the COMPOSITUM pathway in barley differs from the RAMOSA pathway in maize because *RA1* and *RA3* orthologs are not present outside the tribe Andropogoneae (Bortiri et al., 2006; Vollbrecht et al., 2005). Nevertheless, *RA2* and *REL2* are present in most grasses, including rice and Triticeae species (Bortiri et al., 2006; Gallavotti et al., 2010; Koppolu et al., 2013; Suzuki et al., 2019). Moreover, the expression of *REL2* in barley

might be independent of *VRS4/HvRA2* (Koppolu et al., 2013). Therefore, the *REL2* in barley may interact with a different target protein (i.e., *RA1* equivalent) to regulate branch outgrowth in barley, as seen in maize (Figure 1.3.1)(Koppolu & Schnurbusch, 2019; Vollbrecht et al., 2005). The maize genome has a paralog of *ZmRA3* known as *SISTER OF RAMOSA3 (SRA)* (Satoh-nagasawa et al., 2006); the orthologue of the *SRA* is present in several types of grass species, including barley (*HvSRA3*) (Koppolu et al., 2013; Satoh-nagasawa et al., 2006). The *HvRA2* regulates *HvSRA3* and the trehalose biosynthetic enzyme trehalose-6-phosphate synthase (*HvTPS1*) (Koppolu et al., 2013; Koppolu & Schnurbusch, 2019). Therefore, inflorescence branching regulation in Triticeae and Andropogoneae species appears to be governed by differential genetic control (Koppolu et al., 2022; Koppolu & Schnurbusch, 2019).

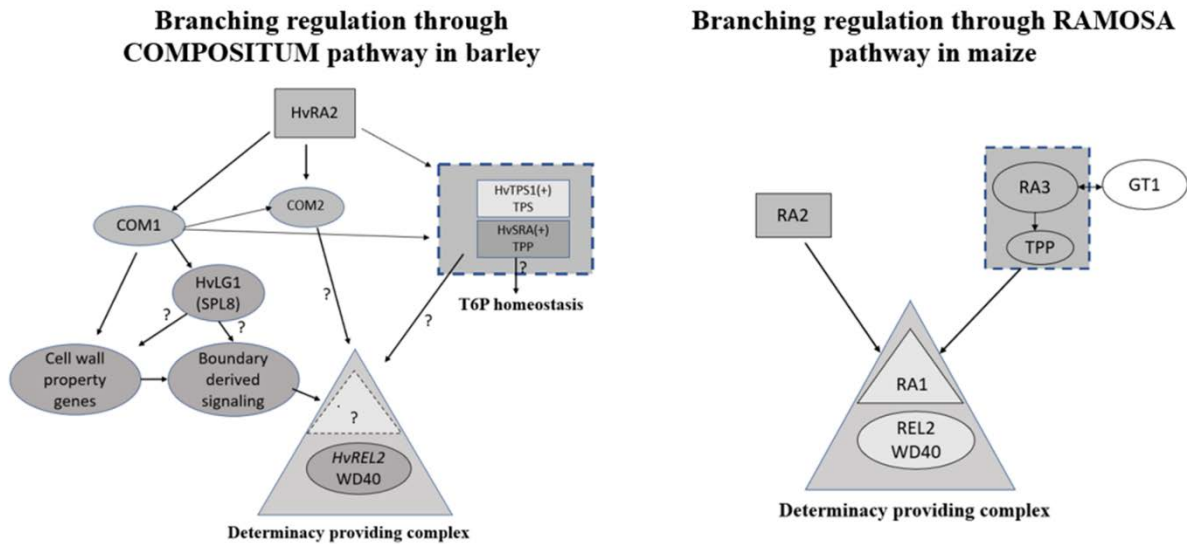


Figure1.3.1. Model for inflorescence branching regulation in barley and maize. *TPS1*, TREHALOSE-6-PHOSPHATE SYNTHASE 1; *RA1*, 2, 3: *RAMOSA 1*, 2, 3; *REL2*, RAMOSA1 ENHANCER LOCUS 2; *TPP*, TREHALOSE-6- PHOSPHATE PHOSPHATASE; *HvSRA*, SISTER OF RAMOSA3; *COM2*, *COMPOSITUM 2*; *GT1*, *GRASSY TILLERS1*; Adopted from (Koppolu & Schnurbusch, 2019; Poursarebani et al., 2020).

1.5. The function of LBD transcription factors

Lateral organ boundaries (LOB) domain (*LBD*) proteins are plant-specific transcription factors that play an important role in plant organ development and metabolic processes in higher plants (Husbands et al., 2007; Shuai et al., 2002).

The LBD proteins are defined by the highly conserved LOB domain in plants, which comprised of a cysteine-rich repeat known as zinc finger-like motif (CX₂CX₆CX₃C) as a DNA-binding motif, followed by highly conserved GAS block (Gly-Ala-Ser) and a leucine-zipper-like coiled-coil motif (LX₆LX₃LX₆L) responsible for protein dimerization (W.Chen et al., 2018; Husbands et al., 2007; Koppolu et al., 2013; Shuai et al., 2002; Xu et al., 2016). The *RA2* orthologs of LBD proteins in grasses (monocots) have a distinct C-terminal carrying a putative activation domain (44 aa) that is absent from *Arabidopsis* and other eudicots, and the final four amino acids of the N-terminal domain (PGAG) are highly conserved across grass species (Koppolu et al., 2013).

The LBD proteins have been identified in several plant species. Approximately 823 LBD genes have been identified in 18 plant species (Shuai et al., 2002). Based on protein sequences and phylogenetic analysis, the LBD proteins were divided into two main classes (Class I and Class II). Class I can be further divided into four subclasses, Class IA, Class IB, Class IC, and Class IE. Class II were sub-grouped into two classes (IIA and IIB) (Shuai, et al., 2002; Zhang et al., 2020). The LBD proteins are involved in different functions in plant development and metabolic processes, such as inflorescence development, auxin signaling, photomorphogenesis, shoot differentiation, regulating callus formation, leaf development, embryogenesis, lateral root formation, abiotic and biotic response, vascular patterning, anthocyanin synthesis, and nitrogen responses (J. Wang et al., 2021; Y. Zhang et al., 2020).

In *Arabidopsis thaliana*, a total of 43 *LBD* genes were reported (Shuai et al., 2002). The first identified member of LBD protein in *Arabidopsis thaliana* was *AtLOB*, the loss of function mutant of this gene displayed boundary formation defects and organ fusion phenotypes (Bell et al., 2012). The Ectopic expression of *AtLOB* resulted in stunted growth as a consequence of the reduction of the brassinosteroid (BR) responses. The *AtLOB* negatively regulates BR accumulation, by targeting the promoter region of *PHYB ACTIVATION TAGGED SUPPRESSOR1 (BAS1)* to regulate BR accumulation in the boundary regions resulting in limited growth (Bell et al., 2012; Gendron et al., 2012). The orthologous genes of *AtLOB* were identified in barley (*HvRA2*), maize (*RAMOSA2/RA2*), and rice (*OsRA2*).

In barley, *HvRA2* is a key regulator of spike architecture (see section 1.2.2.2). In rice, *OsRA2* regulates panicle architecture by modifying pedicel length (H. Lu et al., 2017). The genetic analysis for *OsRA2* indicates possible relation between miR156 and *LAX1*, *LAX2*, *RCN2*, and *OsRA2* in regulating panicle architecture (X. Yang et al., 2019). In maize, *ZmRA2* is involved in regulating inflorescence development (Bortiri et al., 2006). The conservation of the expression pattern of *RA2* and the high similarity of the protein sequence among different grass species suggest that *RA2* may have a conserved function, which is essential for regulating inflorescence architecture in grasses (Bortiri et al., 2006; Koppolu et al., 2013; H. Lu et al., 2017).

1.5. Functional Genomics

With the availability of complete genome sequences of several organisms, the focus has moved from structural genomics to functional genomics to assign functions to newly identified DNA sequences (Radhamony et al., 2005). There are two ways to link the sequence and function of a specific gene: forward and reverse genetics; whereas reverse genetic strategies start with a

DNA sequence and then seek a plant line mutated in that gene, forward genetic approaches study the phenotype first and then the genotype (Alonso & Ecker, 2006; Bouchez & Ho, 1998; Krysan, 1999; Peters et al., 2003).

In Arabidopsis, reverse genetics has become a general practice for characterizing genes with unknown functions due to the completion of its genome sequence (Provart et al., 2021; The Arabidopsis Genome Initiative, 2000; Ülker & Weisshaar, 2011; B. Wang et al., 2021). Moreover, the advancements in next-generation sequencing technology enabled whole genome sequencing in many species providing unprecedented discovery and characterization of molecular polymorphisms.

Furthermore, sequencing of other crops such as rice (H. Du et al., 2017; Goff et al., 2002; Kishor et al., 2020; Yu et al., 2002), *brachypodium distachyon* (The International Brachypodium Initiative, 2010), sorghum (Cooper et al., 2019; Paterson et al., 2009) and barley (Mascher et al., 2021; Sakkour et al., 2022; The International Barley Genome Sequencing Consortium, 2012), which make reverse genetics a practical procedure to a variety of plant species (Kumar et al., 2022). Moreover, when more than one gene coding for a particular function, reverse genetics is the right tool to analyze this redundancy (Krasileva et al., 2017; Z. Li et al., 2018; Meissner et al., 1999). Therefore, combining forward with reverse genetics will be the best way to analyze plant gene functions (Alonso & Ecker, 2006; Capilla-Perez et al., 2018).

1.5.1. Reverse genetics approaches to study gene function

Both reverse and forward genetics approaches are used to study the function of a particular genomic sequence. Although both methods usually proceed in the opposite direction, the final aim

is to study gene function. The reverse genetics approach starts with known genomic or protein sequences and then tries to identify the phenotypic or molecular function of this sequence by altering that sequence, Whereas forward genetics begins with a mutant phenotype and then seeks to discover the disrupted sequences relevant to that phenotype (Aklilu, 2021; Zakhrabekova et al., 2013).

The main tools for forward genetics are the mutants causing phenotype change and then looking for the sequence responsible for this phenotype. The barley researchers have spent many years identifying and characterizing barley mutants that provided the raw material for forward genetic approaches (Aklilu, 2021; Kurowska et al., 2011; Lundquist, 2005). Several mutagens have been used effectively to induce mutations in barley, such as X-rays, gamma-rays, Ethyl Methyl Sulfonate (EMS), and sodium azide (Lundqvist & Franckowiak, 2003).

In addition, barley scientists have collected spontaneous and artificially induced mutants and systematically maintained them in geneticist and breeder collections centers at the National Small Grain Collection, Aberdeen, ID (<https://www.ars.usda.gov/pacific-west-area/aberdeen-id/small-grains-and-potato-germplasm-research/docs/barley-wheat-genetic-stocks-collections/>), and the Nordic Genetic Resource Center, Alnarp, Sweden (<https://www.nordgen.org/en/plants/plant-material/seed-collections>) (Lundqvist & Franckowiak, 2003).

Many of these mutants were backcrossed to a near-isogenic line in the Bowman background, which provides a rich resource for functional studies and gene cloning. Thus, the barley community has an extensive collection of mutants, to begin with, forward genetic approaches. In addition, recently, additional genomics tools developed will accelerate forward genetics approaches (Druka et al., 2011).

Several reverse genetics tools have been developed to study gene function for the identified sequence. Due to the extensive collection of EST (Expressed Sequence Tag) from different plant tissues in barley, which put the basis for the prediction of gene function to study the function of the identified sequences, a variety of reverse genetics tools have been developed to study gene function. This includes transgenesis of plants, in vitro mutagenic approaches (Abdeeva et al., 2012), and genome editing tools, such as TILLING (Targeting Induced Local Lesions IN Genomes) and CRISPR / Cas9 technology (Jaganathan et al., 2018; Rasheed et al., 2021; Zakhrabekova et al., 2013).

1.5.1.1. Transgenic plants

Testing genes of interest by creating transgenic lines is a common functional genetics approach (Abdeeva et al., 2012). There are two systems for barley transformation; particle bombardment and *Agrobacterium*-mediated genetic transformation (Hensel et al., 2011). The transformation of barley was first reported in 1994 using particle bombardment (Wan & Lemaux, 1994), and the first reports of *Agrobacterium tumefaciens* mediated barley transformation were published by Tingay et al., (1997). Although successes with these approaches have been limited in barley due to low transformation efficiency several efforts have been made to overcome the problems associated with low transformation efficiency with varying success (Dahleen & Manoharan, 2007; Han et al., 2021; Kumlehn & Hensel, 2009).

The transgenic plant can identify the gene function by several means. Such as complementation of a loss-of-function mutant by complementing the mutated gene with its functional form to recover the wild-type phenotype, or via co-suppression and downregulation of the target genes by introducing several copies of an overexpression construct; or by RNA interference (RNAi), in

which the transgene consists of an inverted repeat of the target sequence, which leads to the formation of hairpin RNA molecules. This hairpin loop will be recognized and degraded via post-transcriptional gene silencing machinery of the host plant (Abdeeva et al., 2012; Kochetov & Shumny, 2017; Kumlehn & Hensel, 2009). The RNAi approach is considered an ideal tool to downregulate genes and overcome gene redundancy in a gene family. It is also beneficial where a completely loss-of-function mutant is lethal because RNAi only knocks down the expression of the target gene rather than completely knocking it out. Moreover, RNAi could give a better understanding of gene function when combined with tissue-specific or development stage-specific promoters, but the main drawback of RNAi is that it may not produce a complete loss-of-function phenotype (Boettcher & McManus, 2015; Daly et al., 2019).

With the rapid progress in the development of genetic engineering, genome editing has emerged as a new tool for targeting specific genome sequences, which provide a means to create mutation at specific DNA sites. These mutations could be insertions, deletions, or gene replacements (D. Du et al., 2021; Verma et al., 2021; Wada et al., 2020). Genome editing tools such as zinc-finger nucleases (ZFNs) (Carroll, 2011; Shukla et al., 2009), Transcriptional Activator-Like Effector Nucleases (TALENs) (Christian et al., 2010, 2013; Khan et al., 2017; T. Li et al., 2012; Ma et al., 2015), and bacterial CRISPR-associated protein nine nucleases (Clustered Regularly Interspaced Short Palindromic Repeats) (Křenek et al., 2021; Lawrenson et al., 2021) have been successfully used in plants.

Both ZFNs and TALENs systems rely on protein-DNA binding interactions by designing a construct in the desired combination. The DNA binding domain is attached to a nuclease domain of FokI to cleave in a targeted DNA sequence specifically (Malzahn et al., 2017). Wendt et al.,

(2013) successfully applied TALENs technology in barley by inducing double-stranded breaks in a specific site of the barley genomic through a customized TALENs, leading to a deletion in the targeted site; also Gurushidze et al., (2014) successfully created a homozygous knockout mutant in barley, by applying TALENs methodology, and the offspring of the mutated plants showed the mutant phenotype.

In addition to barley, TALENs were successfully applied for mutagenesis in other plants such as wheat (Y. Wang et al., 2014), maize (Liang et al., 2014), rice (T. Li et al., 2012), tobacco (Y. Zhang et al., 2013), sugarcane (Jung & Altpeter, 2016), tomato (Lor et al., 2014), *Brachypodium* (Shan et al., 2013), *Brassica oleracea* (Sun et al., 2013), soybean (Haun et al., 2014) and *Arabidopsis* (Christian et al., 2013).

For more efficient genome editing, the CRISPR/ Cas9 system has been widely adopted and modified in plants. By using an **R**NA-guided **en**donuclease (RGEN) approach, which relies on the small sequence of non-coding RNA known as a single guide RNA that binds with the target DNA sequence, to direct the Cas9 nuclease to the targeted sequence (Jinek et al., 2012; Malzahn et al., 2017). The RGEN system, unlike ZFNs and TALENs, which are difficult to assemble, and are labor-intensive and costly, RGEN is easy to design, easy to implement, and a relatively cheap method for genome editing, which makes it an ideal tool for genome editing in plants (El-Mounadi et al., 2020; Hilscher et al., 2017; Hsu et al., 2014; Matres et al., 2021; Zegeye et al., 2022).

Lawrenson et al., (2015) induced heritable mutations in barley and *B. oleracea* with the help of RGEN by targeting multi-copy genes, the transgenic loci from the created mutation segregated and produced transgene-free plants having the desired mutation, the percentage of the induced mutation in this study was between 10 to 23%. Later reports by Kapusi et al., (2017) and Zeng et

al., (2020) successfully produced targeted knock-outs in barley using the RGEN system with a higher percentage, around 78% of the plants.

The RGEN system has been successfully applied to different plant species to generate transgene-free plants including barley (Gasparis et al., 2019b; Q. Yang et al., 2020; Zeng et al., 2020), rice (Dong et al., 2020; J. Li et al., 2016; Shen et al., 2018; Zhou et al., 2019), maize (Barone et al., 2020; R. Chen et al., 2018) and wheat (Liang et al., 2017; Y. Zhang et al., 2016). Therefore, RGEN is considered one of the most beneficial tools for reverse genetics in plants.

1.5.1.2. Targeting induced local lesions in genomes (TILLING)

TILLING is a molecular biology technique that can directly identify the mutation in a specific gene and link this mutation to phenotypic change leading to identifying the function of this gene. This method was developed in 2000 for Arabidopsis (McCallum et al., 2000). It combines the advantage of chemical mutagenesis for a known sequence with the sensitivity of high throughput screening for nucleotide polymorphisms in a targeted sequence. It has been applied to many crop plants regardless of their genome size and ploidy levels, such as corn, wheat, rice, tomato, and barley (Kurowska et al., 2011).

There are different TILLING populations available for barley that has been created from different barley cultivars, such as Golden Promise (Schreiber et al., 2019), barley landrace “Hatiexi” (HTX) (C. Jiang et al., 2022), Optic (Caldwell et al., 2004), Morex (Talamè et al., 2008), Barke (Gottwald et al., 2009), Lux (Lababidi et al., 2009), Mannenboshi (Kawamoto et al., 2020), RGT Planet (Knudsen et al., 2022) and Sebastian (Szarejko et al., 2017).

The mutation density in these TILLING barley populations is very high. For example, the Golden Promise TILLING population was estimated by one mutation per 154 kb (Schreiber et al., 2019); the Morex population constitutes 4,906 families, with a mutation density of one SNP per 374 kb (Talamè et al., 2008). The Optic population was developed with an average mutation density of one per 1000 kb (Caldwell et al., 2004). Lux population has been made by using a sodium azide with a mutation density of one per 2500 kbp (Lababidi et al., 2009) (Lababidi et al., 2009), and the population Sebastian has been developed by using double treatment with sodium azide and N-methyl-N-nitrosourea (NMU) with mutation load one per 477 kbp (Szarejko et al., 2017). The Barke TILLING population contains around 10,279 M2 lines with a mutation density of one per 0.5 kb (Gottwald et al., 2009). Such a high mutation density percentage coupled with a high-quality reference genome assembly will help elucidate the genes' function in mutants of interest (C. Jiang et al., 2022).

1.6. Cis-regulatory elements and regulation of gene expression

The regulation of gene expression is a highly dynamic and complicated process that comprises multiple proteins and transcription factors. It involves cis-regulatory elements localized in the promoter regions upstream of the transcriptional start site, which control gene expression at different developmental stages and tissues (Biłas et al., 2016; Hernandez-Garcia & Finer, 2014; Mithra et al., 2017).

The promoter region consists of the core and two regions upstream of the core region, the proximal and distal promoter regions (Fig. 1.6.1) (Hernandez-Garcia & Finer, 2014; Mithra et al., 2017; Pandey et al., 2018). The core promoter region is located within 40 bp upstream of the coding region. Moreover, it contains the Transcriptional Start Site (TSS) where RNA polymerase II

(RNAPII) binds and initiates the basal level of the transcription, which is enough for the basal level of transcription. The core promoter sequences contain several essential elements for the transcription process, which include the TATA box, initiator (INR), downstream promoter elements (DPE), and CAAT box (Ijaz et al., 2020; Mithra et al., 2017). The main feature of the core promoter elements is to facilitate the binding of the preinitiation transcription complex. Therefore, any alteration in the plant core promoter leads to changes in gene expression (Srivastava et al., 2014).

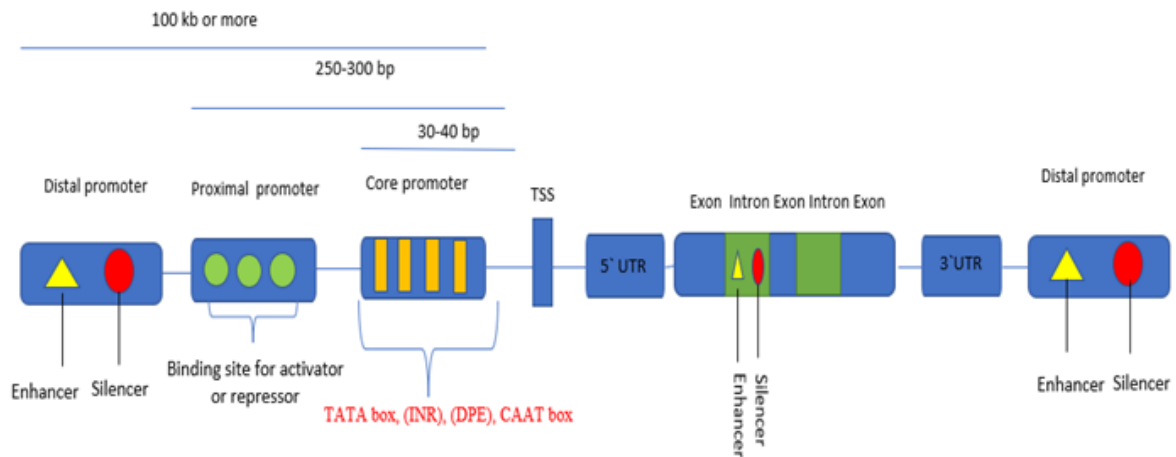


Figure 1.6.1: Schematic representation for promoter elements in plant

The proximal promoter region is generally located several hundred nucleotides around the TSS. The proximal region contains many binding sites for activators or repressors, which assist transcription factors in different developmental processes (Pandey et al., 2018; Shahmuradov et al., 2003). The distal promoter region is mostly located thousands of nucleotides away from TSS. This region includes regulatory elements such as enhancers, silencers, and insulators that contribute to the fine-tuned regulation and spatiotemporal gene expression and allow to control of cell type and growth pattern (Hernandez-Garcia & Finer, 2014; J. Li, Wang, et al., 2019; Maul et al., 1998; Shahmuradov et al., 2003).

1.6.1. Enhancers and Silencer

Enhancers and silencers are cis-regulatory elements that contain multiple transcription factor binding sites (TFBS) required to enhance or repress the transcription of the target gene (Hardison & Taylor, 2012; Kolovos et al., 2012; Pandey et al., 2018; Rusche et al., 2003). The interaction between promoters and enhancers depends on their distance (Y. Yang et al., 2011). The enhancer or silencers can be located several thousand base pairs (bp) away from the TSS, either upstream or downstream of the core promoter, and they can be located within the intron sequences (Gupta & Tsiantis, 2018; Hong et al., 2003; Z. Lu et al., 2019).

In maize, Stam et al.,(2002) identified a 6-kb enhancer region located 100 kb upstream of the transcription start site (TSS) of the *b1* gene. This cis-element is required for B-I enhancer activity and paramutation in maize. Another study on maize made by Zheng et al., (2015) identified a 3.9 kb cis-element for the *Bx1* (*benzoxazinless1*) gene located 140 kbp away from the TSS. This distal cis-element was required for higher transcript levels for *Bx1* during later developmental stages. The variation in physical enhancer position in the genome with its multiple components makes the prediction of enhancers a difficult task (Hardison & Taylor, 2012).

The Enhancers control expression via multiple enhancer modules that interact with several TFs and regulatory proteins, including chromatin interactions that allow functional diversity independent of its location in the genome (Biłas et al., 2016; Kolovos et al., 2012; Long et al., 2016; Y. Peng et al., 2019; Schmitz & Grotewold, 2022). The enhancer element regions are characterized by increased nuclease sensitivity, reduced nucleosome density, modifications of core histone proteins, and low DNA methylation. Which allows the accessibility of chromatin by TF

interactions to regulate gene expression independently of the distance and orientation to their target genes (Z. Lu et al., 2019; Perlot & Alt, 2008; Ricci et al., 2019; Zhao et al., 2019).

Four models have been proposed for gene regulation by enhancer elements. As it was reviewed by Kolovos et al., (2012) Figure (1.6.2); (1) the Tracking model, the regulatory proteins bind to the enhancer complex and move towards the core promoter to enhance the transcription; (2) the linking model, after the protein binding of the regulatory protein it drives the polymerization toward the core promoter; (3) the relocation model, the gene relocates to the place where it can interact with its enhancer machinery complex (4) and the looping model, the most accepted model, where the enhancer complex form a loop to bind to the core promoter to activate the transcription.

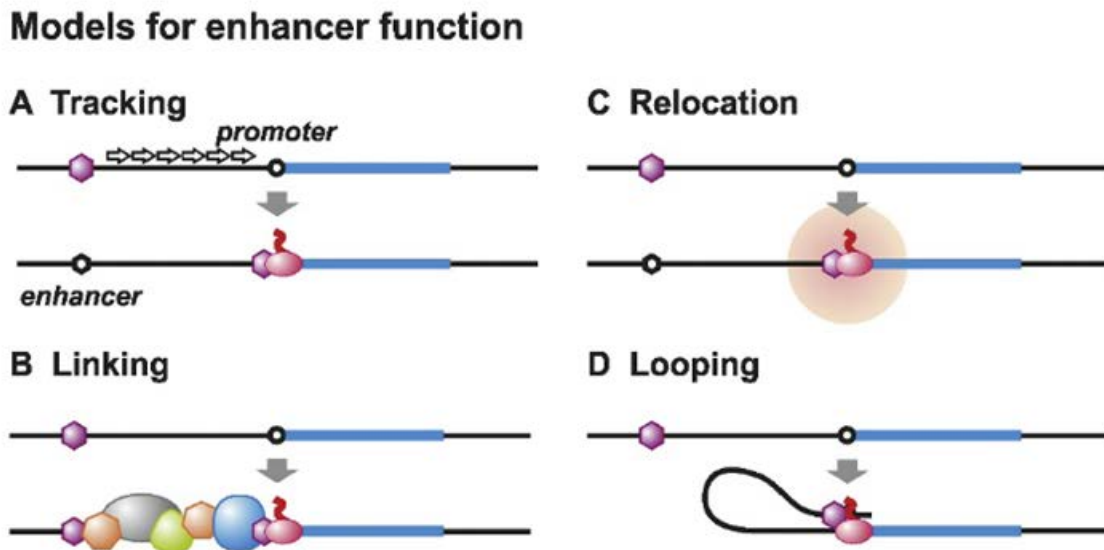


Figure 1.6.2 proposed models for the function of enhancers (Kolovos et al., 2012) (A) tracking model, the transcription factor (purple hexagon) binds to the enhancer and moves towards the core promoter, to interact with the polymerase (pink oval). (B) In the linking model, the transcription factor drives the polymerization of proteins in the direction of the core promoter. (C) Relocation model, the gene itself relocates to nuclear sub-compartments (pink halo), where it can interact with the enhancer-promoter

complex. (D) In the looping model, where the enhancer complex forms a loop comes into proximity with the relevant promoter and triggers transcriptional regulation. (Kolovos et al., 2012).

The silencer elements work similarly as enhancers. It can downregulate gene expression by forming a silencer complex via binding with several TFs with corepressor proteins. This silencer complex can establish precise, tissue-specific expression patterns by blocking expression in cells, where the gene should be silenced, and preventing ectopic gene expression (R. Liu et al., 2020; Privalsky, 2004; Schmitz & Grotewold, 2022; Xiao et al., 2017). The silencers can regulate gene expression directly or indirectly through silencing the enhancers (R. Liu et al., 2020). For example, it has been shown that the Enhancer of *AGAMOUS* (*AG*) in Arabidopsis is responsible for tissue specificity for the *AG* to be expressed in flower tissue (Elliot, 1997; Hong et al., 2003; Yanofsky et al., 1990). The functional genomic study on *AGAMOUS* second intron enhancer (*AGI*) derived from tobacco reveals that The *AGI* cis-element contains a conserved GAGA binding motif. The *AGI* functions as a silencer by suppressing the effect of the enhancer in vegetative tissue through histone modification and significantly increases the activity in the inflorescence tissue (R. Liu et al., 2020).

1.6.2. Insulators

Insulators are specific proteins known as boundary elements. For proper gene regulation, the insulator is located between enhancer or silencer elements and promoters (Kurbidaeva, 2021). The insulator can block an enhancer effect on the target gene by blocking the interaction between an enhancer and the relevant promoter; it can also prevent the spread of repressive chromatin (Kurbidaeva, 2021; Kyrchanova & Georgiev, 2014).

The insulators achieve their function by interacting with each other to generate chromosomal loops via specific DNA motifs that act as binding sites allowing this interaction to occur (Kurbidaeva,

2021). Furthermore, the insulators can maintain the stabilization of the chromosome organization and the integrity of the regulatory elements. Therefore insulator sequences were used in the transgenic experiment to avoid positional effects, stabilize their expression and protect a transgene from unwanted interactions with endogenous genetic elements (W. Jiang et al., 2017; Pérez-gonzález & Caro, 2019; Singer et al., 2011).

1.7. Aims and underlying working hypotheses of the present thesis

Understanding the molecular genetic regulation of inflorescence development in grasses is essential for increasing crop yields. Knowing the mechanisms behind the repression of branching and spikelet differentiation will help reduce the abortion of spikelet formation and increase crop yield. From previous research studies, it was proposed that temporal gene expression and dosage of *HvRA2* (*VRS4*) are essential for establishing the barley-specific row-type pathway (Koppolu et al., 2013; Koppolu & Schnurbusch, 2019) as well as the branch repression COM pathway (Poursarebani et al., 2015, 2020). The transcriptional expression of *SbRA2* during the panicle branching of sorghum starts after the initiation of the primary branch meristems (Brown et al., 2006). Whereas in branchless barley and wheat spikes, *VRS4/HvRA2/TaRA2* mRNA expression is initiated at a very early developmental stage after the differentiation of the SAM into leaf primordia (Koppolu & Schnurbusch, 2019).

Such an expression pattern indicated that the transcriptional regulation of *VRS4/HvRA2* and *TaRA2* is temporally advanced in barley or wheat (Triticeae), respectively, compared to sorghum. We therefore hypothesized that this early expression might cause branch suppression in barley and wheat spikes. Notably, the expression level of *TaRA2* in wheat spike is much higher compared to its expression in barley spikes. Such expression differences between barley and wheat spikes could

potentially be linked with the observed differences in spikelet number per rachis node (one spikelet vs. three spikelets for wheat and barley, respectively) between both species.

In general, it is a challenging task to relate the observed morphological spikelet differences of different species to temporal gene expression changes. However, one way of validating such temporal comparative gene expression dynamics in different species is to conduct transgenic experiments by swapping species' promoters for the gene of interest and evaluating the resultant phenotypes (McSteen, 2006; Strable et al., 2022). Therefore, in the current proposed research work, we tried to test whether the cis-regulatory elements for different, species-specific *RA2* promoter sequences might cause differences in inflorescence architectures between barley, wheat, and sorghum.

To achieve this, we conducted transgenic experiments by swapping the beginning of the putative promoter region upstream of the start codon ATG of *RA2* CDS from barley (2166bp), wheat (2228bp), and sorghum (2418bp) and transformed these constructs to complement the *hvra2(vrs4)* barley mutant, followed by a detailed phenotypic and molecular characterization of *vrs4* transgenic complementation lines compared to azygous lines.

1.7.2. The major objectives of the present study are:

1. Generation of promoter-swapped *RAMOSA2* (*HvRA2*) constructs from barley, wheat, and sorghum, transform them into *vrs4* mutants and evaluate the outcome of the transgenic plants at the phenotypic and molecular level.
2. Promoter activity localization of the barley, wheat, and Sorghum *RA2* promoters within the barley spike using transgenic GFP reporter lines.

3. Generation of *vrs4* knockout mutants using a highly efficient RNA-guided Cas9 gene editing system in the *cv.* Golden Promise (model genotype for efficient, stable transformation) which will be a valuable resource for further functional analysis studies.
4. Complementation studies using promoter swapped *RAMOSA2* (*HvRA2*) constructs in *vrs4(hvra2)* knockout mutant (created by RGEN) followed by functional characterization.

1.8. Data contributions

The author of this thesis (*Omar Heliel*) performed the majority of the presented results. However, some results were obtained in collaboration with other researchers, their contributions are listed below:

1-Prof. Dr. Thorsten Schnurbusch and Dr. Ravi Koppolu, Plant Architecture Research Group, IPK.

Conceived the idea/ research plan and supervised the candidate.

2-Dr. Goetz Hensel - Research Group Plant Reproductive Biology, IPK

Supervised Mrs. Sabine Sommerfeld for barley transformation and transgenic plant production.

He also generated the RGEN construct for supertransformation. The author of this thesis (*Omar Heliel*) participated in this step for a short time only to learn the barley transformation technique.

3-Dr. Ravi Koppolu - Plant Architecture Research Group, IPK.

Generated all the complementation constructs containing the species-specific putative promoter sequences, except for the complementation construct tagged with GFP, which was made by the main author (*Omar Heliel*) of this thesis.

4-Dr. Twan Rutten - Research Group Structural Cell Biology, IPK.

Supported the Scanning of fluorescence microscopic images for GFP visualization.

5-Dr. Jozefus Schippers - Seed Development Research Group, IPK.

Supported the transient assay expression analysis of *RA2* promoters in rice protoplasts.

2.0. Materials and Methods

2.1. Plant materials and growth conditions

Barley genotypes Bowman, Golden Promise, two *vrs4* mutant genotypes, which includes Bowman backcross derived lines BW–NIL(*mull.a*) (Koppolu et al., 2013) and Golden Promise *vrs4* RGEN mutant, as well as stable transgenic plants were used in this study. Grains were planted in 96 well plastic trays and germinated under greenhouse conditions (16 hours light, 15 °C and 8 hours dark, 14 °C.) for four weeks, and then the germinated seedlings were transferred to the vernalization room at 4°C. After four weeks of vernalization, seedlings were transferred to the greenhouse at 15 °C for two days. Afterward, the seedling was transferred to 11 cm diameter pots and allowed to mature in the greenhouse. For expression analysis by qRT-PCR, the grains germinated in 24-well planting trays were grown under greenhouse conditions (16 hours light, 18 °C, and 8 hours dark, 14 °C). The germinated seedlings were kept to reach the glume/stamen primordia stage. Then the seedlings were dissected by extracting the entire meristems without taking any surrounding leaf tissue and then placed in 2 ml Eppendorf tubes in liquid nitrogen.

2.2. Fluorescence Microscopy

The GFP fluorescence was analyzed using either LSM 510 META or LSM780 confocal laser scanning microscopes (Carl Zeiss Microscopy GmbH, Jena, Germany) established at IPK (Structural Cell Biology, SZB, Dr. Michael Melzer). GFP was visualized by excitation with a 488 nm laser line in combination with a 490-530 nm band-pass filter; whereas chlorophyll fluorescence will be analyzed by excitation with a 633 nm laser line in combination with 650 nm long-pass filter. In all samples, the authenticity of the GFP signal will be analyzed by photo spectrometric unmixing using the Lambda detector.

2.3. Molecular analysis

2.3.1. Genomic DNA extraction

DNA was prepared using a modified protocol from Rogowsky et al., (1991). Leaf sampling for Genomic DNA extraction was done either in 96 well-plate or individual 2ml Eppendorf tube extractions containing two glass balls and then frozen in liquid nitrogen, followed by grinding with mixer mill MM 200 (RETSCH, Germany) as a fine powder. The same protocol for DNA extraction was used for both plate and tube, except that for the plate, half of the volume from each reagent was added to each well in the plate compared to the Eppendorf tube.

The samples collected in the tube were lysed by adding 800 μ L of extraction buffer (1% N-Lauryl-Sarcosin, 100 mM Tris-HCl pH 8.0, 10 mM EDTA pH 8.0, 100 mM NaCl) and mixed vigorously by Vortex at high speed until all lumps have disappeared. And then, add 800 μ L of Phenol/Chloroform/Isoamyl alcohol (25:24:1) and shake for 5 min/300rpm, Followed by centrifugation at maximum speed for 10 min at 4°C. The supernatant was carefully transferred into a new 1,5 ml Eppendorf tube. The DNA was precipitated by adding 1/10 Vol of 3 M sodium acetate (pH 5.2), 3/4 Vol of cold Isopropanol, and mixed by gently inverting the Eppendorf tube until streaks of DNA were visible and then centrifuged at 14,800 rpm for 10 min at 4°C (tubes). The supernatant was removed from the tube, leaving the DNA pellet intact. The pellet was then washed with 800 μ l Of 70% Ethanol and vortexed to release the pellet from the bottom of the Eppendorf and precipitated by centrifugation at 14,800 rpm for 5 min at 4°C. And then, decant out the supernatant carefully and let the pellet dry completely at room temperature or 37 °C in an incubator. Finally, dissolve the pellet in 50 to 100 μ L of Tris-HCl (pH 8.0) containing 40 μ g/ml RNase and incubate at 37 °C for 1 hour, or incubate the tubes overnight on a shaker at 4°C.

2.3.2. Polymerase chain reaction (PCR) conditions

All PCR amplification assays in this experiment were done by using Taq DNA polymerase from Qigene and High-Fidelity DNA Polymerase PrimeSTAR GXL (TAKARA), Annealing temperatures in PCR protocols varied based on the melting temperature of the primer pairs.

The PCR condition was as follows for the Taq polymerase from Qigene:

5 μ l Q buffer and 2.5 μ l 10x reaction buffer and 1 μ l 5 μ M Forward Primer, 1 μ l 5 μ M Reverse Primer, 0.125 μ l Taq DNA Polymerase, and then complete the total volume with sterile water to 25 μ l reaction. The PCR amplification was performed under the following thermal cycle conditions: 94°C 3min, followed by 35 cycles of 94°C for 1min, 55-60 °C for 1 min, and an extension at 72 °C for 1 min per 1 kb, and then the final extension at 72°C 10mins, 4-10°C hold.

The High-Fidelity DNA Polymerase PrimeSTAR GXL (TAKARA) condition was carried out by using the following mixture:

10 μ l 5X PrimeSTAR GXL Buffer, and 4 μ l 1X dNTP Mixture (2.5 mM each), and 2 μ l 5 μ M Forward Primer, 2 μ l 5 μ M Reverse and PrimeSTAR GXL DNA Polymerase 0.5 μ l 1.25 U/50 μ l, and 1 μ l 500ng CDNA And, finally complete the final volume with Sterile purified water to 50 μ l. The thermal cycle conditions were done using either two steps or three steps. For two steps the cycle condition was as follows:

For 35 cycles at 98°C for 10 sec, 68°C for 20 sec/kb

For three-step the cycle condition was as follows:

35 cycles at 98°C for 10 sec, 55-60 for 10 sec, and 68°C for 20 sec/kb.

2.3.3. Purification of PCR products

PCR products were purified using column or 96 well plates using the PCR Purification Kit from (QIAGEN, Hilden, Germany) following the manufacturer's protocol.

2.3.4. Sequencing

The extracted plasmid DNA or purified PCR products were verified by sanger sequencing at the company LGC Genomics GmbH (Berlin, Germany). The sequencing results obtained were analyzed using the Sequencher software.

2.3.5. Southern Blotting

The T-DNA copy number in transgenic plants was determined by performing the Southern hybridization technique. 10 µg of genomic DNA (from transgenic or wild-type plant leaves) was digested by the appropriate (Selected based on the construct map). Digested DNA was electrophoretically initially for 1 hour at 100 volts and then left overnight at 20 volts, separated in 1% agarose gel using 1X TAE buffer (40 mM Tris-acetate, 1 mM EDTA, pH 8.2 to 8.4).

Afterward, the gel was placed in a container with the solution, and the container was gently agitated) for 5 min in 'Solution-I' (0.25 M HCl), two times of a 15 min treatment in 'Solution-II' (1.5 M NaCl and 0.5 M NaOH), and two times of a 15 min treatment in 'Solution-III' (0.5 M Tris-HCl and 3 M NaCl).

After each treatment, the gel was rinsed in distilled water. The fragmented DNA was transferred from the treated gel to a Hybond Nitrocellulose membrane by capillary transfer with 20X SSC buffer (175 g NaCl, 88 g Sodium citrate dihydrate in 1 L water). The transferred membrane was rinsed two times in 2X SSPE buffer (3.6 M NaCl, 0.2 M Sodium phosphate, and 0.02 M Disodium

EDTA, pH 8.0) for 10 min. A gene-specific probe for hygromycin phosphotransferase(*hpt*) was labeled with DIG as recommended by the supplier (Roche, Mannheim, Germany).

2.3.6. RNA extraction

Total RNA was extracted from the immature spikes at an early developmental stage and from leaves. The samples were collected in 2mL Eppendorf tubes containing two small glass balls in liquid nitrogen. Later on, the Frozen samples were ground with MM 200 (RETSCH, Germany) as a fine powder. The grounded samples were lysed by adding 500 μ L of TRIzol (Invitrogen, Thermo Fisher SCIENTIFIC) to each sample, vortexed twice for 45 seconds, and then incubated at RT for 5 min, followed by adding 100 μ l chloroform, shaking 15 times vigorously and incubate at RT for 3min. And then, samples were centrifuged at 13,000 rpm at 4°C for 15 min.

The aqueous phase of about 200 μ l was carefully transferred into a new 1.5 mL Eppendorf tube and to this added an equal volume of 2-propanol, mix, incubate at RT for 10min, followed by centrifugation at 13,000 rpm at 4°C for 10 min. The supernatant was decanted, leaving the RNA pellet intact to the bottom of the tube. The good RNA pellet should be colorless, and when the pellet is more visible, it indicates more contamination from DNA and protein. The pellet was then washed with 1 ml of 75% Ethanol and vortexed, centrifuged at 7000g for 5min at 4°C. And then, remove the supernatant carefully and let the pellet dry.

Finally, dissolve the pellet in 50 μ l of DEPC (diethylpyrocarbonate) treated water at 55-60°C, 10 min, short vortex, and short spin down. The RNA concentration was measured by using NanoDrop. Genomic DNA potentially present in RNA samples were removed by incubating the RNA with RNase-free DNase I (Roche, Germany) for 2 hours at 37°C using the following mixture per 50 μ l reaction: about ~50 μ g RNA sample, 5 μ l DNase I Buffer (10x), 2.0 μ l DNase I (5U/ μ l), 0.5 μ l

RNaseOUT (40U/ μ l), and complete the volume to 50 with DEPC treated water. And then, the DNase treatment was stopped by adding 2.5 μ l 0.5M EDTA per reaction Incubating at 80°C for 2 min and then completing the volume to 100 μ l by DEPC water.

The RNA was precipitated by adding 3.3 μ l of 3 M sodium acetate (pH 5.2) to each sample and mixed well by vortexing. Then, an equal volume of isopropanol was mixed by gently inverting the Eppendorf tube, then centrifuged at 15,000 rpm for 10 min at 4°C. The supernatant was decanted from the tube carefully, followed by washing of the recovered RNA Pellet with 75% ethanol by centrifugation at 7000g for 5min at 4°C.

Finally, the recovered RNA pellet was resuspended in 20-30 μ l diethylpyrocarbonate (DEPC) treated water. The RNA integrity was verified by electrophoresis of 1 μ l of total RNA on a 1.5 % standard agarose gel using freshly prepared 1x TAE buffer for 30 min at 120 Volte. Furthermore, RNA concentration was determined using Qubit Fluorometers from Invitrogen. All RNA solutions were treated with DEPC to prevent RNase contamination, and RNase-free tubes/tips were used. To ensure that the DNA was completely removed from the RNA samples, one essential PCR reaction was performed using 1 μ L RNA as a template and two pairs of primers spanning Intron-exon junction, if amplification was obtained, the DNase treatment had to be repeated.

2.3.7. Synthesis of cDNA

500 ng total RNA was reverse-transcribed into first-strand cDNA using superscript III RT (200U/ μ L) (Invitrogen) according to the manufacturer's instructions. By the addition of 0.5 μ L of 50 μ m oligo (dT), 0.5 μ L of 10 mM dNTPs mix to 500 ng RNA and complete the volume with double distal H₂O treated with DEPC to 5 μ L, and then incubate the samples at 65 °C for 5 minutes, then place on ice for at least 1 min. Prepare the following mixture, 2 μ L 5X first-strand

Buffer, 2 μ L 25mM MgCl₂, 0.5 μ L from 0.1 M DTT, 0.5 μ L RNaseout (40U/ μ l), 0.5 μ L superscript III RT (200U/ μ L).

And then, add this mixture to each sample, followed by gently mixing and short spin; afterward, the total mixture was incubated for 50 minutes at 50 °C. Then terminate the reaction at 85 °C for 5 minutes, chill on ice for a few seconds, and then collect the sample by a short centrifuge. As a final optional step, degrade the remaining non-converted RNA to cDNA by adding 1 μ l RNaseH to the total mixture and incubating at 37°C for 20 minutes.

2.3.8. Real-time PCR analysis

The gene expression analysis was relatively quantified using real-time PCR on the Applied Biosystems 7900HT Fast Real-Time PCR system (ThermoFisherSCIENTIFIC). Total RNA extracted from the leaf and Immature spike samples were reverse-transcribed as described above (see section 2.3.7) and the cDNA samples were used for real-time PCR. The RT-PCR reaction was performed by adding 5 μ L of SYBR® Green PCR Master Mix (ThermoFisherSCIENTIFIC), 1 μ L diluted 1:20 cDNA as a template, 2 μ L of each 0.5 μ M forward and reverse primers in 10 μ L total reaction volume.

The RT PCR amplification was performed under the following thermal cycle conditions: 50 °C for 2 min, 95 °C for 10 min, followed by 5 cycles touch down program to increase the specificity of the PCR, at 95 °C for 15 Sec and 60 °C for 1 min, during this touchdown program the annealing temperature will be decreased by 1 °C per cycle until the T_m of the primers is reached, and then 40 cycles of 95 °C for 15 Sec and 55 °C for 1 min and a final extension at 95 °C for 15 sec.

The gene-specific primers were designed using Primer3web <https://primer3.ut.ee/>. Genes like *Actin* were used for normalization. The expression analysis experiments were conducted using three biological replicates, and three technical replicates represented each biological replicate. The Relative expression levels of target genes were calculated by the $2^{-\Delta\text{CT}}$ method (Livak & Schmittgen, 2001), and the data was analyzed by SDS 2.3 software (Applied Biosystems®, ThermoFisherSCIENTIFIC). The sequences of the primers used for qRT-PCR are provided in Appendix Table 1.

2.4. Transgenic constructs generation and barley transformation

2.4.1. Generation of complementation constructs

2.4.1.1. Barley construct

The *HvRA2* gene was synthesized and subcloned into a pUC57 vector by GenScript Biotech (Netherlands). The total synthesized fragment is 3,483bp and contains 774 bp CDS, 2,166bp upstream region as a putative promoter, and 413 bp as 3'UTR. The synthesized fragment of about 3,483bp was released using EcoRI & BamHI and then subcloned into the pNOS vector. Later on, the gene cassettes were subcloned from the pNOS cloning vector using the restriction enzyme *SfiI* into the final destination binary vector p6i-d35S-TE9.

The resulting construct was transformed into the *Agrobacterium tumefaciens* strain *AGL1* by electroporation. PCR and restriction enzyme confirmed the presence of plasmids in selected clones, and finally, the positive clones were verified by Sanger sequencing before using it for stable transformation. The verified clone was transformed into barley *hvra2* mutants (BW NIL(*mull-1-a*) and *ra2* mutant in Golden Promise background) using *Agrobacterium tumefaciens* mediated transformation as described previously by Hensel et al., (2009).

2.4.1.2. Barley construct tagged with GFP

The same cloning approach used to make barley complementation constructs were applied here. *GFP* CDS was introduced into Barley complementation constructs once before the *HvRA2* CDS (N-terminus) and once after the *HvRA2* CDS (C-terminus). The verified clones were transformed into *ra2* mutant in the Golden Promise background. Only the verified transgenic plants with GFP at the C-terminus were analyzed. The transgenic plants with GFP at the N-terminus were not ready for analysis by the time of writing this manuscript

2.4.1.3 Wheat complementation construct

The 3,688 bp fragment containing the entire *HvRA2* coding region and the cis-regulatory regions of *RA2* from wheat (*Aegilops tauschii*), which contains 2,229 bp 5' upstream sequences as a putative promoter, and the 689-bp 3' downstream sequence, was synthesized, then it was cloned into pUC57 vector (Genscript). The same cloning approach was followed as described in the previous section (section 2.4.4.1) to be cloned into the final destination vector using the same restrictions site.

2.4.1.4. Sorghum complementation construct

The cis-regulatory regions of *RA2* from sorghum, which consists of 2,418 bp as a putative promoter and 974 bp as a 3' downstream sequence, were fused with *HvRA2* CDS following the same methods described above (section 2.4.4.1).

2.4.2. Promoter activity localization constructs

2.4.2.1. Generation of *RAMOSA2* promoter constructs fused with GFP

The same procedure used for cloning the complementation constructs was used for reporter constructs with *GFP*. The *GFP* coding sequence fused with *RA2* regulatory regions (promoter and

UTRs) from respective barley, sorghum, and wheat *RA2* genes were synthesized GenScript Biotech (Netherlands). The verified clones from the three constructs of the final destination vector p*6i*-d35S-TE9 were transformed into cv. Bowman. The GFP expression patterns were evaluated and quantified in the stable transgenic lines. The spike meristems from transgenic plants were collected at various developmental time points. The *GFP* fluorescence was analyzed using LSM 510 META or LSM780 confocal laser scanning microscopes (Carl Zeiss Microscopy GmbH, Jena, Germany).

2.4.2.2. Transient expression assay for promoter activity

For promoter activity analysis, the putative promoters of the *RA2* from barley, sorghum, and wheat were PCR amplified directionally cloned into the pENTR-D topo vector. Once a clone was verified by sequencing, we conducted an LR reaction for subcloning into the destination vector pGWL7 (<https://gatewayvectors.vib.be/collection/pgwl7>) for transient assays; each construct was co-transformed with a normalization vector. The CaMV35S::REN (*Rluc*) into rice protoplast, the transformed cells were incubated overnight at room temperature. The Firefly and Renilla luciferase activity was measured using the Dual-Luciferase Reporter Assay System (Promega, <http://www.promega.com/>). Rice protoplast isolation and transformation were carried out according to He et al., (2016).

2.4.3. RGEN design and vector construction

The *HvRA2* sequences of barley (cultivar Golden Promise) were downloaded from the IPK web blast (<http://webblast.ipk-gatersleben.de/barley/viroblast.php>). Moreover, based on this sequence, two single guide RNAs (gRNAs) were designed for targeting *HvRA2* using the web tool DESKGEN (<https://www.deskgen.com/>). According to (Budhagatapalli et al., 2016), the vector

construction was generated. A synthetic double-stranded oligonucleotide carrying the target-specific part of the gRNA was inserted between the OsU3 (RNA polymerase III) promoter and the downstream gRNA scaffold present in the monocot-compatible intermediate vector pSH91 (Budhagatapalli et al., 2016). Next, the fragment containing the expression cassettes of gRNA and Cas9 was introduced into the binary vector p6i-d35S-TE9 (DNA-Cloning-Service, Hamburg, Germany) using the *SfiI*, and the final destination vector was verified by sequencing before being delivered into *Agrobacterium tumefaciens* strain GV2260 using electroporation protocol.

2.5. Protein-protein interactions study

2.5.1. Yeast two-hybrid assay

A yeast-2-hybrid (Y2H) screening was conducted according to manual kits from (Takara /Clontech /Yeast maker TM Yeast transformation system two-user manual). The coding sequence of *HvRA2* (*HORVU.MOREX.r2.3HG0194160*) without activation domain was amplified using PrimeSTAR GXL (TAKARA). It was cloned in-frame into pGBKT7 into *EcoRI* and *PstI* site as bait by using the Vazyme ClonExpress Ultra One Step Cloning kit following the recommended protocol supplemented with the kit. The bait plasmid was confirmed by sanger sequencing before performing the transformation into Y2H Gold Yeast Strains of *Saccharomyces cerevisiae* supplied by the kit.

2.5.2. Construction of prey clones

The candidate genes that potentially interact with *HvRA2* were selected based on high-resolution gene expression data generated by (Thiel et al., 2021) to generate the Y2H prey clones., The prey clones were generated from a barley genotype Bowman cDNA from the spike at an early

developmental stage, and the full-length CDS of the corresponding genes were cloned into the pGADT7 vector.

Both prey and bait vectors were co-transformed in yeast Gold strain, and positive colonies were screened on a synthetic defined (SD) medium without leucine and tryptophan (SD/-Leu/-Trp). To select for the bait-prey interaction, a quadruple dropout medium lacking leucine, tryptophan, histidine, and adenine was used (SD/-Ade/-His/-Leu/-Trp).

All The primers which have been used in this experiment are listed in the Appendix, Table 1.

2.5.3 Preparation of yeast-competent cells

Protein-protein interaction assay was done by co-transformation of respective prey and bait plasmids as described in the Yeast Protocol Handbook (Takara/Clontech). One single colony of *S. cerevisiae* yeast matchmaker Gold was picked and inoculated into 3 mL of YPDA medium and incubated at 30°C with shaking at 250 rpm for 8-12 hours; 5 µl of pre-culture was transferred into 50 mL of fresh YPDA and incubated with shaking until OD 600 of 0.15-0.3, cells were harvested at 700 g for 5 min at room temperature, and resuspend the pellet in 100ml fresh YPDA and allowed to grow for 3-5 hours at 30°C with shaking at 250 rpm until OD600 of 0.4–0.5 was reached. Divided the culture into two falcon tubes and centrifuge at 700 g for 5 minutes. Discarded the supernatant and washed each pallet in 30 ml sterile deionized H₂O at 700 g for 5 min and then resuspended in freshly prepared sterile 1x TE/1x LiAc solution; the cells now are ready to be transformed with plasmid DNA.

2.5.4 Yeast co-transformation

For co-transformation, 0.1 µg DNA of bait and respective combination of prey candidate and 0.1 mg of denatured Yeast maker carrier DNA (Takara/Clontech) were added to 100 µL of competent cells. For this, freshly prepared 500 µL of PEG (polyethylene glycol)/LiAc solution transformation solution (40 % PEG (MW 3350) in 1x TE/1x LiAc solution) was added, mixed and incubated at 30°C for 30 min in the water bath with gently vortexing every 10 min. 20µl DMSO was added as recommended by the kit, and tubes were subsequently heat-shocked at 42°C for 15 minutes with gentle mixing every 5 min. The yeast-cell suspension was centrifuged for pelleting at high speed for 15 sec and resuspended in freshly prepared sterile 1X TE buffer, and spread gently on SD medium (SD/- Leu/-Trp) to select for both bait (PGBKT7) and prey (pGADT7) and incubated at 30°C for five days or until colonies appeared. For the negative control, different combinations with empty bait vector pGBKT7 and respective prey candidates were used, and of *HvRA2* bait vector with empty prey vector was tested for growth on SD/-Trp/-Leu medium by co-transformation.

Growth on (SD/-Ade/-His/- Leu/-Trp) indicates a potential interaction between the two respective proteins in the yeast cell. For this, a single colony was picked and resuspended on ddH₂O; 5 µL was spotted with a pipette on SD/-Trp/- Leu as a control for growth and on SD/-Ade/-His/-Leu/-Trp/ plate to select for protein-protein interactions. After 5 to 7 days of incubation at 30°C, plates were photographed. For autoactivation, control empty bait vector with prey candidate and empty prey vector with *HvRA2* bait was used and spotted on the same plates.

2.6. Basic cloning methods

2.6.1. Colony PCR

After preparing the PCR mixture and adding all the components except for the template, keep the PCR tube on ice and then use a 200µl pipette sterile tip to pick up the colony from the LB plate and then immerse it inside the PCR reaction; then, with the same tip touch the LB backup plate, after finish picking up a certain number of colonies, place the PCR tube into the PCR machine under the normal PCR cycle condition.

2.6.2. Isolation of plasmid DNA

The isolation of plasmid DNA from transformed *E. coli* or *Agrobacterium tumefaciens* cells was performed using either a manual method or using QIAGEN kit (Hilden, Germany) following the manufacturer's instructions. The isolation of plasmid DNA from transformed *E. coli* or *Agrobacterium tumefaciens* cells was performed using either a manual method or a QIAGEN kit (Hilden, Germany) following the manufacturer's instructions. The manual method starts by harvesting 3 ml overnight bacterial culture by centrifuge for 1 min at maximum speed. Then decant the supernatant, leaving the bacterial pellet as dry as possible. Add 300 µl of solution I (50mM Tris-Cl, pH 8.0, 10mM EDTA, 100ug/mL RNase A). Vortex vigorously to dissolve the pellet. Followed by adding 300 µl of freshly prepared solution II (0.2 N NaOH and 1% SDS). The tube was inverted six times and incubated at RT for 2 minutes. Afterward, 300 µl of solution III (3.0M potassium acetate, pH 5.5) was added to the tube, mixed gently, and incubated at room temperature for 5 min. Then Centrifuge for 10 minutes at full speed, and the supernatant was transferred to a fresh tube. Finally, add 600 µl isopropanol and invert the tube several times to precipitate the plasmid DNA. Followed by centrifugation for 15 minutes. The DNA pellet was washed with 500

μ l 70% ethanol, centrifuge for 5 min, left to dry at room temperature (RT), and dissolved in 50 μ l of TE.

2.6.2. DNA gel extraction

The DNA band was cut under UV from the gel and placed in an Eppendorf; purification of the band was carried out using Qiagen DNA Gel Extraction Kit. By using this Kit, DNA recovery was about 80%.

2.6.3. Digestion of plasmid DNA

Single or double enzyme digestions were performed to check whether the PCR product had been sub-cloned efficiently. The volume of the enzyme used was always less than 10% of the total volume of the digest to prevent inhibition of the reaction. The digestion reaction is carried out by mixing the following components in 1.5 ml microcentrifuge tubes, (~5 μ g) 3 μ l Plasmid DNA, 2 μ l Enzyme buffer, (20 units/ μ l) 0.5 μ l Enzyme, and complete the volume to 20 μ l by ddH₂O and then incubating at 37°C for 3 hours.

2.6.4. DNA ligation

The ligation reaction was carried out in 1.5 Eppendorf tubes by adding 1:3 linearized plasmid to the insert and then T4-DNA ligase (Thermo Fisher Scientific (Waltham, MA, USA) in a total volume of 10 μ L and incubating overnight at 4 °C.

2.6.4. Preparation of bacteria glycerol stocks

0.7 ml of the bacterial overnight culture was added to 0.3 ml of sterile 50% glycerol, mixed well, and frozen on liquid nitrogen. These glycerol stocks were stored at -80°C for further use.

2.6.5. Transformation of *E-coli* competent cells

The competent cells were taken out from -80°C and left to melt on ice for 30 min after adding 2.5 µl of the ligation reaction mixture, and gently mixed with the ligation mixture, afterward the cells were heat-shocked for 30 seconds at 42 °C in a water bath without shaking and immediately chilled on ice. 200 µl of room temperature SOC medium or LB without antibiotic were added, and the tube was shaken horizontally at 220 rpm for 1 hour to induce antibiotic resistance. The transformation was then spread on Luria–Bertani (LB) plates with appropriate antibiotics and left inverted overnight at 37°C.

To prepare SOC medium, add 20g/L of bacto-tryptone, 5g/L of bacto-yeast extract and 0.5 g/L of NaCl were dissolved in water. To this solution, 10 ml of 250 mM KCl were added, the pH was adjusted to 7, and then autoclaved. Before using this solution, 5 ml of sterile 2M MgCl₂ and 20 ml of 1M glucose were added.

2.6.6. Transformation of *Agrobacteria* competent cells

50 µL of competent cells were kept on ice, added 100-200 ng of binary vector (1-2 µL), incubated for 2 min, then transferred to the precooled cuvet. The transformation was performed at 25 µF, 400 Ω, and 2.5 kV on the Bio-Rad electroporator. One mL of SOC medium was immediately added to transformed cells and incubated at 28 °C with shaking for 2 h. Finally, 50 µL and 150 µL of the bacterial culture were placed on selection plates with appropriate antibiotics and incubated at 28 °C for 48 hours.

3.0 Results

Previous research studies have implied that the variation of inflorescence architecture might be due to spatiotemporal activity and dosage of the genes involved in inflorescence meristem specification (Hu et al., 2022; X. Jiang et al., 2022; Koppolu & Schnurbusch, 2019; Périlleux et al., 2019). For example, in species of the tribe *Andropogoneae* (Maize, Miscanthus, Sorghum), temporal changes in the expression pattern of *RA1* appear to be correlated with inflorescence morphologies. In the tassel of maize, the spikelet pairs form long branches at the base, and with the initiation of *RA1* expression, the long branches stop and form spikelet pairs instead of directly on the central axis of the tassel. The same pattern occurs in Miscanthus and Sorghum, where the expression of *RA1* correlates with the imposition of branch repression and determinate spikelet pair identity (Bortiri et al., 2006). Similarly, the expression of *RA2* in barley and wheat spikes initiated after the differentiation of SAM into leaf primordia at an early developmental stage of the spike (Koppolu et al., 2013). In contrast to the branched sorghum panicle, *RA2* was expressed transiently in the axillary meristem of the panicle (Bortiri et al., 2006). Such a spatial-temporal expression pattern of *RA2* among different species might be causative for producing a branchless spike (Koppolu & Schnurbusch, 2019). In addition to the timing, it was noticed that *RA2* was expressed at a higher amount in wheat spikes compared to barley at the early developmental stage (Koppolu & Schnurbusch, 2019). This higher level of *RA2* in wheat spikes might be the cause for limiting the number of the spikelet per rachis node to one compared to three spikelets per rachis node in the barley spike (Koppolu & Schnurbusch, 2019). To test these working hypotheses, transgenic complementation studies were carried out using promoter swapped transgenic lines consisting of *HvRA2* coding sequence fused with either barley, wheat, or sorghum *RA2* putative promoter sequences. Initially, we used these constructs to evaluate the degree of complementation

with different promoters transformed into the *vrs4* mutant BW-NIL(*mull.a*). However, due to the low transformation efficiency of BW-NIL(*mull.a*), we induced the mutations of *HvRA2* in the Golden Promise genotype(GP) (with high transformation efficiency) using the RNA guided endonuclease (RGEN) approach. Transgenic complementation experiments with the promoter swapped transgenic constructs were carried out using the *HvRA2* RGEN KOs created in the GP background. The phenotypic outcomes of these transgenic experiments were evaluated and discussed in the following sections.

3.1 Complementation into BW-NIL(*mull.a*) background

3.1.1 Identification of promoter regions, putative transcription factor binding sites, and cis-motif analysis

The sequences of the putative *RA2* promoter were compared between barley, sorghum, and wheat. About 2 -2.5 kb sequences were selected upstream of the start codon to increase the possibility of including most of the cis-regulatory elements related to the function and expression pattern of *RA2* during spike development. The selected promoter sequences were followed by in silico cis-motif analysis.

The putative 2,166 bp promoter sequence upstream of the start codon of *HvRA2* was aligned against the promoter sequences of the same region of *SbRA2* about 2,418 bp and *AetRA2* 2,228 bp, by using Global multiple alignments of finished sequences from mVISTA (https://genome.lbl.gov/cgi-bin/VistaInput?num_seqs=3), resulting in the identification of four conserved regions between the three selected promoter sequences and two conserved regions between wheat and barley (Figure 3.1.1). The total length of the conserved regions between the three promoters was about 677 bp with 72% identity while the total length of the conserved

sequence between wheat and barley was about 2,096 bp and showed higher homology of about 88%.

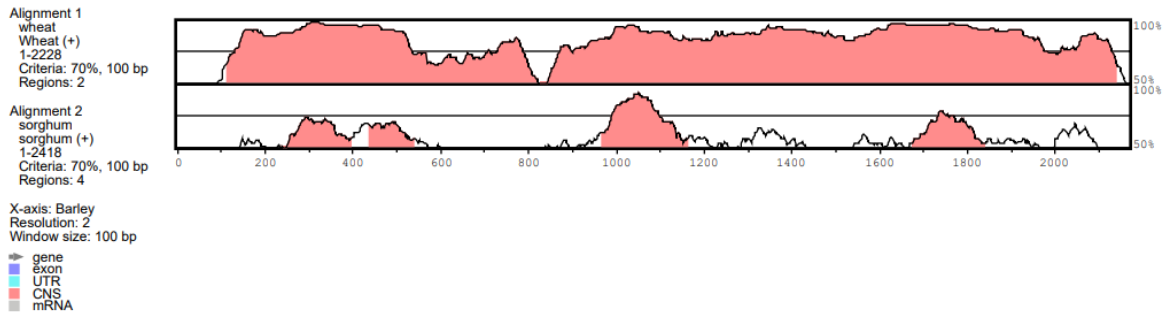


Figure 3.1.1 mVISTA plots of RA2 promoter sequence alignments between barley against wheat and sorghum, the conserved regions are colored and indicate >70% sequence similarity over 100-bp windows.

The potential promoter sequences were analyzed using the PlantPAN database (<http://plantpan.itps.ncku.edu.tw/>) and Plant Transcription Factor Database (<http://planttfdb.gao-lab.org/>); as a result of these analyses, several elements have been identified as predicted transcription factor binding sites (TFBSs) throughout the putative *RA2* promoter sequences of barley, sorghum, and wheat. While there was not much variation in the type of the TFBSs that have been predicted, there was a variation in the number of those predicted sites (Figure 3.1.2; and Appendix Table.2); these elements were mostly related to spike and floral organ development, in addition to light and phytohormone responses.

Evidently, there is a difference in the morphology of the spike between barley and wheat, despite the high similarity of *RA2* promoter sequences between barley and wheat. Therefore, we speculated that the morphological variation between species might be due to non-conserved regions in the *RA2* promoter sequences. By performing further analysis on non-conserved regions using the meme suite (Bailey et al., 2009), we identified one motif of about 50 bp. This motif was

present three times in wheat promoter sequences compared to two times in barley and only one time in sorghum (Figure 3.1.3 A; black box)

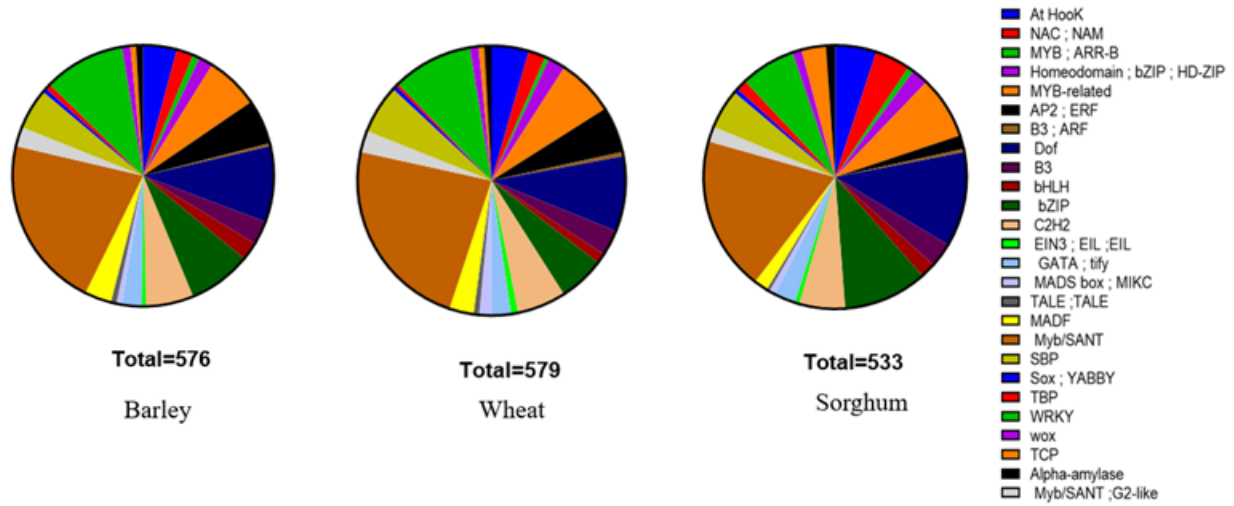


Figure 3.1.2. Frequency of the distribution of the putative TFBSs in *RAMOSA2* promoter between barley, sorghum, and wheat.

This motif was submitted to Tomotom tools (<https://meme-suite.org/meme/tools/tomtom>) utilizing the Arabidopsis DAP v1 database to locate a comparable pattern with a known function. This analysis revealed 53 matches with known motifs (listed in Appendix Table 3). The 53 matches were primarily related to two types of transcription factors: C2C2-Dof transcription factor (Figure 3.1.3 D) and the transcription factor of the vernalization gene 1 (*VRN1*) (Figure 3.1.3 C). The C2C2-Dof transcription factor functions as a transcriptional activator or repressor in plant growth and development (Yanagisawa, 2004), and the *VRN1* encodes a MADS-box transcription factor involved in the regulation of vernalization and flowering by regulating other gene expressions (Deng et al., 2015), suggesting some significance for the discovered 50 bp motif.

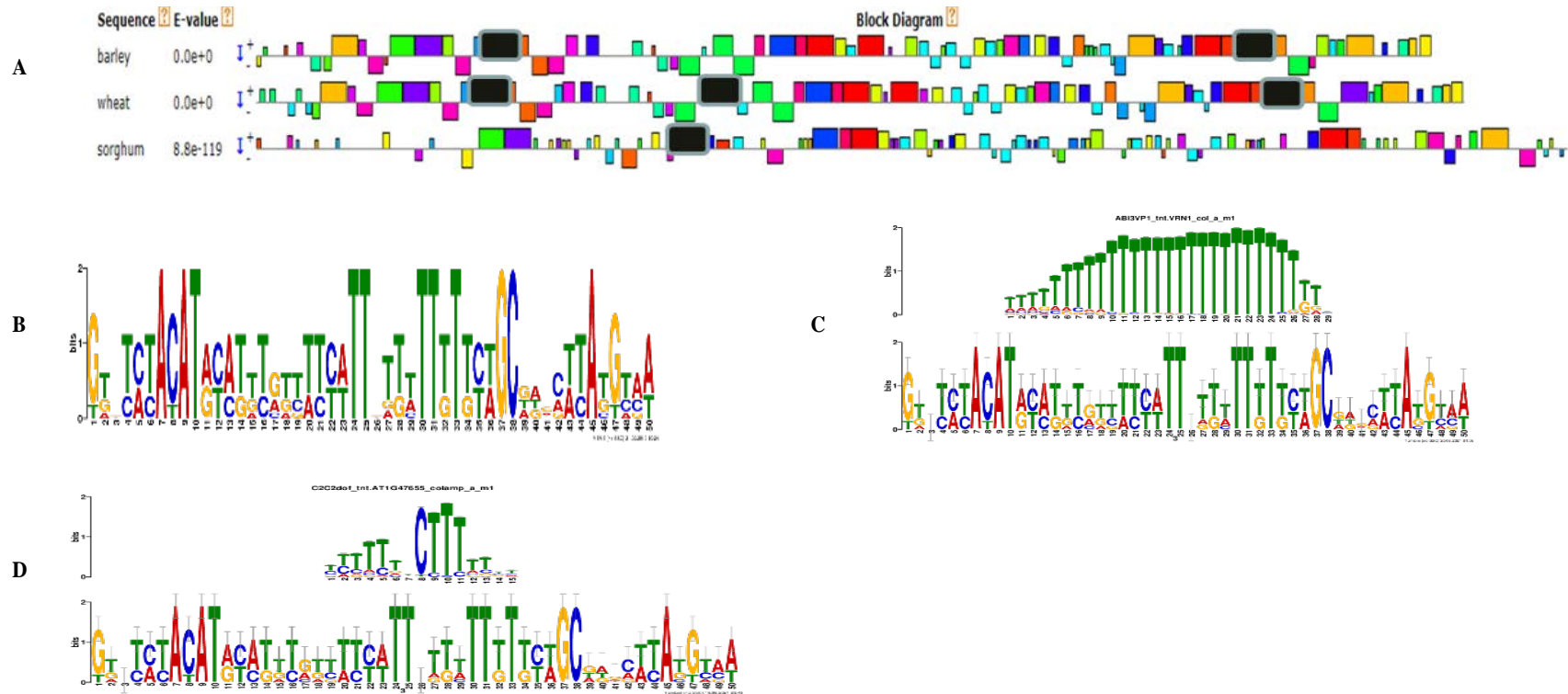


Figure 3.1.3. Motif analysis of RA 2 Promoters sequences; A) putative motif distributions in the selected RA2 promoters between barley, sorghum, and wheat, black boxes represent the discovered motif in the non-conserved region; B) WEBlogo for meme motif presented in black boxes; C) WEBlogos of *VRN1* motif created by Tomotom tools; D) WEBlogos of C2C2-Dof motif created by Tomotom tools.

To validate the function of this motif in barley, we have synthesized a complementation construct with the promoter of *RA2* from sorghum, having this motif inserted several times as illustrated in (Figure 3.1.4) to be transformed into *ra2* mutant. Currently, these constructs are in the transgenic pipeline for stable transformation into Golden Promise RGEN KOs of *HvRA2*.

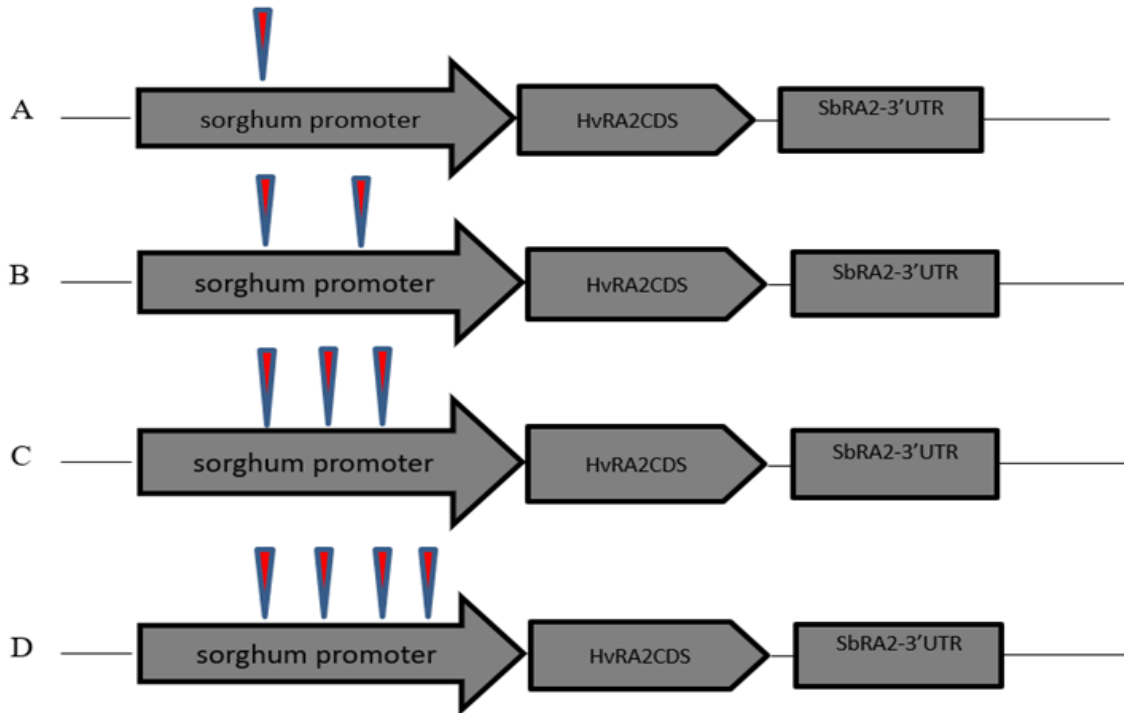


Figure 3.1.4. Schematic representation of complementation construct with modified sorghum promoter; Expression of *HvRA2* is driven by the sorghum *RA2* promoter after inserting the novel motif several times. A) motif inserted once B) motif inserted twice; C) motif inserted three times; D) motif inserted four Times.

3.1.2. The two-rowed wild-type condition was partially restored in *vsr4* mutant complemented with a native gene and parts of the endogenous barley promoter sequence

To study the function of *cis*-regulatory regions of *RA2* in shaping the inflorescences architecture of barley, wheat, and sorghum, we initially complemented the Bowman near-isogenic lines of

barley *ra2* mutants, i.e. BW-NIL(*mull.a*), in a transgenic experiment with the native *RA2* gene sequence of barley (CDS *HvRA2*) driven by a putative promoter of 2.16 kb upstream region of the *HvRA2* CDS, including the 5'UTR, and a 543bp sequence downstream of the *HvRA2* CDS, including the intron of the 3'UTR (Figure 3.1.2.1).



Figure 3.1.2.1. Schematic representation of complementation construct; Expression cassette of *HvRA2* driven by *HvRA2* promoter and *HvRA2* 3'UTR, (*hptII-i*) hygromycin phosphotransferase II as a selectable marker gene driven by (*deCaMV35S*) promoter. *E9-t*, *nos-t*: terminators; *LB* and *RB*: left and right borders.

After multiple attempts of barley transformation, we succeeded in obtaining one transgenic event using the BW-NIL(*mull.a*) background. The complemented transgenic plants from this line showed restoration of wild-type phenotype only at the base of the spike, for which the suppression of spikelet indeterminacy/spike branching and two-rowed condition was observed. However, the upper part of the spike showed fertile lateral spikelets, resulting in a six-rowed condition (Figure 3.1.2.2.), indicating that the phenotype complementation experiment in BW-NIL(*mull.a*) using the above mentioned construct appears to be incomplete.

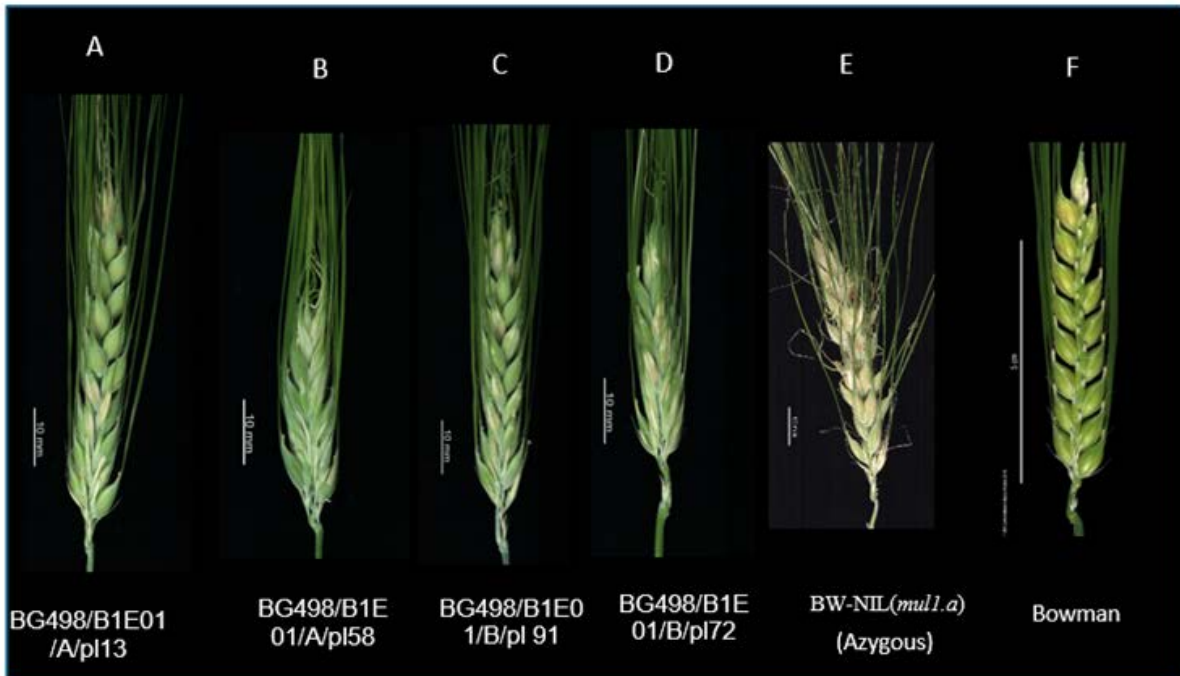


Figure 3.1.2.2 spike phenotype of the transgenic plant complemented with native *HvRA2* gene. (A-D) positive transgenic plants carrying pHvRA2::*HvRA2*CDS::*HvRA2*-3'UTR cassette showing only partial phenotype recovery in the basal spike.

3.1.3. Restoration of wild-type two-rowed condition in transgenic plant complemented with *HvRA2* CDS driven by *RA2* promoter from wheat

To investigate the putatively species-specific transcript differences of *RA2* (dosage and temporal gene expression), we generated transgenic lines expressing the full-length coding sequence of *HvRA2* under the regulation of the 2.22 kb upstream region of *AetRA2* (*Aegilops tauschii* L.) CDS as a putative promoter as well as 689 bp of sequence downstream of the *AetRA2* CDS as putative 3'UTR elements. (**Figure 3.1.3.1**). Again, this construct was introduced into the mutant BW-NIL(*mul1.a*) background.



Figure 3.1.3.1. Schematic representation of complementation construct with RA2 Regulatory element from wheat progenitor species *Aegilops tauschii*; expression cassette of *HvRA2*-CDS driven by *Ae. tauschii* putative RA2 promoter and 3'UTR , (hptII-i) hygromycin phosphotransferase II as a selectable marker gene driven by (deCaMV35S) promoter. E9-t, nos-t: terminators; LB and RB: left and right borders.

Three independent transgenic events were generated for this construct. All the plants from these events showed a complete restoration of a wild-type spike phenotype (two-rowed), with repression of spikelet indeterminacy/spike branching observed in *ra2* mutants (**Figure 3.1.3.2**). A few plants displayed overall stunted growth carrying stunted spikes with a relatively higher tiller number compared to control plants, and most of these plants had poor grain settings, or did not produce grain at all (**Figure 3.1.3.3**).

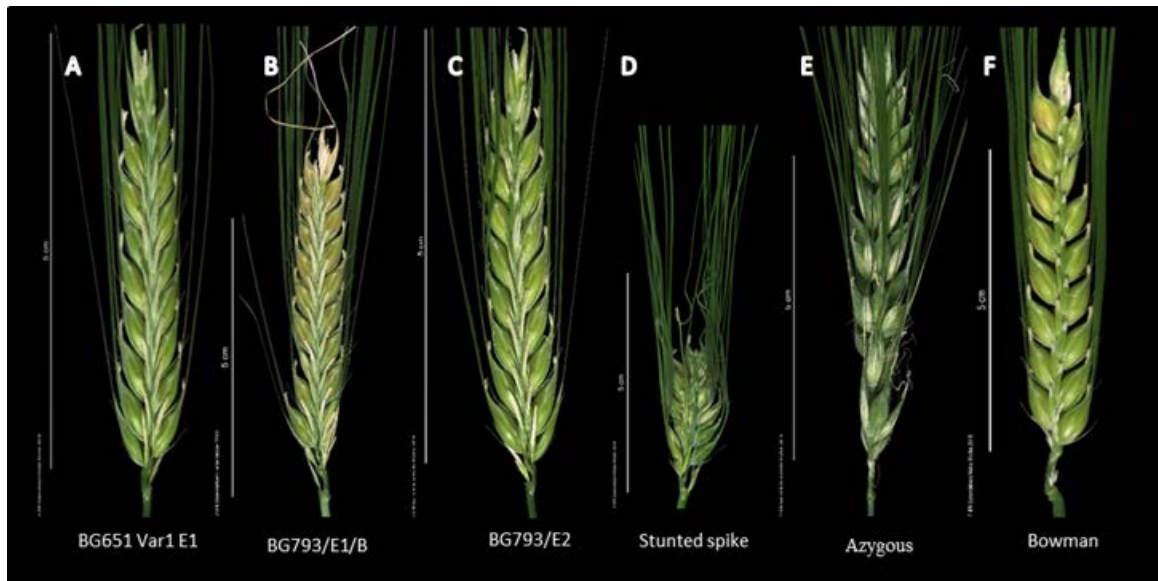


Figure 3.1.3.2. Spike Phenotypes of T2 generation barley pAetRA2::HvRA2CDS::Aet3'UTR transformants. (A-D) BW-NIL(*mull.a*) mutants complemented with pAetRA2::HvRA2CDS::Aet3'UTR construct. (D) stunted spike was observed on all three transgenic events. (E) Azygous, controls containing

no transgene were obtained from the segregating transgenic lines from the same experiment (F) wild type (two-rowed cv. Bowman

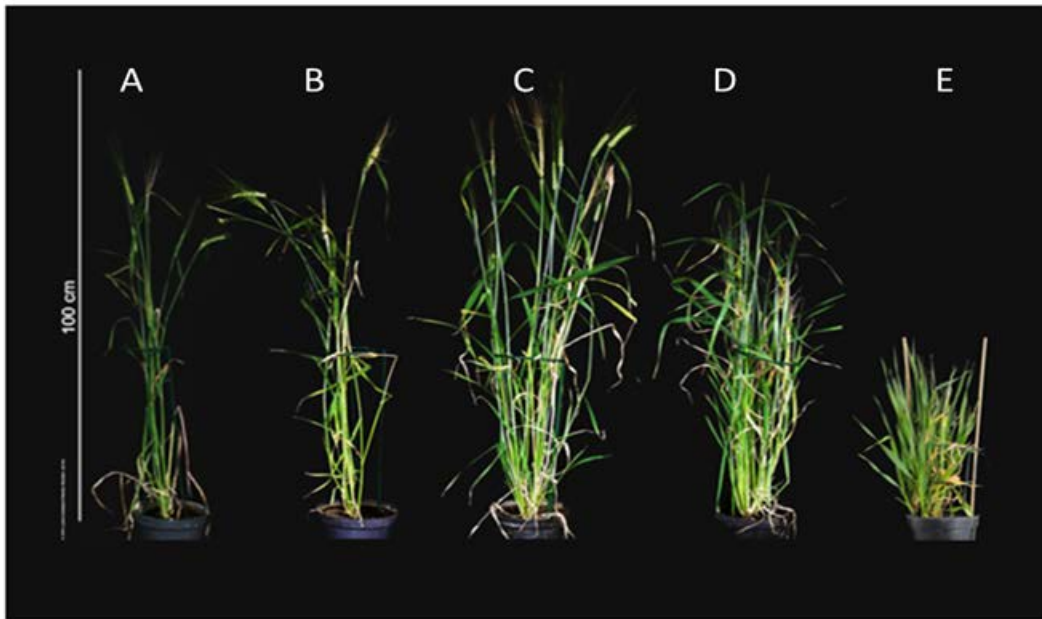


Figure 3.1.3.3 Effect of *HvRA2* expression driven by Wheat regulatory elements on plant height. (C-E) transgenic plants expressing *HvRA2* driven by Wheat regulatory elements compared to Azygous plants (B) and Wildtype (Bowman cultivar) (A)

3.1.4. The two-rowed condition was partially achieved in transgenic plant complemented with *SbRA2* CDS driven by *RA2* sorghum promoter

To study the effect of the temporal expression of *RA2* on inflorescence architecture between barley and sorghum, we synthesized a transgenic construct containing the *SbAR2* CDS, 2.41 kb of the putative promoter region, as well as 974 bp of sequence downstream of the CDS (*pSbRA2::SbRA2CDS::SbRA2* 3'UTR) (Figure 3.1.4.1F). The synthesized cassette was introduced into BW-NIL(*mull.a*) mutants. Transgenic lines from three independent events displayed partial restoration of the wild-type phenotype, where spikelet determinacy was obtained. However, LS sterility could only be observed at the base of the spike, whereas lateral spikelet fertility was recovered at the top of the spike (Figure 3.1.4.1). Moreover, we found stunted spikes similar to

plants transformed with the wheat construct, except that the stunted spikes from the sorghum constructs only partially complemented the wild-type phenotype. This result gave us an exciting indication that the expression of *SbRA2* might be delayed or lower resulting in only partial restoration of the wild-type two-rowed condition.



Figure 3.1.4.1. Spike Phenotypes of T2 generation of transformed barley plants with sorghum cassette pSbRA2::SbRA2CDS::Sb3'UTR. (A-C) BW-NIL(*mull.a*) mutants complemented with pSbRA2::SbRA2CDS::Sb3'UTR construct. (C) A partially complemented short spike was found in all transgenic lines transformed with the sorghum construct. (D) Azygous plant, (E) wild type (F) expression cassette of *SbRA2* driven by Sorghum bicolor RA2 putative promoter and 3'UTR.

3.1.5. There is no clear relation between copy number and spike phenotype and gene expression in the transgenic plants

To investigate whether the *RA2* transgene mRNA transcript levels regulate the observed phenotype in transgenic plants, the *RA2* expression in transgenic plants transformed with different constructs and control plants was quantified. *RA2* transcript levels were measured at different developmental

stages using qRT-PCR (**Figure 3.1.5.1**). The expression levels of *RA2* in plants transformed with sorghum constructs was significantly lower compared to the transformed plant with barley and wheat *RA2* constructs. However, there were no differences in the degree of complementation between the transformed plants with barley and sorghum constructs.

Despite the fact that the wheat construct complemented the wildtype phenotype, the *RA2* transcript levels were slightly lower in transformed plants than those with the barley construct. This result suggests that the complementation of the two-rowed condition in wheat might be achieved by TFs and other regulatory elements that bind to the TFBS located in the used parts of the wheat promoter, which is missing from the promoters of barley and sorghum.

Since the expression of transgenes can be affected by many factors, such as the positional effect of random integration, transgene zygosity, and copy number of the T-DNA insertion (Rajeevkumar et al., 2015), we checked the transgene copy number. To this end, we performed Southern-blot analyses (Figure 3.1.5.2) of transgenic barley plants with different *RA2* constructs (i.e. barley and wheat regulatory elements); for both of which only one copy of the T-DNA insertion was detectable, indicating single-copy transgene insertions. However, for plants transformed with the sorghum constructs, we found three to four copies, suggesting that higher copy numbers in these plants might have caused lower transcript levels due to well-known silencing effects(Čermák & Fischer, 2018; Holubová et al., 2018; Nagaya et al., 2005; Schubert et al., 2004).

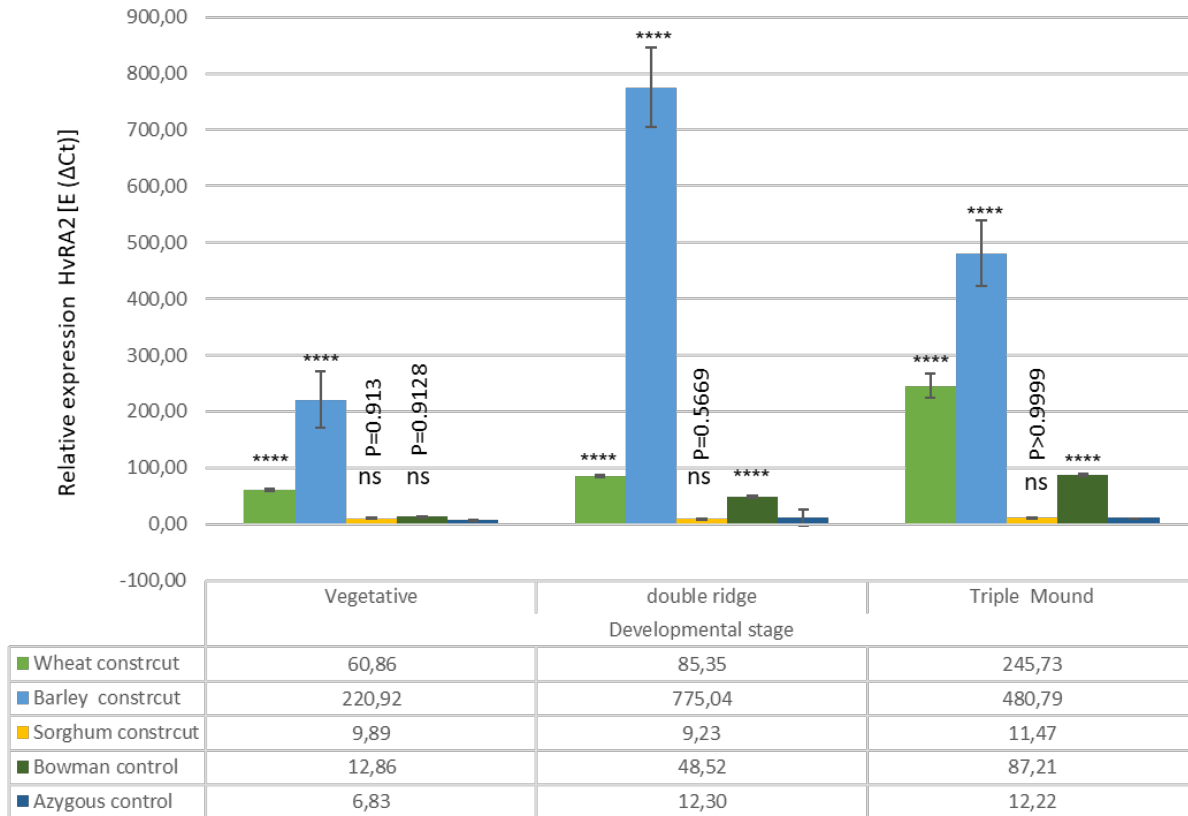
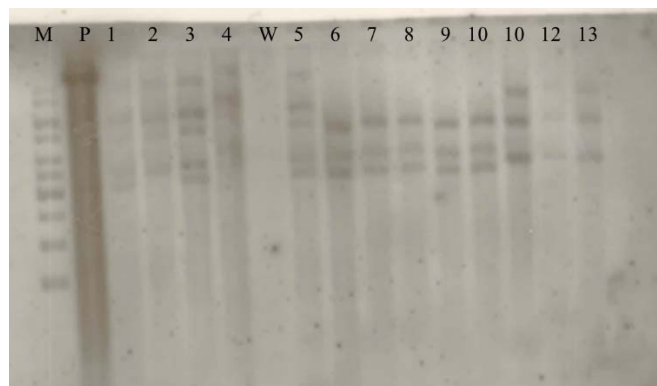
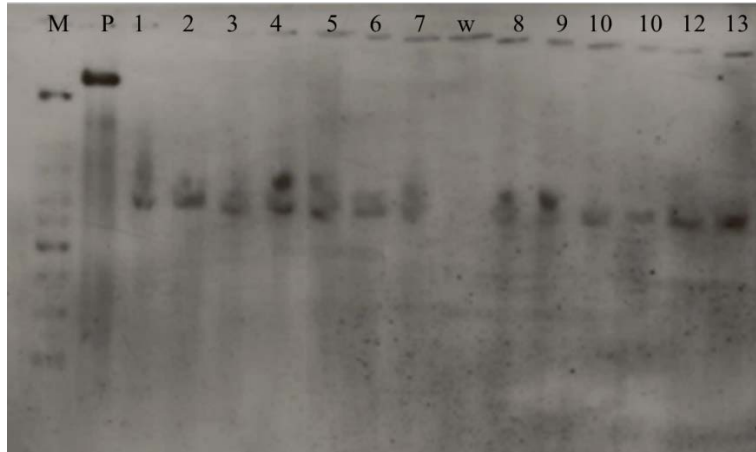


Figure 3.1.5.1 Expression analysis of *HvRA2* in T2 transgenic lines. Relative expression of *HvRA2* is determined by quantitative RT-PCR in the inflorescence spike at various spike developmental stages. Constitutively expressed *HvActin* was used for normalization, Error bars indicate S.D. of three replicates. The median ΔC_t values are given at the bottom of the graph. Significant differences were calculated based on a one-way ANOVA test followed by Tukey's multiple comparisons test compared with Azygous values., **** $P < 0.0001$, ns, non-significant the measured nonsignificant P value are presented in the histogram.

(A)



(B)



(C)

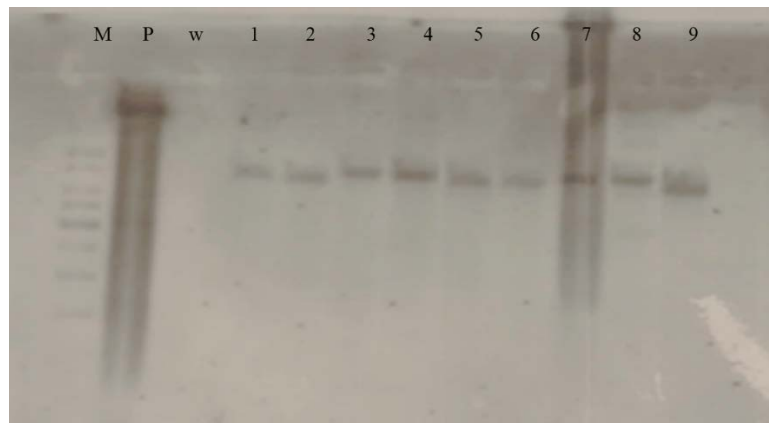


Figure 3.1.5.2: Southern blot analyses of T2 transgenic plants transformed with three different constructs. 20 μ g genomic DNA for each plant were digested with HindIII and the fragments were separated into 0.8% (w/v) agarose gel. hygromycin-specific probes were used for DNA hybridization (A) DNA blot for the transformed plants with sorghum construct (B) DNA blot for a transformed plant with the wheat construct (C) DNA blot for plants transformed with barley construct (M) marker (w) wildtype was used as a negative control, (p) plasmid as a positive control, numbers indicate the transgenic plant individual.

3.2. Constitutive overexpression of *RA2* studies

3.2.1 Constitutive overexpression of *AetRA2* CDS in wheat (cultivar Bobwhite) affects plant morphology

To test whether higher expression levels of *RA2* affect wheat plant architecture or the number of florets per spikelet, we generated constitutive overexpression constructs containing *AetRA2* CDS

driven by maize Ubiquitin promoter and then transformed them into wheat cv. Bobwhite; two transgenic events were obtained. The transgenic plants from the *RA2* overexpression construct were severely stunted with curly leaves and stunted spikes without grain set or grain filling (Figure 3.2.1.1). These results suggest that overly high levels of *RA2* may lead to premature meristem formation, which affects the overall plant development negatively.

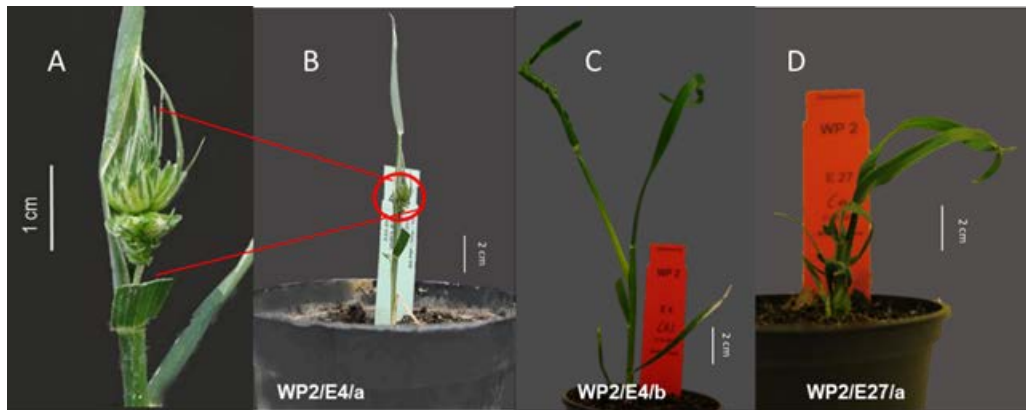


Figure 3.2.1.1 Constitutive over-expression of transgenic wheat plants. (A) the phenotype of the stunted spike with empty grains (B-D). The overall phenotype of overexpressing transgenic lines.

3.3. Promoter activity localization

3.3.1. Temporal gene expression pattern for GFP was not achieved under the cloned *RAMOSA2* promoters from barley, sorghum, and wheat

To study the temporal and spatial expression regulation of *RA2* across different spike developmental stages in barley, we synthesized *GFP* reporter constructs by fusing the *GFP* coding sequence to regulatory regions of *RA2* (promoter and UTRs, identical to those used for the complementation studies) of barley, sorghum, and wheat and transformed into barley cv. Bowman. We successfully generated four independent transgenic lines for each construct. The GFP fluorescence signal was observed ubiquitously in different developmental stages, even in other plant organs such as roots (Figure 3.3.1.1). All constructs showed overall GFP expression;

however, there was no noticeable difference between different types of promoters. These results indicate that the used regulatory regions from the respective species were most likely not complete and may be missing some important cis-regulatory elements related to the spatial and temporal gene expression.

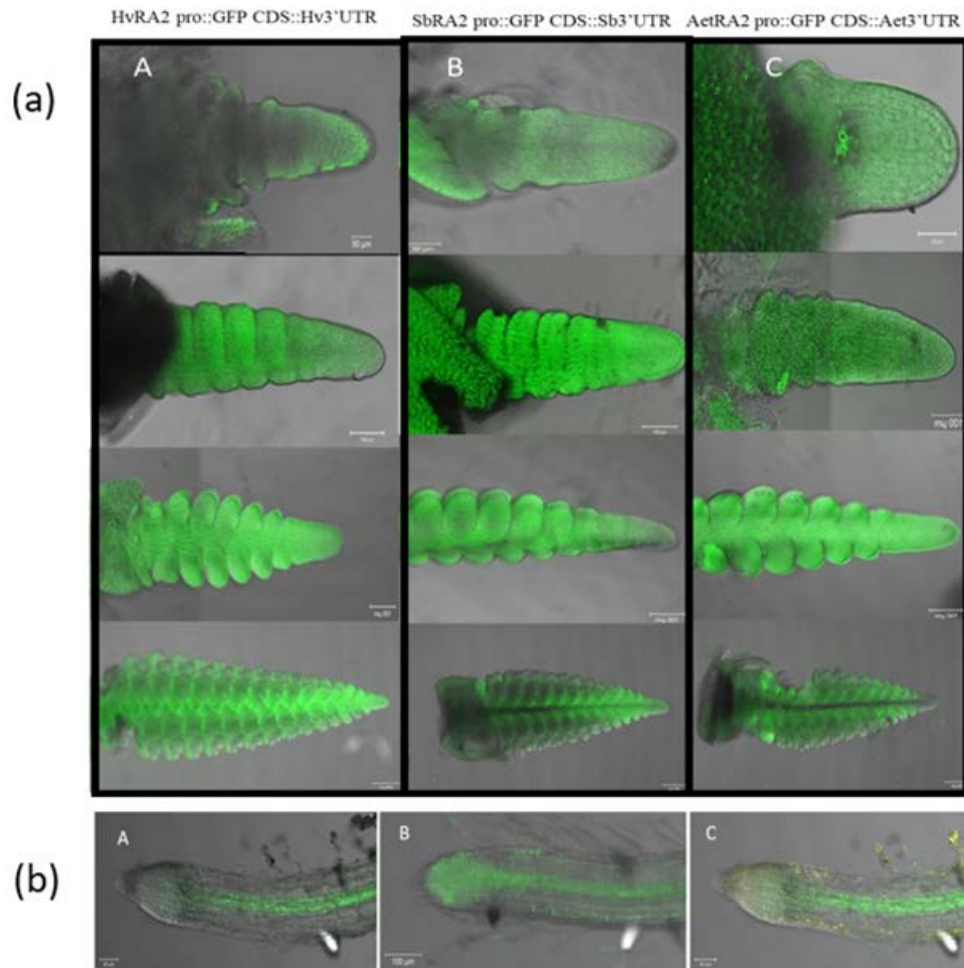


Figure 3.3.1.1. GFP fluorescence in spikes of transgenic plants with GFP driven by different putative promoter constructs. (a) Spike samples, (b) root tip samples (A) GFP fluorescence at different developmental stages in the spikes of transgenic plants carrying *pHvRA2*::GFP constructs, (B) for transgenic plants carrying *pSbRA2*::GFP constructs, and C) for plants carrying *pAetRA2*::GFP constructs.

3.3.2. No clear difference between the amount of expression of the *GFP* driven by different promoters

Since no distinct temporal or spatial expression patterns were detected using the selected species-specific promoter sequences, we investigated whether there is a difference in the overall expression strength or dosage of *RA2* modulated by putative *RA2* promoters of barley, sorghum, and wheat. Hence, we used quantitative real-time RT-PCR to measure the expression level of *GFP* driven by different *RA2* promoters at the stamen primordia stage. The expression analysis was carried out in four independent transgenic lines for each construct. We found that the *GFP* expression levels driven by *RA2* promoters were significantly higher from barley and wheat in some lines compared to the expression level of *GFP* under the putative sorghum promoter, which was most lowly expressed in all tested lines (**Figure.3.3.2.1**).

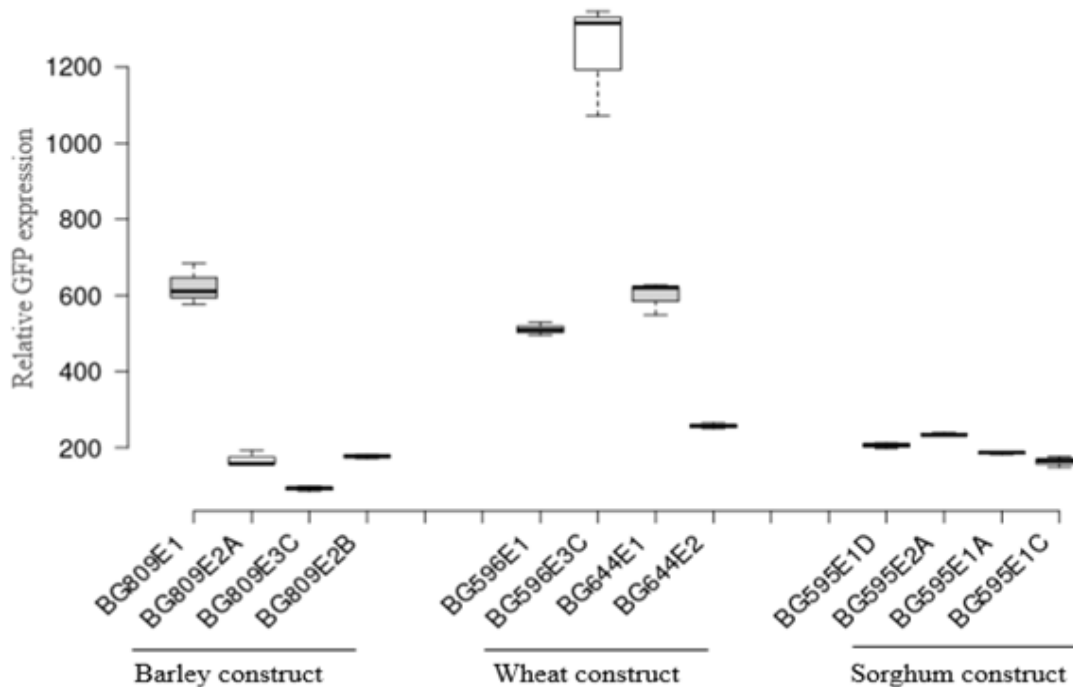


Figure 2.3.2.1 The expression level of *GFP* driven by different promoters; immature spikes were sampled at the stamen primordia stage for qRT-PCR, from transgenic plants transformed with three

different constructs for the respective species under the study; for each construct, four independent transgenic lines were used, the constitutively expressed *HvActin* was used for normalization; the bottom and top of box plots represent the first and third quartile, respectively, the middle line is the median, and the whiskers represent the maximum and minimum values, and the remaining outlier data points are shown as individual dots; the data are representative of 3 independent biological replicates.

3.4. Knockout of *HvRA2* in barley Golden Promise cultivar mediated by RNA-guided endonuclease (RGEN) approach.

Due to the difficulty of obtaining sufficient transgenic lines from the initial complementation experiments into the Bowman near-isogenic lines of barley *ra2* mutants, i.e. BW-NIL(*mull.a*), we therefore created *ra2* mutants in the cv Golden Promise (model genotype for efficient, stable transformation) by using a high-efficiency RGEN approach. The *ra2* mutant produced in the Golden Promise background will be a valuable resource for further functional analyses, and for a better understanding of the molecular mechanisms underlying spike inflorescence development in barley.

3.4.1 Targeted mutagenesis of *HvRA2* induced by RGEN in the T0 generation

To knock out *RA2* in barley cv Golden Promise, two gRNAs were designed at the beginning of the protein-coding region of *RA2* before the conserved region in the LOB domain (Figure 3.4.1.1). The two gRNAs were assembled into two different constructs by integrating each respective sequence of the selected gRNAs between the rice u3 promoter and the gRNA scaffold (Figure 3.4.1.2). The resulting vectors were confirmed by Sanger-sequencing before introducing into the barley genome. The two constructs were co-transformed into immature barley embryos via *Agrobacterium*-mediated transformation. About 54 regenerated primary plantlets exhibited hygromycin resistance, six plantlets could not survive after transfer to soil, and the remaining 48

primary transformants plantlet were evaluated for the presence of cas9 and the presence of mutations in the target sequence using PCR analysis and sanger sequences

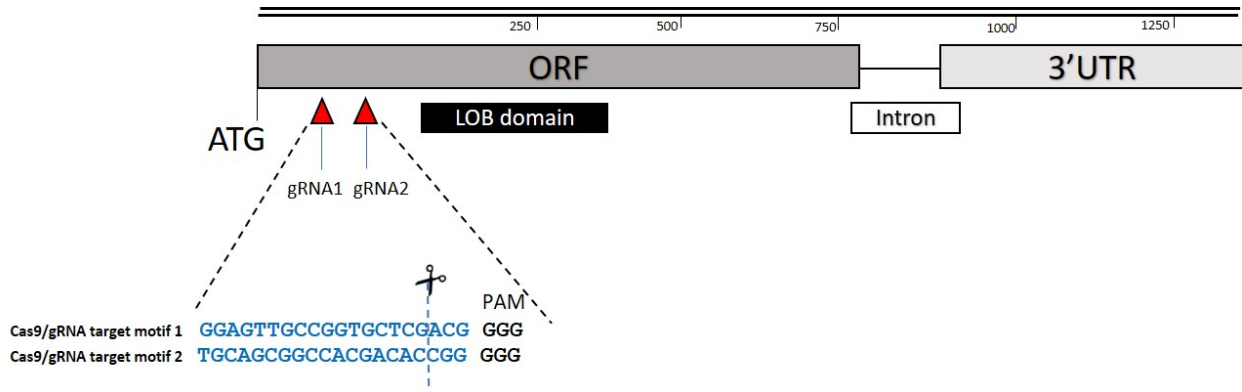


Figure 3.4.1.1: Schematic of *HvRA2* gene structure and Cas9/gRNA target motif. *HvRA2* contains only one exon and one intron. The protospacer adjacent motif (PAM) (GGG) sequence is indicated in black and the target site of the guide is indicated in blue. The scissors indicate the expected cleavage site.

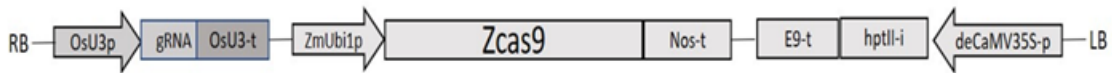


Figure 3.4.1.2: Schematic representation of the RGEN T-DNA in binary vector used for plant transformation. The expression of cas9 is driven by the maize Ubiquitin 1 promoter (ZmUbi1p), and the gRNA is driven by the rice U3 Polymerase III promoter (OsU3-p), (hptII-i) hygromycin phosphotransferase II as a selectable marker gene driven by (deCaMV35S) promoter. E9-t, nos-t, OsU3-t: terminators; LB and RB: left and right borders.

3.4.1.1 Analysis of putative *ra2* mutant plants in T0 generation

The targeted *HvRA2* region was amplified by PCR for DNA sequencing. The amplified *HvRA2* sequences were aligned against the *HvRA2* gene sequence in the wild-type Golden Promise. The sequencing data revealed four mutants for target one, six mutants for target two, and

six mutants located on both targets; overall, 16 independent mutations occurred in 40 stable transgenic lines carrying active cas9. We could not find transgene-free mutants in T0 lines. The data for this initial screening are summarized in (Table 3.4.1.1.1).

Table 3.4.1.1.1: summary of the analysis of putative *ra2* mutant plants in T0 generation.

gRNA	total number of lines	No. of plant with mutation	No. of positive with PCR for Cas9/Hyg	Mutation rate %	Homozygous mutants	Total No. of plants showing the mutant phenotype
Target 1	54	4	40	40%	1	2
Target 2		6				
Target 1&2		6				

The targeted mutation in T0 was heterozygous for all lines, except a homozygous mutant, which didn't produce grains; due to this fact, the *ra2* mutant phenotype was only seen in two lines on a few spikes, and it was quite weak. (Figure 3.4.1.1.1)



Figure 3.4.1.1.1. The phenotype of T0 *ra2* mutant created by RGEN approach: different Mature spikes from different events showing various levels of branch proliferation and indeterminate of the triple spikelet compared to the wildtype.

Mutagenesis efficiency among T0 regenerated plantlets was about 50 % due to the simultaneously expressed two gRNAs targeting *HvRA2*. Most of the mutations were indels (insertion/deletions) or single base substitution, located at 3-7 nucleotides upstream of the PAM sequence. (**Figure 3.4.1.1.2**)

(A)

Plant ID	PAM	Target site 1	Target site 2	PAM	zygosity
WT	←	CGTCGAGCACCGGCAACTCCATCGTCTCCGTGGTGGTTGCAGCGGCCACGACACCGGGCCGGGGCCCGCTG	CGTCGAGCACCGGCAACTCCATCGTCTCCGTGGTGGTTGCAGCGGCCACGACACCGGGCCGGGGCCCGCTG	→	
BG757E1 T0	←	CGTCGAGCACCGGCAACTCCATCGTCTCCGTGGTGGTTGCAGCGGCCACGACACCGGGCCGGGGCCCGCTG	CGTCGAGCACCGGCAACTCCATCGTCTCCGTGGTGGTTGCAGCGGCCACGACACCGGGCCGGGGCCCGCTG	→	het
BG757E2 T0	←	CGTCGAGCACCGGCAACTCCATCGTCTCCGTGGTGGTTGCAGCGGCCACGACACCGGGCCGGGGCCCGCTG	CGTCGAGCACCGGCAACTCCATCGTCTCCGTGGTGGTTGCAGCGGCCACGACACCGGGCCGGGGCCCGCTG	→	het
BG757E26 T0	←	CGTCGAGCACCGGCAACTCCATCGTCTCCGTGGTGGTTGCAGCGGCCACGACACCGGGCCGGGGCCCGCTG	CGTCGAGCACCGGCAACTCCATCGTCTCCGTGGTGGTTGCAGCGGCCACGACACCGGGCCGGGGCCCGCTG	→	het
BG757E27 T0	←	CGTCGAGCACCGGCAACTCCATCGTCTCCGTGGTGGTTGCAGCGGCCACGACACCGGGCCGGGGCCCGCTG	CGTCGAGCACCGGCAACTCCATCGTCTCCGTGGTGGTTGCAGCGGCCACGACACCGGGCCGGGGCCCGCTG	→	het
BG757E28 T0	←	CGTCGAGCACCGGCAACTCCATCGTCTCCGTGGTGGTTGCAGCGGCCACGACACCGGGCCGGGGCCCGCTG	CGTCGAGCACCGGCAACTCCATCGTCTCCGTGGTGGTTGCAGCGGCCACGACACCGGGCCGGGGCCCGCTG	→	het
BG757E29 T0	←	CGTCGAGCACCGGCAACTCCATCGTCTCCGTGGTGGTTGCAGCGGCCACGACACCGGGCCGGGGCCCGCTG	CGTCGAGCACCGGCAACTCCATCGTCTCCGTGGTGGTTGCAGCGGCCACGACACCGGGCCGGGGCCCGCTG	→	het
BG757E31 T0	←	CGTCGAGCACCGGCAACTCCATCGTCTCCGTGGTGGTTGCAGCGGCCACGACACCGGGCCGGGGCCCGCTG	CGTCGAGCACCGGCAACTCCATCGTCTCCGTGGTGGTTGCAGCGGCCACGACACCGGGCCGGGGCCCGCTG	→	het
BG757E34 T0	←	CGTCGAGCACCGGCAACTCCATCGTCTCCGTGGTGGTTGCAGCGGCCACGACACCGGGCCGGGGCCCGCTG	CGTCGAGCACCGGCAACTCCATCGTCTCCGTGGTGGTTGCAGCGGCCACGACACCGGGCCGGGGCCCGCTG	→	het
BG757E37 T0	←	CGTCGAGCACCGGCAACTCCATCGTCTCCGTGGTGGTTGCAGCGGCCACGACACCGGGCCGGGGCCCGCTG	CGTCGAGCACCGGCAACTCCATCGTCTCCGTGGTGGTTGCAGCGGCCACGACACCGGGCCGGGGCCCGCTG	→	het
BG757E40 T0	←	CGTCGAGCACCGGCAACTCCATCGTCTCCGTGGTGGTTGCAGCGGCCACGACACCGGGCCGGGGCCCGCTG	CGTCGAGCACCGGCAACTCCATCGTCTCCGTGGTGGTTGCAGCGGCCACGACACCGGGCCGGGGCCCGCTG	→	het
BG757E47 T0	←	CGTCGAGCACCGGCAACTCCATCGTCTCCGTGGTGGTTGCAGCGGCCACGACACCGGGCCGGGGCCCGCTG	CGTCGAGCACCGGCAACTCCATCGTCTCCGTGGTGGTTGCAGCGGCCACGACACCGGGCCGGGGCCCGCTG	→	het
BG757E48 T0	←	CGTCGAGCACCGGCAACTCCATCGTCTCCGTGGTGGTTGCAGCGGCCACGACACCGGGCCGGGGCCCGCTG	CGTCGAGCACCGGCAACTCCATCGTCTCCGTGGTGGTTGCAGCGGCCACGACACCGGGCCGGGGCCCGCTG	→	het
BG757E52 T0	←	CGTCGAGCACCGGCAACTCCATCGTCTCCGTGGTGGTTGCAGCGGCCACGACACCGGGCCGGGGCCCGCTG	CGTCGAGCACCGGCAACTCCATCGTCTCCGTGGTGGTTGCAGCGGCCACGACACCGGGCCGGGGCCCGCTG	→	het
BG757E54 T0	←	CGTCGAGCACCGGCAACTCCATCGTCTCCGTGGTGGTTGCAGCGGCCACGACACCGGGCCGGGGCCCGCTG	CGTCGAGCACCGGCAACTCCATCGTCTCCGTGGTGGTTGCAGCGGCCACGACACCGGGCCGGGGCCCGCTG	→	het

(B)

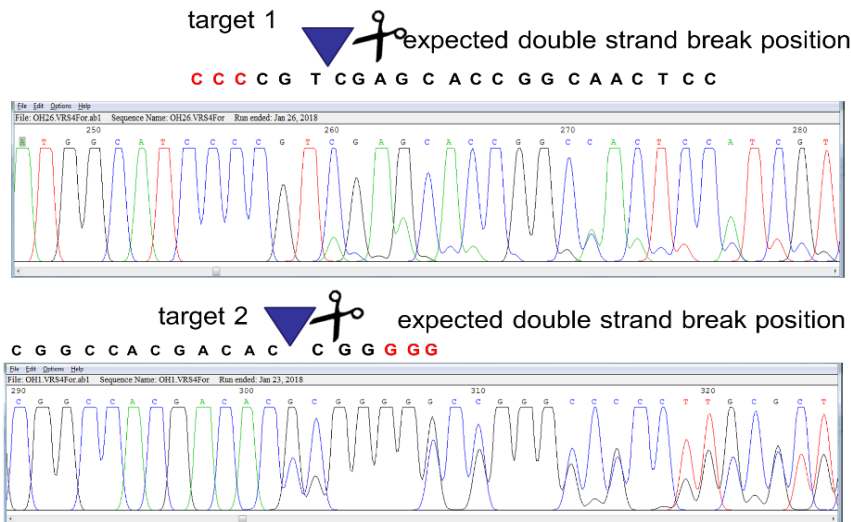


Figure 3.4.1.1.2 Mutation types in primary transgenic plants. (A) The sequence marked in blue represents the gRNA-specific part of the targeted motif, the underlined sequences indicate the protospacer-

adjacent motif PAM. Lines ID are given on the left-hand side, deletions are highlighted with red dashes and inserted nucleotides with subscript red letters, single-base substitutions are shown in red type, and zygosity status of the mutants are given on the right side either heterozygous(het) or homozygous (hoz) (B) an example of typical chromatogram which shows the position of a double-strand break at the target site, causing INDEL mutation in T₀ detected 3 bp upstream the PAM motif shown in red type

3.4.2. Analysis of targeted mutagenesis of *HvRA2* in the T1 generation

The progeny of 9 lines from T₀ plants were selected for further analysis; 10 to 20 grains per line were germinated in the S1 greenhouse. DNA was extracted from leaf material, and the target sites were sequenced. Most InDel mutations in T₀ plants were transmitted to the T₁ generation. However, additional mutation types were discovered in T₁ due to T₀ plants' heterozygosity and the presence of active gRNA/Cas9 transgene, which caused new mutation types at target locations. For example, the progeny analysis of the BG757 E52 line in T₁ revealed a 60 bp deletion in 14 plants, six plants carried 1 bp insertion (+A), and one plant had several InDel mutations, whereas the T₀ mother plants had a 56 bp deletion, the complete segregation pattern for this line is illustrated in (Figure 3.4.2.1A).

Another example of an unusual segregation pattern was found in line BG757 E23 line, whereby the mutant in T₀ was not transferred to T₁, and the offspring showed various indel/bp substitution mutants in T₁, which were not detected in the mother plant. These results indicate that this line had a chimeric mutation (Figure 3.4.2.1B).

A

Plant ID	PAM	Target site 1	Target site 2	PAM	zygosity	T-DNA		
WT	GCCGGCAATGGCAT	<u>CCC</u> CGTCGAGCACCGGCAACTCC	ATCGTCTCCGTGGTGGT	TGCAGCGGCCACGACACCGG	GGG	CCGGGGCGCCGTG	het	+
BG757E52 T0		<u>CCC</u> CGTCGAGCACCGGCAACTCC					het	-
BG757E52 PL11T1		<u>CCC</u> CGTCGAGCACCGGCAACTCC					het	-
BG757E52 PL3T1		<u>CCC</u> CGTCGAGCACCGGCAACTCC					het	-
BG757E52 PL5T1		<u>CCC</u> CGTCGAGCACCGGCAACTCC					het	-
BG757E52 PL7T1		<u>CCC</u> CGTCGAGCACCGGCAACTCC					het	-
BG757E52 PL8T1		<u>CCC</u> CGTCGAGCACCGGCAACTCC					het	-
BG757E52 PL9T1		<u>CCC</u> CGTCGAGCACCGGCAACTCC					het	-
BG757E52 PL10T1	GCCGGCAATGGCAT	<u>CCC</u> CGTCGAGCACCGGCAACTCC	ATCGTCTCCGTGGTGGT	TGCAGCGGCCACGACACCGG	GGG	CCGGGGCGCCGTG	hoz	-
BG757E52 PL11T1	GCCGGCAATGGCAT	<u>CCC</u> CGTCGAGCACCGGCAACTCC	ATCGTCTCCGTGGTGGT	TGCAGCGGCCACGACACCGG	GGG	CCGGGGCGCCGTG	hoz	-
BG757E52 PL12T1	GCCGGCAATGGG	<u>CCC</u> CGTCGAGCACCGGCAACTCC	ATCGTCTCCGTGGTGGT	TGCAGCGGCCACGACACCGG	GGG	CCGGGGCGCCGTG	het	+
BG757E52 PL13T1		<u>CCC</u> CGTCGAGCACCGGCAACTCC					hoz	+
BG757E52 PL14T1		<u>CCC</u> CGTCGAGCACCGGCAACTCC					het	+
BG757E52 PL15T1		<u>CCC</u> CGTCGAGCACCGGCAACTCC					het	+
BG757E52 PL16T1		<u>CCC</u> CGTCGAGCACCGGCAACTCC					hoz	+
BG757E52 PL17T1		<u>CCC</u> CGTCGAGCACCGGCAACTCC					hoz	-
BG757E52 PL18T1	GCCGGCAATGGCAT	<u>CCC</u> CGTCGAGCACCGGCAACTCC	ATCGTCTCCGTGGTGGT	TGCAGCGGCCACGACACCGG	GGG	CCGGGGCGCCGTG	hoz	+
BG757E52 PL19T1		<u>CCC</u> CGTCGAGCACCGGCAACTCC					hoz	+
BG757E52 PL20T1	GCCGGCAATGGCAT	<u>CCC</u> CGTCGAGCACCGGCAACTCC	ATCGTCTCCGTGGTGGT	TGCAGCGGCCACGACACCGG	GGG	CCGGGGCGCCGTG	hoz	-
BG757E52 PL21T1		<u>CCC</u> CGTCGAGCACCGGCAACTCC					het	-
BG757E52 PL22T1	GCCGGCAATGGCAT	<u>CCC</u> CGTCGAGCACCGGCAACTCC	ATCGTCTCCGTGGTGGT	TGCAGCGGCCACGACACCGG	GGG	CCGGGGCGCCGTG	hoz	+
BG757E52 PL23T1		<u>CCC</u> CGTCGAGCACCGGCAACTCC					het	+
BG757E52 PL24T1	GCCGGCAATGGCAT	<u>CCC</u> CGTCGAGCACCGGCAACTCC	ATCGTCTCCGTGGTGGT	TGCAGCGGCCACGACACCGG	GGG	CCGGGGCGCCGTG	hoz	+

B

Plant ID	PAM	Target site 1	Target site 2	PAM	zygosity	T-DNA		
WT	GCCGGCAATGGCAT	<u>CCC</u> CGTCGAGCACCGGCAACTCC	ATCGTCTCCGTGGTGGT	TGCAGCGGCCACGACACCGG	GGG	CCGGGGCGCCGTG	het	+
BG757E23 T0		<u>CCC</u> CGTCGAGCACCGGCAACTCC					het	+
BG757E23 PL11T1		<u>CCC</u> CGTCGAGCACCGGCAACTCC					het	+
BG757E23 PL3T1		<u>CCC</u> CGTCGAGCACCGGCAACTCC					het	+
BG757E23 PL4T1		<u>CCC</u> CGTCGAGCACCGGCAACTCC					het	+
BG757E23 PL5T1		<u>CCC</u> CGTCGAGCACCGGCAACTCC					het	+
BG757E23 PL7T1		<u>CCC</u> CGTCGAGCACCGGCAACTCC					hoz	+
BG757E23 PL8T1		<u>CCC</u> CGTCGAGCACCGGCAACTCC					hoz	+
BG757E23 PL9T1		<u>CCC</u> CGTCGAGCACCGGCAACTCC					het	+
BG757E23 PL10T1		<u>CCC</u> CGTCGAGCACCGGCAACTCC					hoz	+
BG757E23 PL14T1		<u>CCC</u> CGTCGAGCACCGGCAACTCC					het	+
BG757E23 PL15T1		<u>CCC</u> CGTCGAGCACCGGCAACTCC					hoz	-
BG757E23 PL16T1		<u>CCC</u> CGTCGAGCACCGGCAACTCC					hoz	-
BG757E23 PL17T1		<u>CCC</u> CGTCGAGCACCGGCAACTCC					hoz	-
BG757E23 PL18T1		<u>CCC</u> CGTCGAGCACCGGCAACTCC					hoz	-
BG757E23 PL20T1		<u>CCC</u> CGTCGAGCACCGGCAACTCC					hoz	-

Figure 3.4.2.1: segregation pattern from T0 to T1 of the induced mutations of BG757 E52 line(A) and line BG757 E23 (B), the sequence marked in blue represents the gRNA-specific part of the targeted motif, the underlined sequences indicate the protospacer-adjacent motif PAM. Plant ID is given on the left-hand side, deletions are highlighted with red dashes and inserted nucleotides with subscript red letters, single-base substitutions are shown in red type, and the zygosity statue of the mutants is given on the right side. the presence of T-DNA was indicated by (+) as a plant carrying transgene and (-) as a transgene-free plant.

3.4.2.1. Selection of transgene-free homozygous barley mutants T1

To avoid the possibility of forming novel mutations created by active gRNA/ Cas9 transgenic plants. Homozygous mutations for *HvRA2* without any transgenic components were investigated in T1 plants by PCR and DNA sequencing. Among at least 160 plants from nine T1 lines tested,

41 plants without the Cas9 T-DNA were obtained (found within 6 lines of T1). Among these 6 lines, we found 19 T1 homozygous plants carrying In/Del mutations, causing loss of function of *HvRA2* due to frameshift in the open reading frame (ORF) of *HvRA2*, resulting in different protein types or truncated protein (Figure 3.4.2.1.1). The summary of the homozygous transgene-free T1 selection is listed in (Table 3.4.2.1.1).

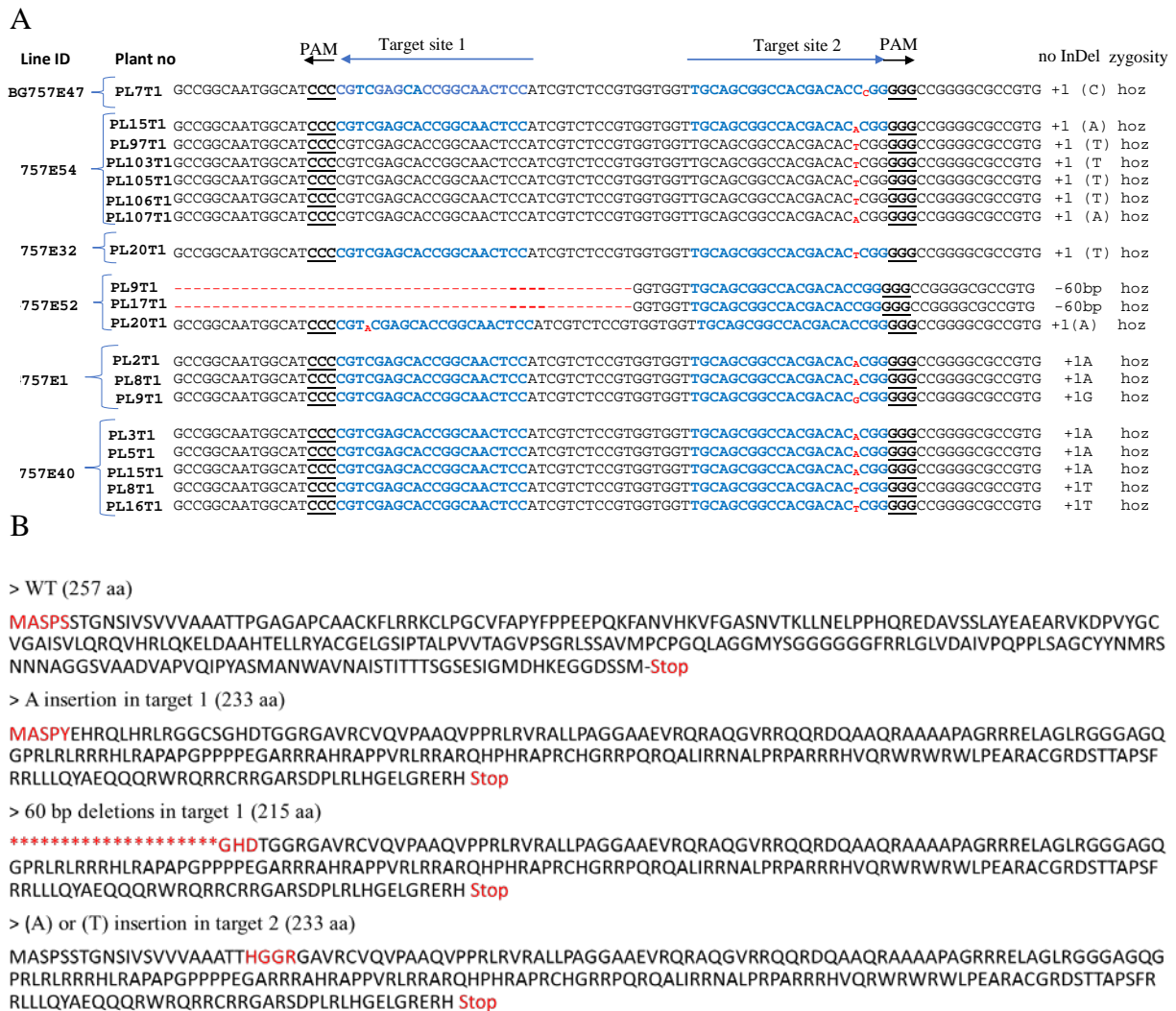


Figure 3.4.2.1.1. Types of mutations detected in the selected homozygous transgene-free plants; (A) Type of mutation at the DNA level. the sequence typed in blue represents the target sequences of the RNA-guided Cas9 nuclease, the underlined sequences indicate the protospacer-adjacent motif PAM. Plant ID is

given on the left-hand side, deletions are highlighted with red dashes, and inserted nucleotides with subscript red letters, The number of modified nucleotides either deleted (-) or inserted (+) is shown on the right side of each sequence. hoz, homozygous, B) Amino acid changes due to InDel mutations. Wt, wildtype; aa, amino acid, conserved aa between the mutants allele and wt are typed in red

In summary, the majority of the plants in T1 were mutated. However, they segregated in the non-Mendelian pattern, and a new type of mutation in the T1 generation indicated the chimeric status of T0 transgenic plants. Therefore, it is necessary to obtain homozygous transgene-free plants for fixed mutations, to be used for the complementation studies, which will be presented in the upcoming section.

Table 3.4.2.1.1: Overview of the selection of the Transgene free homozygous mutant.

T1 mutant lines	No of plants tested	No of positive plants for Cas9	No of mutated plants	No of mutated plants Cas9 free	No of homozygotes mutated plants Cas9 free	type of mutation
BG757E16	20	15	9	0	0	7 plant with bp substitution ,1Plant +1bp, 1plant -30 bp
BG757E47	11	9	10	1	1	7plant+1bp(C),1plant-25bp,1plant-135bp
BG757E23	14	13	6	0	0	3plant with bp substitution ,1Plant +1bp(A), 1plant -12 bp,1plant -3 bp
BG757E32	14	5	10	4	1	8plant+1bp(A),2 plant+1bp(G)
BG757E37	15	7	3	0	0	2 plant with bp substitution , 1plant -21 bp,
BG757E52	21	10	21	10	5	6plant+1bp(A),1plantbp substitution,14plant-61bp
BG757E54	22	11	17	8	6	5plant+1bp(A),10plant+1bp(T),
BG757 E1	28	16	13	10	4	6plant+1bp(A),3 plant bp substitution,4plant+1bp(T)
BG757 E40	18	9	16	8	5	6plant+1bp(A),1 plant bp substitution,9plant+1bp(T)

3.4.2.2. Spike phenotype of homozygous *HvRA2* T1 mutants

The phenotypic changes in the spike phenotype from two-rowed to six-rowed and irregular spike forms were observed in *ra2* T1 knockout mutants (Figure 3.4.2.2.1), this phenotype was similar

to that of *ra2* mutants in BW-NIL(*mull1.a*) background (Koppolu et al., 2013). The *ra2* mutant displays lateral spikelet fertility and loss of spikelet determinacy and identity, resulting in the formation of additional spikelets and or additional florets.

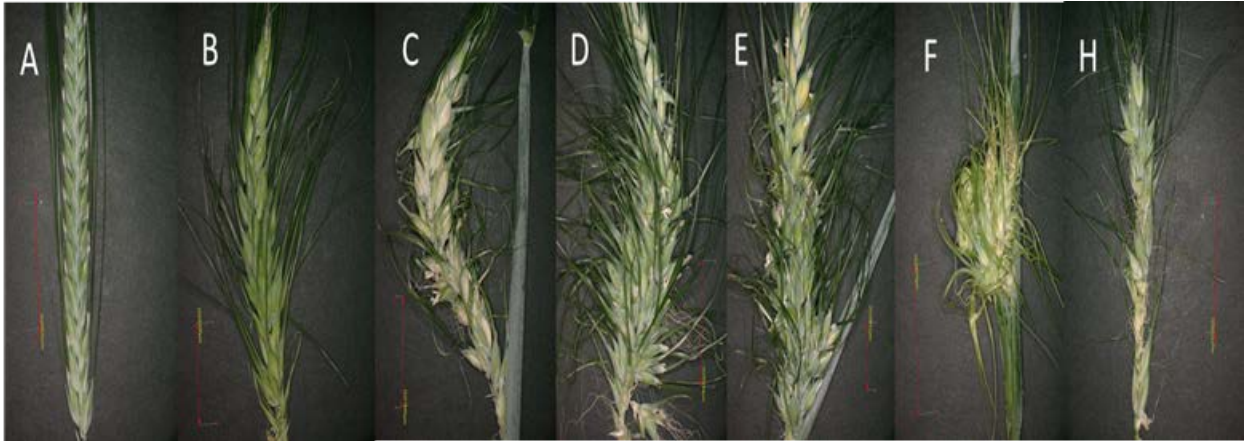


Figure 3.4.2.2.1. Spike phenotypes of *HvRA2* RGEN knock out mutant. The phenotype of the targeted mutation in *HvRA2* was detected on all the mutated plants, the spike showed six-rowed-like, with different levels of spike branching combined with the development of additional spikelet and additional florets(A) Mature spike of two-rowed wild type (Golden Promise) with determinate spikelet at each rachis internode. (B-H) Mature spikes of *ra2* RGEN knock out mutant, showing various levels of indeterminacy of the spikelets.

3.4.3. Validation of *HvRA2* knockout by qRT-PCR

The previous study by Koppolu et al., (2013) showed that expression of the major row-type gene *VRS1* was significantly lowered in BW-NIL(*mull1.a*) mutants. Therefore, to investigate whether CRISPR/Cas9-mediated targeted mutagenesis of *HvRA2* affected the expression level of *VRS1*, RNA was extracted from the immature spike at the triple mound (TM) stage of homozygous mutants T1 lines, as well as BW-NIL(*mull1.a*) mutants and Wild type plants as a control and the relative quantification analysis of *VRS1*, was carried out using quantitative real-time RT-PCR (qRT-PCR), the results of the expression analyses indicate that *VRS1* was highly reduced in the

RGEN *ra2* mutants as well as BW-NIL(*mull1.a*) mutants compared to the wild type (Golden Promise) plants as shown in (Figure 3.4.3.1). These results are consistent with data obtained by Koppolu et al.,(2013)

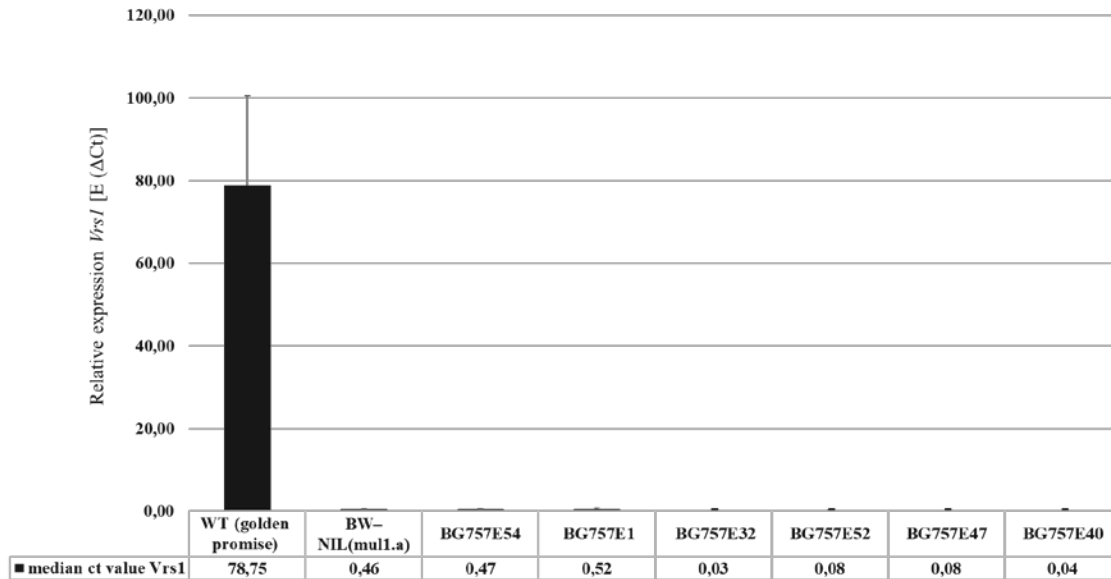


Figure 3.4.3.1. Expression analysis of *VRS1* in *ra2* RGEN knockout mutants. Relative expression of *Vrs1* determined by quantitative RT-PCR in spike at triple mound stage of the RGEN Knock out *ra2* mutants compared to BW-NIL(*mull1.a*) and wild type (Golden Promise cultivar). Constitutively expressed *HvActin* was used for normalization, Expression values are given at the bottom of the graph, error bar represents the SD. of 3 independent biological replicates.

3.4.4. Putative off-target analysis for homozygous *HvRA2* mutants

While designing CRISPR KO guides, the potential off-targets were bioinformatically excluded by selecting guides unique to the target region (*HvRA2*) with the tool Cas-OFFinder, (<http://www.rgenome.net/cas-offinder/>). A single mismatch within the seed region of the guide sequence considerably decreased gRNA activity but was not completely abolished, whereas an additional mismatch or the absence of a PAM sequence will eliminate gRNA activity (Arndell et al., 2019). A few potential off-targets were predicated by the deskgen.com tool, where there is a

high similarity in the seed region for potential off-target (Figure 3.4.4.1). Therefore, to rule out the possibility of the off-target effect, those regions were amplified by PCR and prepared for sanger sequencing, the results of sequencing showed that no mutation was found in the predicted off-target regions (Figure 3.4.4.2).

	Seed region	PAM	Similarity	Mismatch	Gene	Locus		
gRNA1	GGAGTTGCCGGTGCCTCGACG	GGG	100		yes	chr3@ 35980662-35980685	On-target	HvRA2 gene
	GGAGCTGCCGGAGCTCGACG	CGG	3	5,12	No	chr1@ 435581031-435581054	Off-target 1	
	GGGATGGCGGTGCCTCGACG	AGG	2	3,5,8	No	chr4@ 143088748-143088771	Off-target 2	
gRNA2	TGCAGCGGCCACGACACCGG	GGG	100		yes	chr3@ 35980702-35980725	On-target	HvRA2 gene
	ACCAGCAGCCACGACACCGG	CGG	2	1,2,7	No	chr7@ 288246466-288246489	Off-target 3	

Figure 3.4.4.1 Putative off-target analysis for *HvRA2* mutant plants. The seed region is surrounded by two red dashed lines, and the length of the seed region is about 12-bp fragment upstream of the PAM sequences; off-target 1 has only one single mismatch inside the seed region, while off-target two and off-target three, there was no mismatch in the seed region.

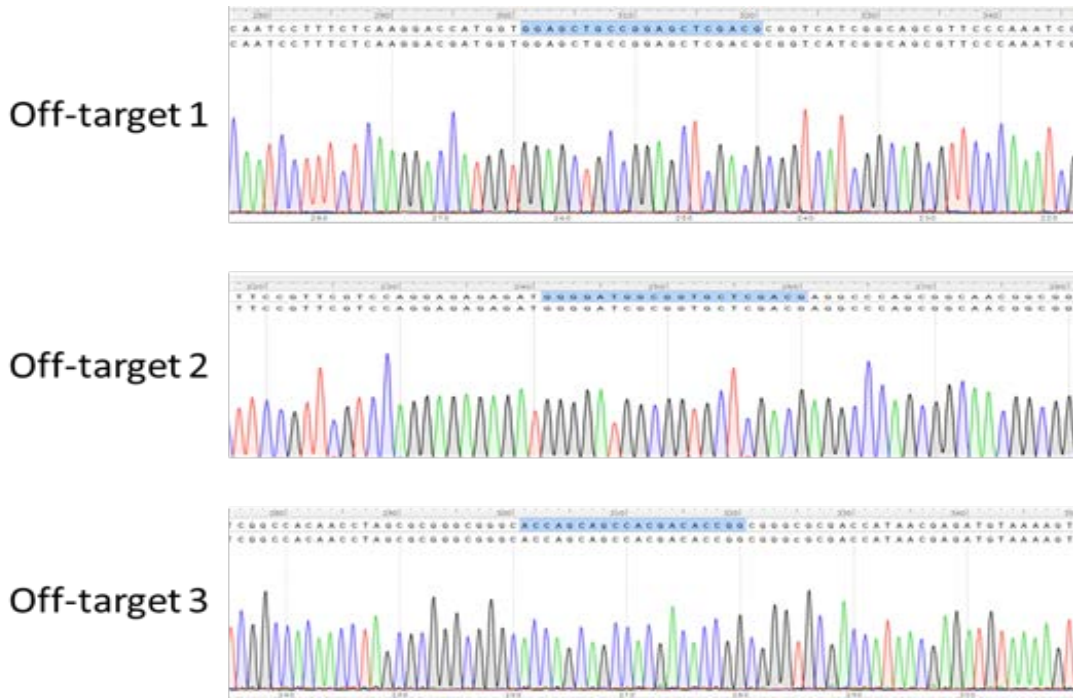


Figure 3.4.4.2 Sequence analysis of potential off-targets in T1 plants homozygous knockout mutants. The analyses of the potential off-targets for *HvRA2* knock-out mutant with clean chromatograms displayed no mutation at those sites compared to the reference sequence

3.5. Complementation of *HvRA2* RGEN *KOs* with promoter swapped *RA2* transgene cassettes

After successfully obtaining *ra2* knockout transgene-free homozygous mutants in the Golden Promise background (see section 3.4.2.1), the homozygous transgene-free *hvra2* RGEN KO mutant was used for the following complementation studies. To address this study's main question, whether differences in *RA2* expression in different grasses might be causative for the difference in inflorescence architectures (Koppolu & Schnurbusch, 2019), we carried out transgenic experiments in barley by super transforming the *ra2* mutant (cv. Golden Promise) with different constructs containing the *HvRA2* coding sequence, fused with gene cis-regulatory regions of *RA2*, either from barley (named barley construct), sorghum (named sorghum construct), or wheat from *Aegilops tauschii* (named wheat construct) (Figure 3.5.1).

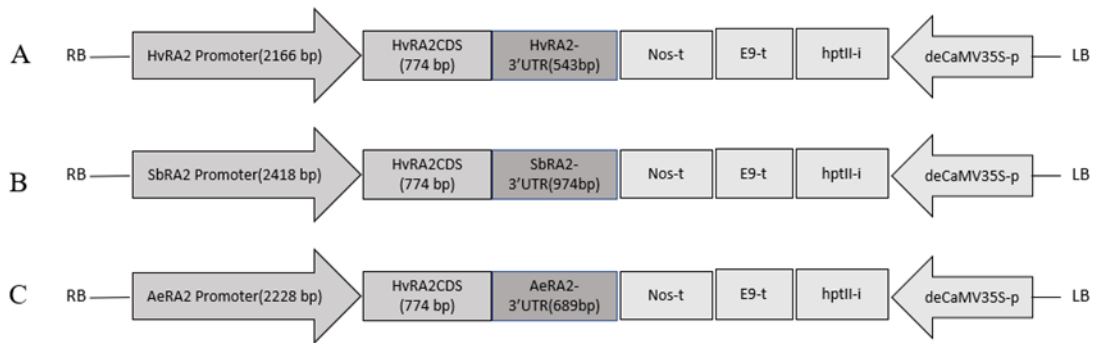


Figure 3.5.1: Schematic representation of the T-DNA constructs used for barley transformation. A) expression cassette for complementation construct of *HvRA2CDS* under the regulation of barley *RA2* promoter and 3'UTR; B) expression cassette for *HvRA2CDS* under the regulation of *Sorghum RA2* promoter and 3'UTR; C) expression cassette for *HvRA2CDS* under the regulation of *Aegilops tauschii RA2* promoter and 3'UTR.

3.5.1. Phenotypic analysis of the super transformed *HvRA2 Golden Promise* KOs with *HvRA2* CDS driven by different *RA2* promoters from sorghum, barley, and wheat

3.5.1.1. Phenotypic analysis of the super transformed T1 plants

The successful integration of T-DNA into different transgenic lines was confirmed by PCR using a specific primer for each construct. Eight to six independent transgene-positive lines for each construct from the T0 plant were selected, and 20 grains per line were germinated in the S1 greenhouse for phenotypic analysis.

The inflorescence of the T1 transformants derived from transgenic plants transformed with the three different constructs barley, sorghum, and wheat showed a restoration of the wild-type phenotype with different degrees of complementation between different lines and within the same line, i.e., reversion to complete or partial two-rowed condition and repression of spikelet indeterminacy/spike branching. The phenotype was quantified by giving each plant phenotype a certain degree from zero(0) to four(4) (named complementation degree as shown in (Figure 3.5.1.1.1). The degree of complementation was based on the quantitative differences of the row-type phenotype, with either two- or six-rowed spikes and indeterminate spikelets. Zero-degree complementation was defined as a spike that was fully six-rowed with indeterminate spikelets; degree one was a six-rowed spike with fewer numbers of developing additional structure than zero degrees. Degree two, the spike displays an intermedium-spike phenotype, the upper parts of the spike were six-rowed, and the basal parts appeared two-rowed. In contrast, in complementation degree three to degree four (highest complementation achieved), the spike was completely two-rowed with differences in spike length.

The comparative phenotyping analysis of spike architecture in the complemented transgenic plants indicated no significant difference in spike phenotype between the three constructs. However,

there was considerable variation within and between lines. Moreover, three independent transgenic lines from the three constructs, barley (BG863CE30A), sorghum (BG864E05), and wheat (BG865E01/D), displayed more stunted or short spikes but complementation degree four. The summary for the different degrees of complementation are shown in the boxplot in (Figure 3.5.1.1.2). Overall, the complementation was achieved in all transgenic lines without noticeable species-specific differences. This result suggests that the difference in inflorescence architectures between barley, sorghum, and wheat is mainly related to potential cis-acting factors upstream of the used promoter regions and most likely is missing from the currently used putative promoter or 3'UTR sequences.



Figure 3.5.1.1.1 The phenotype of T1 super transformed plant with HvRA2 coding sequence and heterologous promoters and UTRs of barley, sorghum, and wheat (*Aegilops tauschii*); (A-F) different mature spikes from different lines showing a different degree of complementation and spikelet indeterminacy compared to Azygous as control; (G) azygous plant are the progenies of transgenic parents and lost the transgene through segregation and kept as control, complementation degrees are given under each spike from 0 to 4.

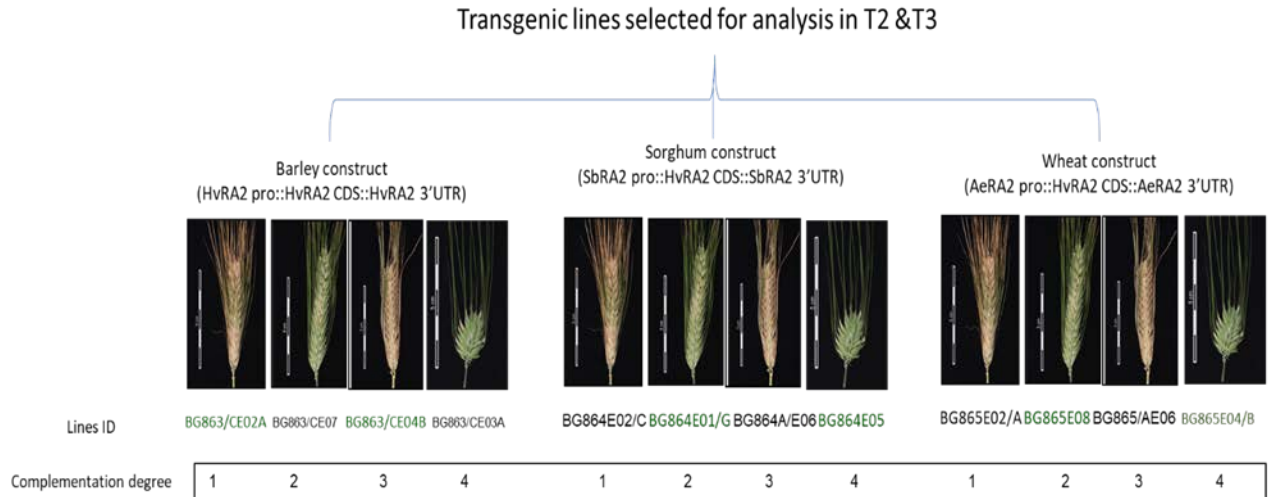


Figure 3.5.1.2.1. Schematic representation of line selection for T2 and T3 for transgenic analysis.

The phenotype analysis of T2 & T3 showed that inflorescences of the transgenic lines could complement the wildtype phenotype compared to azygous plants (Figure 3.5.1.2.2) with different degrees of complementation as was observed in T1, without any noticeable difference between barley, sorghum, and wheat constructs. The observed variation in the T2 & T3 phenotypes was much reduced in comparison to T1 (Figure 3.5.1.2.3), and some lines displayed shorter condensed or stunted spikes, which were quantified as complementation degree four (Figure 3.5.1.2.2A). The line BG863/CE07 from barley constructs displayed the mutant phenotype despite being tested as transgene-positive (Figure 3.5.1.2.2G)



Figure 3.5.1.2.2 The phenotype of T2 & T3 supertransformed plants with *HvRA2* coding sequence and heterologous promoter and UTRs of barley, sorghum, and wheat (*Aegilops tauschii*); (A-G) different mature spikes from different events showing a different degree of complementation and spikelet indeterminacy compared to azygous as control; (H) azygous plants are the progenies of transgenic parents and lost the transgene through segregation and were therefore kept as control.

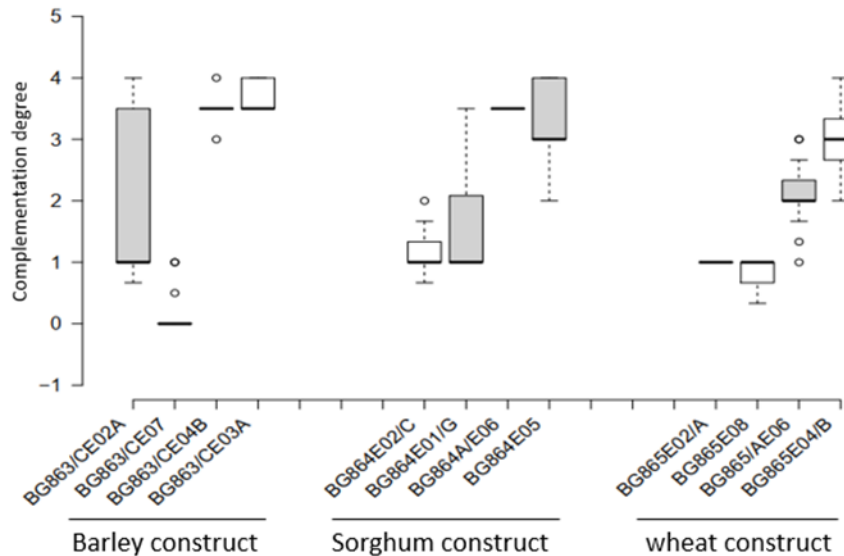


Figure 3.5.1.1.3. Degree of complementation across different T2 lines transformed with different constructs, quantitative analysis showing different degrees of complementation between different lines with different constructs, the bottom, and top of boxes represent the first and third quartile, respectively, the middle line is the median, and the whiskers represent the maximum and minimum values, and the remaining outlier data points are shown as individual dots.

3.5.2. Expression analysis of the *HvRA2* in Transgenic plants

3.5.2.1. Expression analysis by qRT-PCR indicates that complementation is achieved regardless of the expression dosage

To investigate whether the expression level of the transgene is linked to the displayed inflorescence phenotypes, immature spikes were collected at the stamen primordia stage, and qRT-PCR was carried out. The expression analyses show that *HvRA2* expression in transgenic plants transformed with sorghum constructs was significantly lower compared to transgenic plants that were

transformed with wheat or barley constructs (Figure 3.5.2.1.1). The highest expression level was detected in plants transformed with barley constructs, the respective transgenic lines showed the most severe stunting phenotypes in terms of plant height, and some of these plants failed to develop floral structures and subsequently could not produce grains. Surprisingly, although the expression in plants transformed with sorghum was the lowest, the complementation was achieved with the observation of stunted spike phenotype. These results indicate that even the lowest amount of *RA2* expression using these constructs is sufficient to mediate spikelet meristem determinacy and identity, which is otherwise lost when the *HvRA2* is mutated.

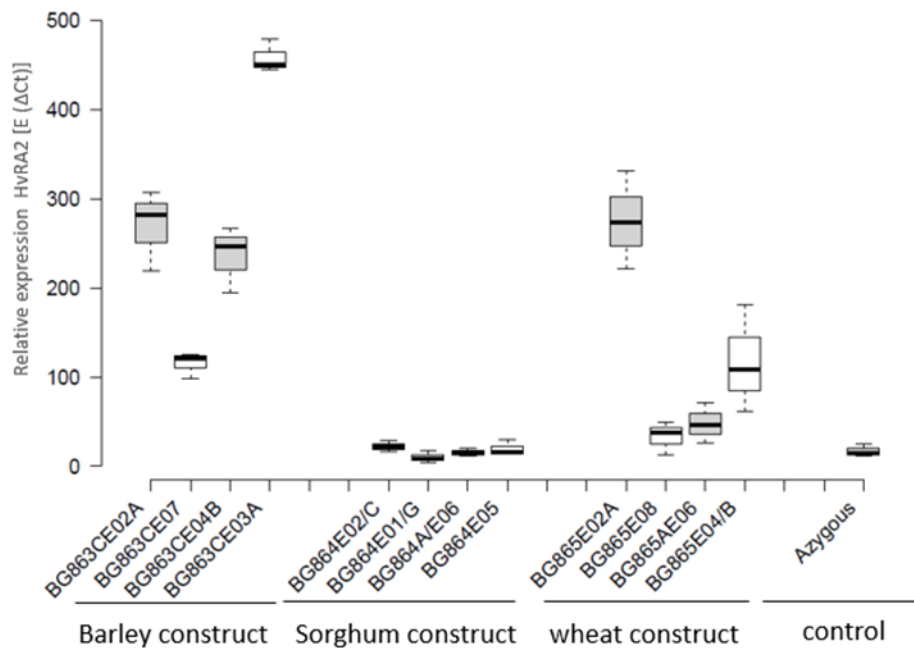


Figure 3.5.2.1.1 Expression analyses of *HvRA2* in T3 transgenic lines. Relative expression of *HvRA2* determined by quantitative RT-PCR in the inflorescence spike at stamen primordia stage of the super transformed with barley, sorghum, and wheat construct as azygous plants as control. the bottom and top of box plots represent the first and third quartile, respectively, the middle line is the median, the whiskers represent the maximum and minimum values, and the remaining outlier data points are shown as individual dots; the data are representative of 3 independent biological replicates.

3.5.2.2 Analysis of *RA2* promoter expression in rice protoplast.

The transgene expression level depends on several factors, such as the positional effect of random integration into the genome, transgene zygosity, and the copy number of the T-DNA insertion. These factors result in variations of gene expression levels from independent transformants (Holubová et al., 2018). To avoid these arbitrary effects and to achieve a better expression comparison among different constructs, transient expression systems, such as a dual-luciferase system (Promega), are an alternative. Following this approach, we thus sought to measure the promoter activities of *HvRA2* based on barley, sorghum, and wheat *RA2* putative promoter sequences. The *RA2* promoter sequences from the respective species were cloned in frame with a plasmid harboring the *Renilla reniformis luciferase* gene (*Rluc*) driven by a constitutive promoter for normalization. The dual-luciferase system enables differentiation between different reporter activities in a single tube due to the different substrates used for each reporter gene.

The barley *RA2* Promoter showed relatively high luciferase (LUC) activity, whereas sorghum and wheat *RA2* Promoters displayed much lower activity (**Figure 3.5.2.2.1**). These findings are consistent with qRT-PCR expression analysis data which was explained in the previous section (see section 3.5.2.1).

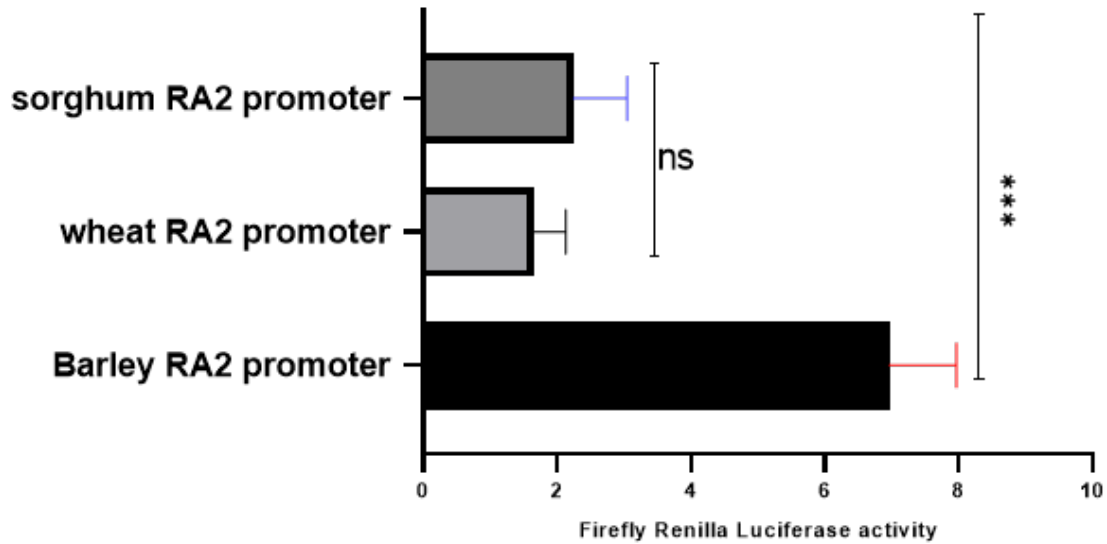


Figure 3.5.2.2.1 Analysis of RA2 promoter activity in rice protoplasts. Rice protoplasts were transformed with HvRA2Pro::*FLUC*, AetRA2Pro::*FLUC*, SbRA2Pro::*FLUC*, each construct was co-transformed with a normalization vector (Rluc) that allows for normalizing, and the transformed cells were incubated overnight, the firefly and Renilla luciferase activity was measured using the Dual-Luciferase Reporter Assay System. Each bar represents the SD. of 3 replicate samples and the data are representative of two independent experiments. The asterisk denotes statistically significant differences between the indicated samples. statistical analysis was performed by one-way ANOVA followed by Tukey's multiple comparisons test, *** $P < 0.0003$, ns $P = 0.6480$

3.5.3. Transgenic plants showed a negative effect on the entire plants' elongation

To investigate whether the transformed constructs affect other traits of the plant, therefore several other morphological traits in the transgenic plants have been measured, including plant height, spike length, spike node number, tiller number, and the number of additional spikelets/florets. For the spike node number and tiller number, there were no significant differences between transgenic plants and Azygous plants at $P < 0.05$ applying one-way ANOVA followed by Dunnett's multiple comparisons test (Figure 3.5.3.1)

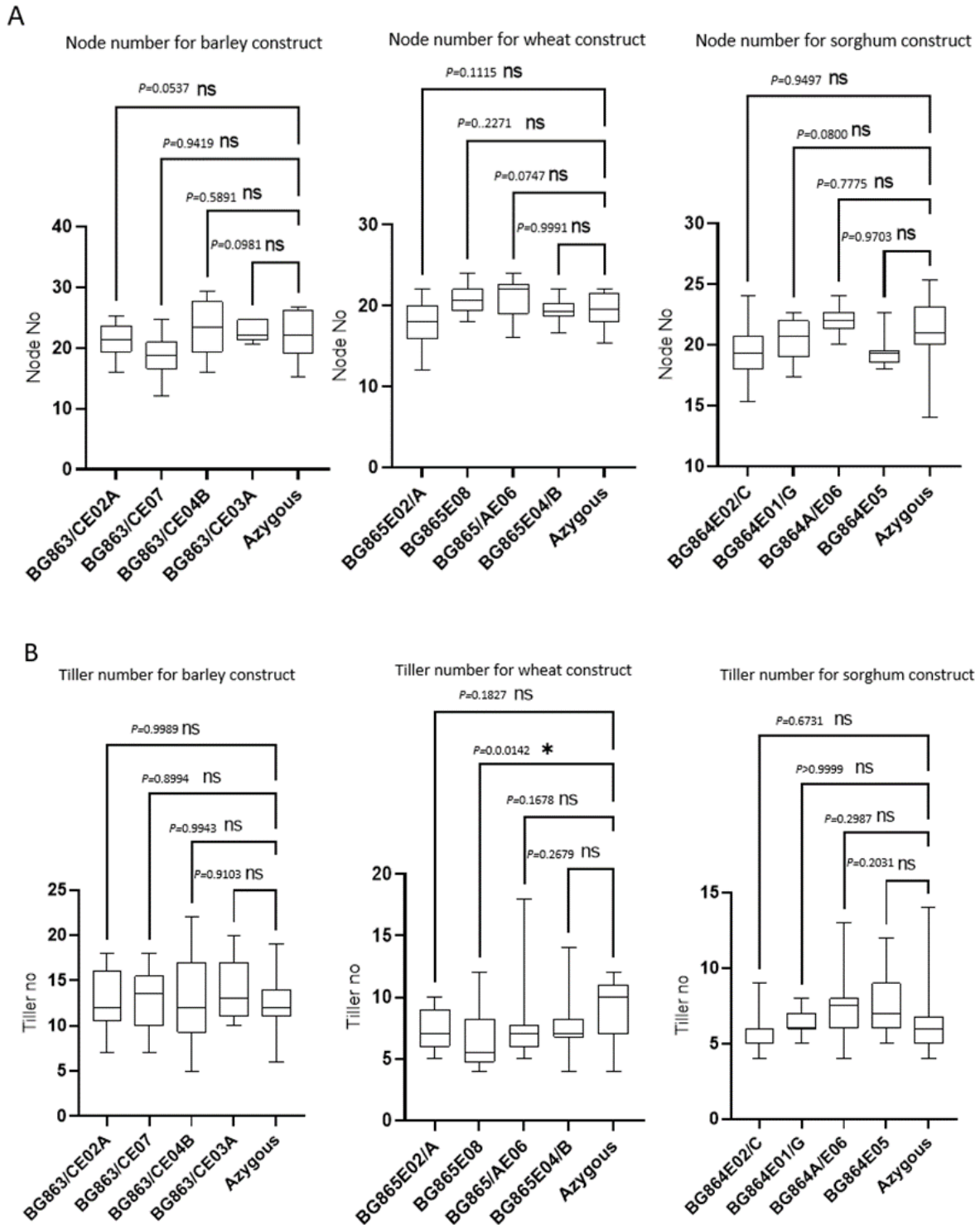


Figure 3.5.3.1. Effect of *HvRA2* transgene expression on the number of tiller and spike node number. A) boxplot display spike node number between different constructs compared to azygous; B) boxplot display tiller number between different constructs compared to azygous, the bottom, and top of

box plots represent the first and third quartile, respectively, the middle line is the median, and the whiskers represent the maximum and minimum values; one-way ANOVA test (Dunnett's multiple comparisons test) for transgene vs. azygous was performed. ns: not significantly different at $P < 0.05$ the p -value are presented above each box

The number of additional structures (spikelets/florets) was significantly reduced in transgenic plants compared to Azygous, without a noticeable difference between the three constructs (Figure 3.5.3.2). There were no significant differences between barley, sorghum, and wheat constructs for most of the measured traits. However, the effect of the expression of the *HvRA2* transgene was observed on the entire plant elongation compared to azygous control, such as plant height and spike length. The spike length was significantly reduced in barley and sorghum constructs compared to the azygous control, and the spike length reduction in the wheat construct was observed only in one line, but the rest of the wheat constructs lines were not significant compared to the azygous control (Figure 3.5.3.3)

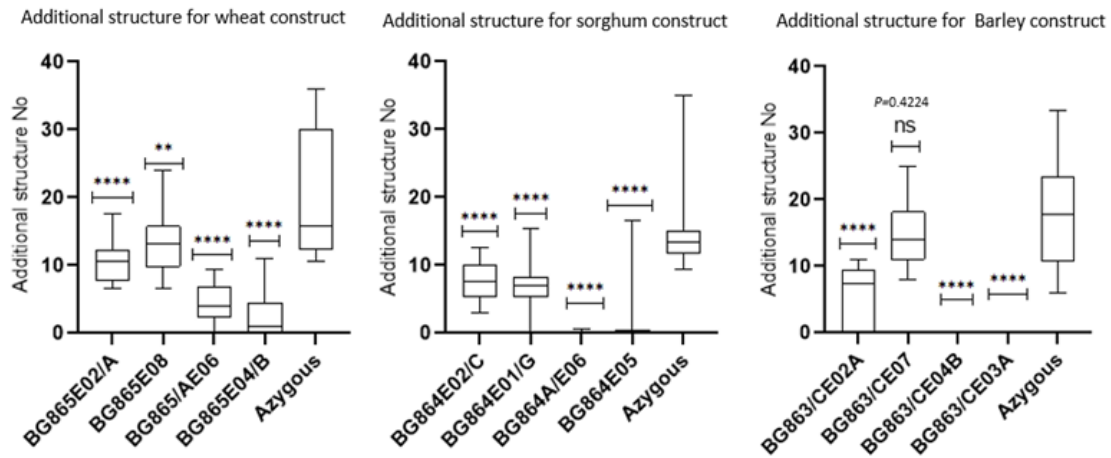


Figure 3.5.3.2. Effect of *HvRA2* transgene expression on the number of additional structures. The number of extra structures was significantly reduced in the transgenic plant compared to the control plant, the bottom and top of box plots represent the first and third quartile, respectively, the middle line is the median, and the whiskers represent the maximum and minimum values; one-way ANOVA test (Dunnett's multiple comparisons test). for transgene vs. azygous was performed **** $P < 0.0001$, ** $P < 0.0025$, ns not significantly p -value=0.4224

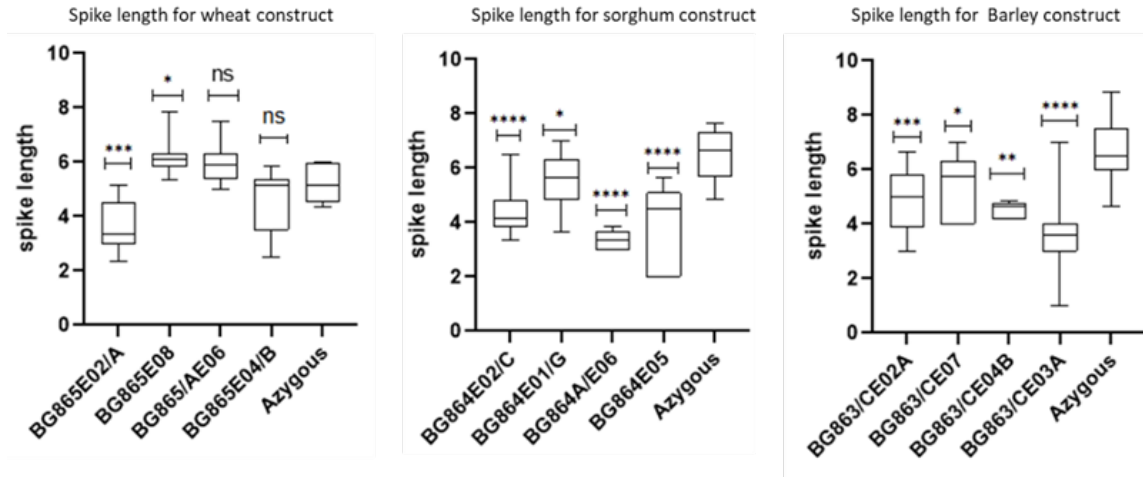


Figure 2.5.3.3. Effect of *HvRA2* transgene expression on the spike length. The spike length was significantly reduced in the transgenic plant compared to the control plant, the bottom and top of the boxes represent the first and third quartile, respectively, the middle line is the median, the whiskers represent the maximum and minimum values, and the remaining outlier data points are shown as individual dots; one-way ANOVA test for transgene vs. azygous was performed **** $P < 0.0001$, *** $P < 0.0003$, ** $P < 0.0025$, * $P < 0.05$.

Plant height was significantly reduced in barley constructs with higher expression of *HvRA2* compared to sorghum and wheat constructs (**Figure 3.5.3.4.**). As a result, the entire plant development, including the inflorescence, becomes more compact compared to the control plant. These observations indicate that ectopic expression of *HvRA2* may potentially negatively affects plant cell proliferation and overall plant development. Similar phenotypes have been observed in Arabidopsis lines that ectopically express the *LOB* gene thereby lowering the accumulation of (BR) in organ boundaries (Bell et al., 2012; Shuai et al., 2002). Which results in stunted plant growth.

A



B

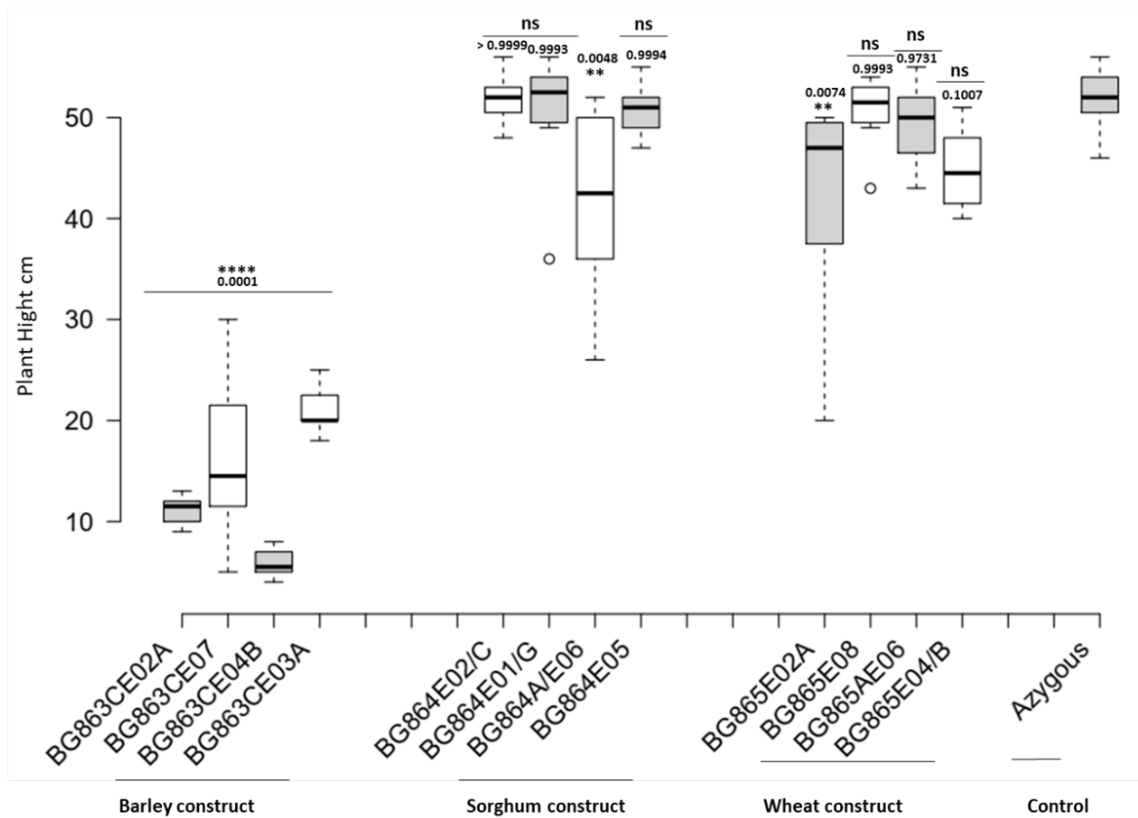


Figure 3.5.3.4. Effect of *HvRA2* expression on the plant height. A) Photographs show the transgenic plant's height from barley, sorghum, and wheat construct compared to azygous plants. B) box blot displays

the variation in plant height between the transgenic plant. The bottom and top of the boxes represent the first and third quartile, respectively, the middle line is the median, the whiskers represent the maximum and minimum values, and the remaining outlier data points are shown as individual dots; one-way ANOVA test (Dunnett's multiple comparisons test) for transgene vs. azygous was performed. ns: not significantly different at $P < 0.05$ the *p-value* are presented above each box

3.5.4 Complementation lines with *HvRA2* tagged with GFP display varied GFP expression patterns between different transgenic lines.

Since we observed different degrees of complementation with plants transformed with the barley construct, it would be ideal for linking this morphological difference with the localization of the expression pattern of *HvRA2* between different phenotypes. To achieve this, we have tagged *HvRA2* with the GFP reporter gene (**Figure 2.5.4.1**) and transformed it into the RGEN Knockout *ra2* mutant in the Golden Promise background.

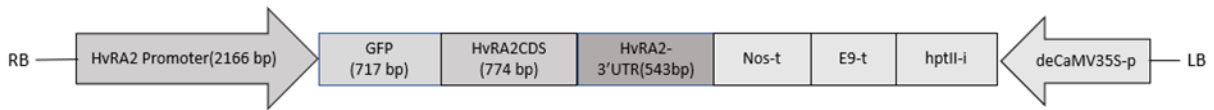


Figure 3.5.4.1 Schematic representation of the T-DNA constructs used for barley complementation constructs tagged with *GFP*.

Eight independent transgene-positive lines from the T0 plant were selected, and 20 grains per line were germinated in the S1 greenhouse for *GFP* visualization and phenotypic analysis. Four independent transgenic lines showed ectopic expression of *GFP* all over the entire spike (**Figure 3.5.4.2. B & D&G**). Two lines of *GFP* expression were not detected at the outer cell layers of the spike tip (**Figure 3.5.4.2 A & H&F**), one line showed expression restricted to the spikelet ridge (**Figure 3.5.4.2 C**), and in one line we could not observe any *GFP* signal. However, it was positive for the T-DNA insertion (**Figure 3.5.4.2. E**).

The remaining plants for these transgenic lines are currently still in the greenhouse for phenotype evaluation (at the time of writing this manuscript, the emergence of the spikes was not observed).

Collectively, the variations observed in the GFP pattern in this experiment with variations obtained in the phenotype of the complementation lines could be attributed to the random integration of the T-DNA into the genome and transgene zygosity status.

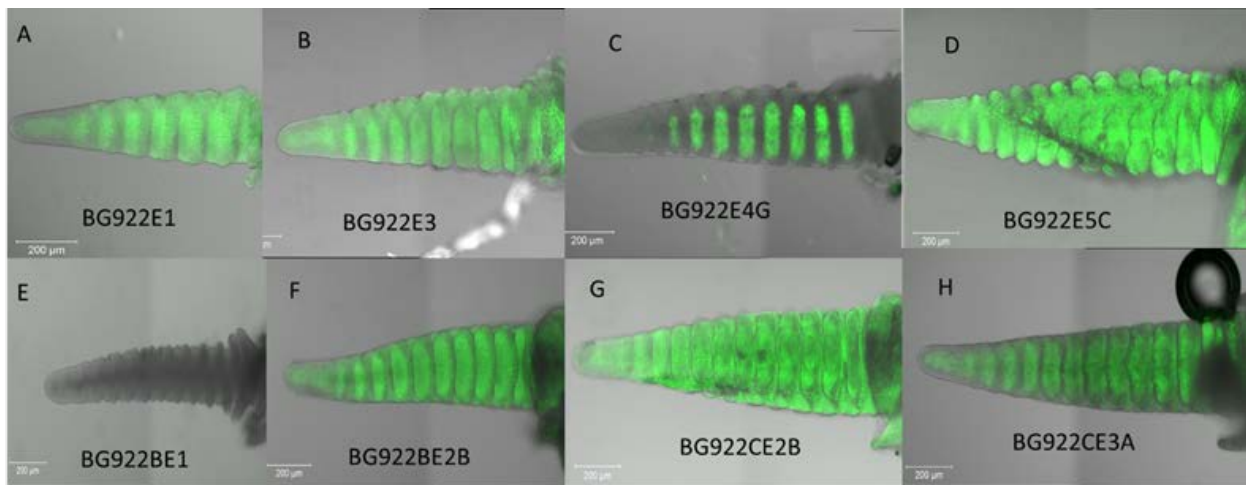


Figure 3.5.4.2. GFP fluorescence in the spike of transgenic plants with GFP fused in frame with *HvRA2* at the C-terminal end. The variation of the fluorescence signal from the fusion protein was observed between different lines.

3.6. Possible interaction between *HvRA2* and other genes related to spike development

Utilizing the high-resolution gene regulatory networks in barley generated by Thiel et al., (2021), a targeted yeast two-hybrid assay was performed to investigate the possible protein-protein interactions between *HvRA2* and other proteins located within the same regulatory network.

All potential candidate genes listed in (Table 3.6.1) which might interact with *HvRA2* were cloned into the pGADT7 vector in frame with the activation domain (AD) of the GAL4 transcription factor as prey. The pGADT7 vector has selectable marker leucine, which will allow the yeast cells

to grow on the leucine-deficient medium, whereas the *HvRA2* CDS without activation domain were cloned into pGBKT7 in frame with the DNA binding domain (BD) as bait, the pGBKT7 has a selectable marker tryptophan, which will allow the yeast cells to grow on the tryptophan-deficient medium. When both preys and baits vectors are successfully co-transformed into the same yeast cells, it will allow the yeast to grow on a double drop-out medium without amino acids tryptophan and leucine (SD/-Trp/- Leu). Whereas in case there is an interaction between two proteins that were cloned into pGADT7 and pGBKT7 vectors, this would bring the AD-domain and the BD-domain together, resulting in transcriptional activation and synthesis of the two amino acids adenine and histidine in yeast cells, allowing the yeast to grow on a quadruple drop-out medium SD/-Trp/-Leu/-His -Ade.

To avoid autoactivation, a negative control was included by co-transforming the empty AD prey plasmid pGADT7 with *HvRA2*- pGBKT7 and BD- pGBKT7 empty with AD-pGADT7 recombinant; thus, the growth of yeast colonies on SD/-Trp/- Leu indicates the presence of both bait and prey plasmids, while the absence of growth on SD/-Trp/-Leu/ His-Ade indicate that the recombinant construct is not auto-activated by itself.

To test the potential interactors of *HvRA2* after co-transformation, yeast cells were plated onto selective double drop-out media SD/-Trp/- Leu, which indicates the successful transformation, followed by drop assay on the quadruple dropout on SD/-Trp/-Leu/ His-Ade medium, the growing cells indicates an interaction between *HvRA2* and the respective proteins (**Figure 3.6.1**).

Out of all combinations, 9 genes could grow in quadruple dropout SD/-Trp/-Leu/ His-Ade, without showing growth from their negative control on the same media, indicating an interaction between the *HvRA2* and those genes. Except for one gene with ID:

HORVU.MOREX.r2.4HG0328540.1 showed growth with an empty vector on SD/-Trp/-Leu/His-Ade medium, indicating that this gene is autoactivated. Some of the genes that show interaction with *HvRA2* were predicted for their role in floral organ development and hormone signaling. For example, the Auxin response factor 14 like (*ARF 14 Like*), was predicted to have a function in the auxin signaling pathway and transcriptional regulation, providing a possible role between auxin signaling and lateral organ development and branching (Eveland et al., 2014; Gallavotti et al., 2008; Strable et al., 2022; D. Zhang & Yuan, 2014). The *OFP8*-like transcriptional repressor is predicted to be the negative regulator for BR signaling, which might be having a role in lowering BR accumulation in organ boundaries to facilitate proper organ boundary formation (Bell et al., 2012; Gendron et al., 2012). In addition to hormonal signaling genes, other genes have a function in axillary meristem formation and organ boundary specification, such as *DEPI*, *CULA*, *SPL14* (*SQUAMOSA-PROMOTER BINDING PROTEIN*), (*LAX1*) *Basic helix-loop-helix (bHLH)* transcription factor, *laxatum-a* (*lax-a*), which may indicate a potential regulation with RAMOSA pathway in grasses (Husbands et al., 2007; Kellogg, 2022; Thiel et al., 2021). The proposed links between these genes need to be confirmed in future experimental studies.

The summary of these results is listed in (Table 3.6.1), including the predicted function for each protein and its interaction status with *HvRA2*. This experiment was repeated five times with consistent results; however, these results required further analysis by using other means to confirm the protein-protein interaction, such as Bimolecular fluorescence complementation (BIFC)(Galli et al., 2022).



Figure 3.6.1: Targeted yeast two-hybrid assay for HvRA2 with different potential interaction partners. The Growth of yeast on SD-Leu/-Trp confirms the presence of both bait and prey vectors for protein expression, growth on SD-Leu/-Trp/-His/-Ade indicates protein-protein interaction, and No growth of the negative control, which is empty bait vector + candidate prey, confirms the absence of autoactivation except for HORVU.MOREX.r2.4HG0328540.1 which is showing interaction even with an empty bait vector.

Table3.6.1 Selected genes for Targeted yeast two-hybrid assay with HvRA2

Gene ID:	Interaction with HvRA2	Predicted biological function
<i>1-HORVU.MOREX.r2.6HG0506770.1</i>	Yes	<i>LEAFY COTYLEDON 1 (LEC1)</i> transcriptional activator, regulates genes involved in photosynthesis
<i>2-HORVU.MOREX.r2.6HG0501740.1</i>	no	<i>Glucan synthase-like 9</i> , involved in the synthesis of the cell-wall
<i>3-HORVU.MOREX.r2.1HG0062930</i>	Yes	<i>Auxin response factor 14 like</i> , involved in Auxin activate signaling pathway and regulation of transcription
<i>4-HORVU.MOREX.r2.1HG0049440.1</i>	no	ALOG domain protein, (DUF640) -developmental regulator by promoting cell growth in response to light
<i>5-HORVU.MOREX.r2.4HG0328540.1</i>	Yes	Pathogenesis-related thaumatin-like protein,
<i>6-HORVU.MOREX.r2.2HG0100560.1</i>	no	Calmodulin-binding family protein, regulating plant growth and development,
<i>7-HORVU.MOREX.r2.6HG0512340.1</i>	no	<i>Galactoside 2-alpha-L-fucosyltransferase</i> , Involved in cell wall biosynthesis
<i>8-HORVU.MOREX.r2.4HG0343960.1</i>	no	Plant-specific remorin protein plays roles during cellular signal transduction processes.
<i>9-HORVU.MOREX.r2.3HG0250320.1</i>	Yes	<i>OFP8</i> -like, transcription repressor plant growth and development, a negative regulator of (BR) signaling.
<i>10-HORVU.MOREX.r2.4HG0336070.1</i>	no	Transcription factor protein (ILI3), regulate cell elongation and plant development.
<i>11-HORVU.MOREX.r2.3HG0266940.1</i>	Yes	<i>BTB-ankyrin repeats unculme 4.24 (cul4)</i> , plant organ development, Boundary specification
<i>12-HORVU.MOREX.r2.2HG0162930.1</i>	no	Zf-FLZ domain (Zinc fingers) - plant growth and development, stress mitigation, sugar signaling, and senescence.
<i>13-HORVU.MOREX.r2.2HG0138000.1</i>	no	Protein IDA, a peptide signal controlling floral organ abscission
<i>14-HORVU.MOREX.r2.5HG0397930.1</i>	Yes	Hordeum vulgare <i>DEPI</i> , involved in the regulation of cell proliferation
<i>15-HORVU.MOREX.r2.2HG0100560.1</i>	no	Calmodulin-binding family protein, is an important calcium-binding protein, cellular signaling
<i>16-HORVU.MOREX.r2.3HG0258640</i>	no	RING/U box superfamily protein, regulation of programmed cell death
<i>17-HORVU.MOREX.r2.1HG0052240</i>	no	GDSE esterase/Lipase, regulation of plant development, morphogenesis, synthesis of secondary metabolites,
<i>18-HORVU.MOREX.r2.5HG0400110</i>	no	HST (Hydroxycinnamoyl coenzyme A-quininate transferase) transferase activity, Auxin transport and cell growth
<i>19-HORVU.MOREX.r2.2HG0099010</i>	no	Peptidase C15, the release of the N-terminal pyro glutamyl group from a peptide or protein
<i>20-HORVU.MOREX.r2.3HG0264500</i>	no	BRUNO-LIKE1 (nucleic acid binding) salicylic acid signaling
<i>21-HORVU.MOREX.r2.6HG0506430</i>	no	WD40 protein binding-signal transduction and transcription regulation
<i>22-HORVU.MOREX.r2.7HG0564420</i>	Yes	<i>SPL14</i> (SQUAMOSA-Promoter BINDING PROTEIN) boundary specification
<i>23-HORVU.MOREX.r2.3HG0253600.1</i>	Yes	(<i>LAX1</i>) Basic helix-loop-helix (bHLH) transcription factor, Axillary meristem formation
<i>24-HORVU.MOREX.r2.5HG0381550.1</i>	Yes	<i>Laxatum-a (lax-a)</i> -controls internode length, floral organ identity, and rachis development

4.0. Discussion

Inflorescence morphology in grasses displays a widely divergent and complex architecture, such as the branchless form of barley and wheat spikes, and severely branched inflorescence structures like the panicle of sorghum and rice. In the current study, we hypothesized that spatiotemporal activity and dosage of *RA2* expression patterns in different grasses (barley, wheat, and sorghum) might cause differences in inflorescence architectures (Koppolu et al., 2022; Koppolu & Schnurbusch, 2019). To test this hypothesis, transgenic barley experiments were carried out by transforming a *ra2* mutant with different constructs containing the *HvRA2* coding sequence, fused with swapped regulatory regions of *RA2* from barley, sorghum, or wheat. Notably, each construct complemented the mutant with the wild-type phenotype without a noticeable difference between the different constructs. These results could be attributed to the lack of unknown regulatory elements from the selected promoters of *RA2*.

4.1. Identification of *cis*-motifs and promoter's analysis

Regulation of gene expression is controlled by the interaction of transcription factor with *cis*-acting elements in the promoter region known as the transcription factors binding site (TFBS), the variation in TFBS provides more significant contributions to different expression patterns, leading to phenotypic variation between different species, which is attributed to changes in the *cis*-elements of the promoter regions (Signor & Nuzhdin, 2018; Sobel & Streisfeld, 2013; Vatov et al., 2021). The *cis*-regulatory elements determine the spatiotemporal patterns and levels of gene expression. Therefore, changes in these regulatory elements might lead to variability in the activity of the promoter between different species (Galli et al., 2020; X. Wang et al., 2021).

The identification of these regulatory regions remains a challenging task, especially in large genomes such as wheat and barley, which might be located hundreds of kb away from the target gene (Galli et al., 2020; Z. Lu et al., 2019; Stam, Belele, Ramakrishna, et al., 2002), considering this information; selection of the putative promoters must be appropriately carried out to generate meaningful results.

The significant differences in the expression levels of *RA2* were observed between barley and Wheat (Koppolu & Schnurbusch, 2019), which could be attributable to interspecific variability in cis-regulatory sequences in the promoter regions between barley and wheat. The motifs enrichment analysis in the promoter region of the differentially expressed gene in *ral* mutant ears identified several putative TFBS; including TFBS for targets such as bZIP, LEAFY (LFY), and MADS-box TFs, which play important roles in branch determinacy (Eveland et al., 2014).

In the present study, the in-silico analysis for the selected promoter region for *RA2* estimated several putative TFBS presents in the promoter region. These binding sites are mostly associated with TFs families, which are predicted to be involved in the regulation of inflorescence development, such as MADS-box TFs (C. Liu et al., 2009; Wei et al., 2019), Myb (Barg et al., 2005), AP2/ERF (Nakano et al., 2006), C2H2 (Gallavotti et al., 2010; Lyu & Cao, 2018), TCP (Dixon et al., 2018; González-Grandío & Cubas, 2016; Poursarebani et al., 2020), bZIP (Gai et al., 2020; Pourabed et al., 2015), NAC/NAM (G. Liu et al., 2022), Dof (Rojas-Gracia et al., 2019), and AT-hook (F. Y. Peng et al., 2016). The predicted biological function for these TFs is summarized in (Appendix Table 2.).

Previous studies by F.Y.Peng et al., (2016) showed that some genes with similar numbers of predicted TFBSs tend to exhibit similar expression patterns. The current study indicated that the predicted TFBSs for *RA2* are conserved among the three species, which might indicate the

conserved function of *RA2* among different species. Although, the number of the predicted TFBSs of *RA2* varied considerably among barley, wheat, and sorghum (**Figure 3.1.2**). This variation in the number of predicted TFBS could be one of the attributes of the change in the expression pattern of *RA2* among the three species (barley, wheat, and sorghum).

Further analysis by the FIMO motif search tool of the non-conserved sequences of the promoter regions of *RA2* among barley, Sorghum, and wheat, identified a putative motive repeated three times in wheat compared to one in barley and sorghum. This motif is a putative TFBS for two types of transcription factors; the C2C2-Dof transcription factor and the vernalization gene 1 (*VRN1*) binding motif (Figure 3.1.3 C); the C2C2-Dof function as a transcriptional activator or a repressor in plant growth and development (Yanagisawa, 2004), and the *VRN1* encodes a MADS-box transcription factor involved in the regulation of vernalization and plant flowering through regulating other gene expressions (Deng et al., 2015). In our study, the prediction of TFBSs in the *RA2* promoters and their distribution patterns in the selected sequences in all three species proposed that the selected promoter's length of *RA2* might be sufficient for transcriptional regulation; and in turn, might also be sufficient for the transgenic analysis study.

4.2. Promoter activity localization

The spatial-temporal gene expression patterns often correlate with plant morphology. As was shown by (Vollbrecht et al., 2005), in which differences in inflorescences morphology between maize, Sorghum, and Miscanthus correlated with the onset of *RA1* expression. *RA2*, as a transcriptional regulator of *RA1* in maize, starts expressing after primary branch meristem initiation (Bortiri et al., 2006). Compared to the branched inflorescences of rice, maize, and sorghum, the *RA2* expression in barley and wheat spikes, is initiated at an earlier developmental

stage. In barley, *RA2* expression starts at the vegetative stage and reaches its highest expression at the Triple mound/Glume primordia, and afterward, the expression goes down (Koppolu et al., 2013). Therefore, it was hypothesized that the spatial-temporal activity of *RA2* expression in Triticeae species compared to sorghum could be one of the reasons for the differences in the inflorescence morphology between barley, wheat, and sorghum (Koppolu & Schnurbusch, 2019). In the current study, contrary to our hypothesis, we could not pinpoint the spatial-temporal expression localization using the GFP reporter lines for barley, wheat, and Sorghum *RA2* promoter sequences. The GFP fluorescence signal was observed ubiquitously across different developmental stages, without noticeable differences between different *RA2* promoters cloned from barley, wheat, and sorghum (Figure 3.3.1.1). A possible explanation for these results is that the cloned promoters from the species in our studies were not complete and might be missing some cis-regulatory elements related to the spatial and temporal expression regulation of the species-specific *RA2* genes.

Previous studies conducting promoter analysis broadly support this finding, indicating the importance of cis-elements for the temporal and spatial expression pattern (G. Tang et al., 2021). For example, it was shown that the removal of cis-elements from the 5' terminal end of seed-specific promoter *AhLECIA* led to constitutive expression of the gene in roots, rosettes, stems, flowers, and seeds of Arabidopsis (G. Tang et al., 2021). Also, the deletion of 20 bp in the fruit-specific promoter for the curcumin gene, which contained an enhancer element, led to constitutive expression of the gene in leaf epidermal cells (Yamagata et al., 2002).

Furthermore, the loss of spatial and temporal control of seed-specific promoters from wheat and barley transformed in rice was attributed to differences in the cis-element differences between these species (Furtado et al., 2008). A gain-of-function mutant of *LEAFY COTYLEDON1 (LEC1)*

in Arabidopsis resulted in the ectopic expression of *LECI* due to a deletion in the promoter region (Casson & Lindsey, 2006). These studies indicate that the most important limitation lies in the limitation of information concerning cis-regulatory elements. What makes the mechanism for the spatial-temporal expression profile of a gene remains unclear.

4.3. No clear difference between the amount of expression of the GFP driven by different RA2 promoters

The expression analysis of *GFP* driven by the different promoters from barley, wheat, and sorghum *RA2* showed a variation in the expression pattern in T2 generation between and within transgenic lines. With the exception that the expression of *GFP* driven by sorghum regulatory element was much lower in all lines compared to barley and wheat constructs (Figure 3.3.2.1). Such differences in the transgene expression could be explained by transgene copy number and positional effects from different transgenic events. In line with the positional effects, the *HvRA2* CDS tagged with *GFP* transgenic lines displayed different *GFP* expressions pattern among different events for the same construct (Figure 3.5.4.2). This finding is supported by several studies that showed that transgene expression pattern is dependent on the site of integration and copy number, and zygosity level (Bag & Ryde, 1993; Campus & Road, 2009; Hensel et al., 2011; Holubová et al., 2018; Peach & Velten, 1991). Despite the place of integration into the genome and copy number not being determined in the current study, we propose that the sorghum *RA2* promoter is potentially weaker than the barley and wheat *RA2* promoters.

4.4. Complementation of RA2 fused with different promoters into BW-NIL(*mull.a*) background

In the barley spike, a predetermined developmental program controls the number of spikelets and florets produced at one rachis node. It produces three spikelets at one rachis node and one floret

on a determinate rachilla. However, in some barley mutants such as *Six-rowed spike 4 (vrs4)*, *compositum 1 (com1)*, and *compositum 2 (com2)*, such a canonical developmental program is disturbed, leading to the development of more than three spikelets and more than one floret (Forster et al., 2007; Koppolu et al., 2013; Poursarebani et al., 2015, 2020).

In many of the *vrs4(hvra2)* mutant alleles, spikelet determinacy and identity are lost, resulting in the production of additional spikelets and florets or branching inflorescence-like structures (Koppolu et al., 2013). Functional *HvRA2* is a crucial regulator of row type and in parallel controls spikelet and floret determinacy and identity (Koppolu et al. 2013; van Esse et al. 2017; Zwirek et al. 2019). For example, it negatively affects lateral spikelet fertility by regulating *VRS5* and *VRS1* (de Souza Moraes et al., 2022; Komatsuda et al., 2007; Koppolu et al., 2013).

In the current study, initially, we transformed *BW-NIL(mul1.a)* with native *RA2* constructs (Figure 3.1.2.1). The transformed plants showed a partial two-rowed condition and repression of spikelet indeterminacy/spike branching observed in *ra2* mutants (3.1.2.2). Similarly, the transformed plants with sorghum constructs (Figure 3.1.4.1F) displayed a similar phenotype to the native *HvRA2* barley construct (Figure 3.1.4.1). In comparison, *HvRA2* CDS fused with regulatory elements from wheat was able to recover wild-type phenotype in the *ra2* mutant *BW-NIL(mul1.a)* background (Figure 3.1.3.2).

These results collectively suggest, though from a low number of independent events, that the cis-elements of the wheat promoter used were sufficient to recover wildtype inflorescence architecture, whereas these elements appear to be missing from barley and sorghum promoters. Therefore, these data needed to be confirmed in additional independent events. In fact, the transformation efficiency in barley is highly genotype-dependent (Harwood, 2012; Hensel et al., 2008; Y. Li, Guo, et al., 2021). To date, the most responsive barley genotype to transformation is

cv. Golden Promise (GP). The transformation efficiency of GP might reach about 86% using *Agrobacterium*-mediated transformation in the immature embryo of barley (Hensel et al., 2008). While the transformation of other genotypes using the established protocol by Hensel et al., (2008) was achievable but at a very low transformation rate, and in some winter genotypes, the transformation was impossible (Hensel et al., 2008) it was difficult to get more transgenic events using the BW-NIL(*mull1.a*) background. Therefore, we could not get a more conclusive answer from this germplasm whether the cis-elements of *RA2* play a role in the morphological difference in the inflorescences of barley, wheat, and sorghum.

To circumvent these obstacles, we further generated *ra2* mutant in the GP background to follow up with our hypothesis by using a high-efficiency RGEN KO approach. The *ra2* knockout mutant in the GP background was used for promoter swapped *RA2* transgenic complementation studies.

4.5. Complementation of *RA2* fused with different promoters into RGEN *ra2* mutant (Golden Promise background)

Three transgenic constructs containing the *HvRA2* coding sequence, fused with gene regulatory regions of *RA2*, from barley, sorghum, and wheat, were transformed in RGEN knockout *ra2* mutants GP background, and they were characterized at the phenotypic and molecular level.

4.5.1. Barley *RA2* fused with regulatory regions from different species showed partly near-complete recovery of wild-type inflorescence architecture.

The phenotypic evaluation of the RGEN *hvra2* *KO* mutant transformed with *HvRA2CDS* fused with *RA2* promoters from barley, wheat, and sorghum showed a restoration of wild-type phenotype, i.e., reversion of complete or partial two-rowed condition and repression of spikelet

indeterminacy/spike or branching without significant differences in the spike phenotype between transgenic plants transformed with different constructs. These results indicate that the *HvRA2* transgene is sufficient to recover regular inflorescence architectures in the *ra2* mutant background regardless of the used promoter length and cis-element architecture.

One possible explanation for these results is that the expression pattern of *RA2* is broadly conserved among different grass species. *RA2* might have a conserved function for shaping the initial steps of the inflorescence architecture in grasses (Bortiri et al., 2006; Koppolu et al., 2013; H. Lu et al., 2017; Y. Zhang et al., 2020). The variation in inflorescence architecture between different species might be due to different modified downstream target genes, which need *RA2* protein to achieve their function (Koppolu et al., 2013). Therefore, it is challenging to determine the actual cause for variation in morphology between different species without investigating downstream target genes.

Previously published data have shown that many genes act downstream of *HvRA2* in maintaining spikelet meristem identity and determinacy. Such as *COMPOSITUM* genes, including *COM1*; (class II TCP TF); and *COM2* (AP2-ERF TF), *SQUAMOSA PROMOTER-BINDING-LIKE 8* gene (*SPL8*), *HvSRA (TPP)*, *HOX1(VRS1)* (de Souza Moraes et al., 2022; Koppolu et al., 2013, 2022; Poursarebani et al., 2020). Loss of function of any of the downstream target genes for *HvRA2* led to the indeterminate nature of spikelets meristem identity and produced a six-rowed phenotype (Komatsuda et al., 2007; Koppolu et al., 2013; Liller et al., 2015; Poursarebani et al., 2020; Zwirek et al., 2019). Therefore, in the current study, we propose that the ectopic expression of the transgene *HvRA2* protein, even only in a small amount, was sufficient for the downstream target gene to maintain spikelet determinacy and identity.

4.5.2. *HvRA2* transgene recovers normal inflorescence architectures in *ra2* mutants independent of the *HvRA2* dosage.

The variation in inflorescence architecture is often influenced by the dosage of gene expression involved in spikelet and floret development in cooperation with other genes in the regulatory network (Debernardi et al., 2017; Dixon et al., 2018; Greenwood et al., 2017; Houston et al., 2013; Miura et al., 2010; Park et al., 2014; Soyk et al., 2017; W. Wang et al., 2018; Z. Zhu et al., 2013). As an example of the gene dosage effect on the spike architecture, the increased dosage of *TBI* causes a paired spikelet phenotype in wheat; here, an additional spikelet is produced dorsally to the primary spikelet and delays inflorescence growth by reducing the expression of meristem identity genes (Dixon et al., 2018).

Barley *INTERMEDIUM-SPIKE C (INT-C)*, also known as *VRS5*, an ortholog of *TBI*, acts downstream of *HvRA2* to suppress the development of the lateral spikelets but not inflorescence branching (Koppolu et al., 2013; van Esse et al., 2017; Zwirek et al., 2019). Moreover, *VRS5* interacts with *COM1* in controlling spikelet meristem identity (de Souza Moraes et al., 2022). Furthermore, *COM1*(CYC/TB1-type) was identified as a downstream target for *HvRA2* in control inflorescence branching via specifying meristem identity (Poursarebani et al., 2020; Shang et al., 2020).

A higher level of *RA2* expression in wheat at an earlier developmental stage might limit the number of spikelets per rachis node to one, compared to three spikelets per rachis node in barley, which has a lower level of *RA2* expression at a similar developmental stage (Koppolu & Schnurbusch, 2019). In the present study, our transgenic analyses showed that the *HvRA2* transgene recovers wild-type phenotype in *ra2* mutants independent of the *HvRA2* dosage, which confirms the

conserved role of *RA2* at the initial step in lateral organ development. Furthermore, other genes in the same pathway may control the rest of the inflorescence development.

The qRT-PCR analysis of the *HvRA2* transgene expression showed a significantly decreased regulation of *HvRA2* driven by *SbRA2* sorghum regulatory elements compared to *HvRA2* expression driven by regulatory elements from barley and wheat. However, while the transcript level was lowest in transgenic plants transformed with *HvRA2CDS* driven by *SbRA2* sorghum regulatory elements, it was still able to recover the normal inflorescence phenotype. Whereas the highest level of expression was observed in transgenic plants transformed with *HvRA2* fused with its regulatory elements. In line with the expression analysis in stable transformants, the transient assay expression analysis in rice protoplasts for measuring basal promoter activity showed that the barley *RA2* promoter gives the highest expression level compared to sorghum and wheat *RA2* promoter (Figure 3.5.2.2.1); however, at this point, we cannot completely rule out the possibility that several other factors might have influenced this result, such as copy number and positional effects (Bag & Ryde, 1993; Campus & Road, 2009; Hensel et al., 2011; Holubová et al., 2018; Peach & Velten, 1991). In conclusion, these results suggest that *RA2* has a conserved role among grasses for the initial steps of inflorescence architecture development in cereals; therefore, low transcript levels were sufficient to trigger the downstream gene to maintain spikelet meristem identity and determinacy.

4.5.3. The constitutive *HvRA2* expression with higher dosage is negatively associated with plant height

In the current study, the most significant phenotypic change associated with gene dosage was the reduced plant height observed in transgenic plants transformed with the barley constructs compared to transgenic plants transformed with sorghum and wheat constructs (**Figure 3.5.3.4**).

The high conservation of *HvRA2* protein sequences among different species, which encodes a LOB domain (LBD) transcription factor, implies a conserved protein function. The LOB transcription factor genes are characterized by their expression in the boundary region between SAM and lateral organs, which play an important role in boundary formation and organ separation (Bell et al., 2012; Bortiri et al., 2006; Koppolu et al., 2013; H. Lu et al., 2017; Shuai et al., 2002). Boundary formation and organ separation are usually characterized by low rates of cell division, expansion, and differentiation (Wang et al., 2016); this might explain the reduction in plants' height combined with the detection of the high transcript level of the *HvRA2* in transgenic plants transformed with the barley construct. In line with plant height reduction in these barley plants, overexpressing *HvRA2* barley and wheat transgenic lines (cv *Bobwhite*) showed stunted growth, upward leaf curling, and a very short spike with no grains in T0 (**Figure 3.2.1.1**). These results are consistent with previously published data, where the transgenic plants overexpressing different *LBD* genes exhibited a similar morphological defect with stunted organs (Bell et al., 2012; Fan et al., 2012; H. Lu et al., 2017; Naito et al., 2007; Shuai et al., 2002). Such phenotypic defects in our transgenic lines overexpressing *RA2* suggest that the overexpression of *RA2* promotes low rates of cell division, expansion, and differentiation in combination with premature organ boundary formation, resulting in stunted plants.

4.6. Knockout of *HvRA2* in barley cultivar Golden Promise mediated by RNA-guided endonuclease (RGEN) approach

Agrobacterium transformation in the BW-NIL(*mull.a*) background was inefficient. As discussed previously(see section 3.1), barley transformation is recalcitrant and highly genotype dependent, the genetic transformation in barley is often an inefficient, laborious, and time-consuming process (Harwood, 2012; Hensel et al., 2008; Y. Li, Guo, et al., 2021). To obtain *ra2 mutant* into a highly

transformable genotypic background, we used the RNA-guided Cas9 endonuclease strategy to knock-out *HvRA2* in the GP cultivar, a model genotype for barley transformation (Hensel et al., 2008; Hisano et al., 2017).

The use of an RNA-guided Cas9 endonuclease approach has evolved as a robust and highly efficient genome-editing tool that has been successfully used in barley (Gasparis et al., 2019, 2018; Kapusi et al., 2017; Lawrenson et al., 2015, 2021; Zeng et al., 2020).

In this study, two gRNAs were used to increase the success rate of the mutation induction. The frequency of the mutation rate in T0 plants was about 40%, which is comparable to the previously reported studies in barley (Holme et al., 2017; Lawrenson et al., 2015; Q. Yang et al., 2020; Zeng et al., 2020). Another important advantage of using dual gRNAs is finding fragment deletion between two gRNA target sites. The dual gRNA-based deletions were previously reported in several plant species such as barley, wheat, tomato, and Arabidopsis (Brooks et al., 2014; Cui et al., 2019; Kapusi et al., 2017; Pauwels et al., 2018; Zeng et al., 2020). Both gRNAs were designed to target *HvRA2* at the beginning of the coding sequences, away from the conservative coding region of the LOB domain, to avoid off-targets in other LOB genes.

In agreement with the previous studies, most of the observed mutations in T0 were indels (insertion/deletions) or single base substitutions, located at 3-7 nucleotides upstream of the PAM sequence (3.4.1.2.2), and most of the mutations found in T0 plants were transmitted to the T1 generation (Holubová et al., 2018; Lawrenson et al., 2015; Zeng et al., 2020); however, few plants showed new mutation types in T1 that were not observed in T0 plants (Figure 3.4.2.1), which could be explained by the heterozygosity and chimeric status of T0 plants. In addition to the presence of an active gRNA/Cas9 transgene, which generates more mutation types in subsequent generations as long as the target site is the wild-type, it also increases the chance of off-target mutation (Feng

et al., 2014; Zeng et al., 2020; H. Zhang et al., 2014; N. Zhang et al., 2020). Therefore, we must select homozygous, transgene-free mutant lines to fix the targeted mutation for our study purposes.

The CRISPR/Cas9 system has been successfully applied to a variety of plant species to generate transgene-free plants (Aliaga-Franco et al., 2019; Gasparis et al., 2019a; Kapusi et al., 2017; Lawrenson et al., 2015; J. Li et al., 2016; Liang et al., 2017; Zeng et al., 2020). In the present study, transgene-free homozygous *hvra2* knockout mutants were successfully obtained in the T1 generation via genetic segregation.

According to previous reports, there is a low possibility of off-target mutations caused by CRISPR/Cas9, which is mainly based on the designed gRNA (Lawrenson et al., 2015; J. Li, Manghwar, et al., 2019; X. Tang et al., 2018; N. Zhang et al., 2020). The target sequences with three or more mismatches are not recognized by the Cas 9 nuclease, and the Cas9 activity is highly reduced, if at least one mismatch is present in the ‘seed’ region, or if three or more mismatches occur in the entire protospacer sequence (Arndell et al., 2019; Gasparis et al., 2019). Therefore, the most effective way to avoid off-target mutations is by designing highly specific gRNAs to the target site with no homology to other genomic regions (N. Zhang et al., 2020). The present study designed the gRNAs using the DESKGEN online platform (Doench et al., 2016), including a detailed off-target analysis for the selected gRNA. Three potential off-targets were determined, and performed PCR and sequencing of these candidate targets revealed no changes in the genome of the selected off-target regions, indicating that the gRNA design was very effective.

4.6.1. The *hvra2* RGEN knock-out mutant lost its spikelet determinacy and identity.

Previous studies identified barley *Six-rowed spike 4 (VRS4)* as an ortholog of the maize *RA2* (Koppolu et al., 2013). In *hvra2* mutants(*vrs4* mutant), spikelets lost their determinacy by

producing more than three spikelets per node and lost their identity by producing branch-like meristems and developing a spike-branching architecture (Koppolu et al., 2013). Additionally, *HvRA2* regulates the barley row-type by promoting transcriptional control over *VRS1*, a (Homeodomain- leucine zipper transcription factor) (Koppolu et al., 2013). In the WT condition, *HvRA2* transcriptionally regulates *VRS1*, which in turn promotes the two-rowed condition (**Figure 4.5.1. A**). However, when *hvra2* is mutated, the transcription of *VRS1* (a negative regulator of LS fertility) is reduced /abolished, resulting in the six-rowed condition (**Figure 4.5.1 C, D**) (Koppolu et al., 2013). In line with this data, our RT-PCR analysis showed that *VRS1* expression was significantly abolished in the *RGEN ra2* mutant (Figure 3.4.3.1), displaying a phenotype with indeterminate spikelets and spike branching (**Figure 4.6.1.D**).

Together, these studies indicate that the functional *HvRA2* is important for regulating spikelet determinacy and branch outgrowth, consistent with a previous report by Koppolu et al., (2013). In the present study, we successfully performed targeted mutagenesis of *HvRA2* genes in barley cultivar Golden Promise via CRISPR/Cas9- mediated genome editing. Furthermore, transgene-free homozygous *hvra2* mutants could be generated in barley transformation for further functional studies.

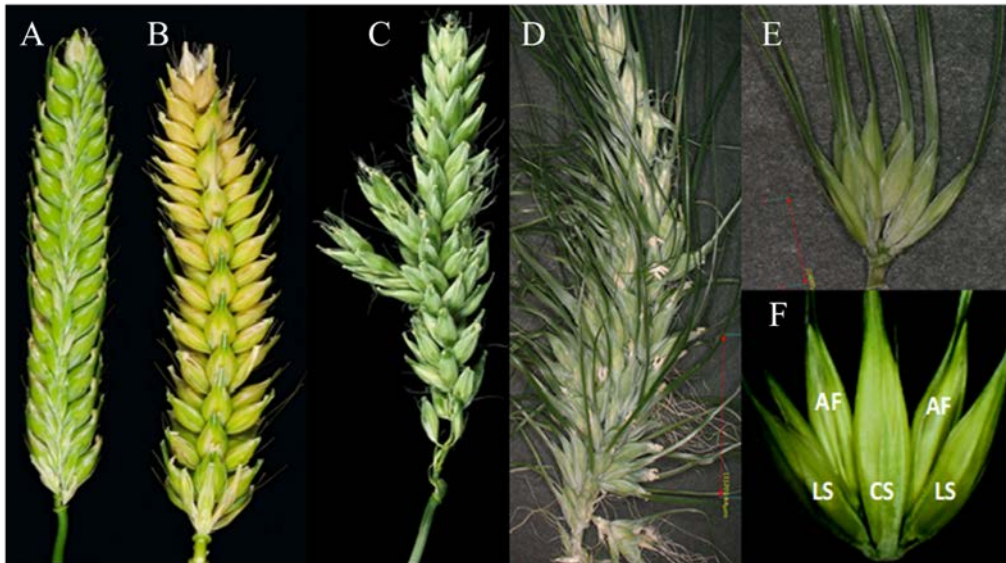


Figure 4.6.1. Spike phenotypes of *HvRA2* RGEN knock out mutant and gamma-ray induced BW-NIL(*mull.a*). (A) two-rowed barley with wild type alleles at *Vrs1* and *RA2(Vrs4)*. (B) Six-rowed barley with wild-type *RA2* and mutated *vrs1* alleles. (C) gamma-ray induced *hvra2* (*vrs4*) mutant displaying six-rowed barleys with indeterminate triple spikelets (D) RGEN knockout mutant in the Golden Promise background, displaying six-rowed barleys with indeterminate spikelet triplets. (E) Indeterminate spikelet triplet of RGEN *hvra2* mutant showing additional florets (F) Indeterminate spikelet triplet of gamma-ray induced *hvra2* (*vrs4*) BW-NIL(*mull.a*) Legend: LS – Lateral Spikelet; CS – Central Spikelet; AF – Additional Floret; F – floret. Figures related to BW-NIL(*mull.a*) were Adopted from (Koppolu et al., 2013)

4.7. Possible interaction between *HvRA2* and other genes related to spike development

To explore the regulation pathway of *HvRA2* in inflorescence development, we utilized the high-resolution RNA-sequencing data generated by Thiel et al., (2021). This dataset identified multiple genes involved in organ boundary formation, signaling, and meristem maintenance. The organ boundaries are maintained to separate different cell groups from each other. Furthermore, they are characterized by low cell division and differentiation rates, resulting in plant height reduction (Q. Wang et al., 2016). These phenomena are achieved by lowered auxin (Cao & Jiao, 2019; Heisler

et al., 2005; Vernoux et al., 2011) and BRs (Bell et al., 2012; Gendron et al., 2012) levels in the organ boundaries. Auxin controls BR biosynthesis by regulating a BR biosynthetic gene. Moreover, BR and auxin have similar distribution patterns (Chung et al., 2011; Rast & Simon, 2008).

In the current studies, a targeted Y2H Assay was performed for protein-protein interactions between *HvRA2* and some of these genes obtained from RNA seq data generated by Thiel et al., (2021). The proteins that interacted with *HvRA2* were involved in different aspects of plant floral organ development and hormone signaling. Such as *HvDEP1*; which is involved in cell proliferation regulation (Bélanger et al., 2014; Thiel et al., 2021; Vavilova et al., 2017; Watt et al., 2020; Wendt et al., 2016); *ARF-14-like* playing a role in auxin that triggers a signaling pathway (Galli et al., 2018; Guilfoyle & Hagen, 2012; Hagen & Guilfoyle, 2002; Okushima et al., 2005); *HvCULA*, involved in plant organ development, boundary specification (Tavakol et al., 2015); *HvSPL14*, having an essential function in boundary specification (Thiel et al., 2021); *laxatum-a* (*lax-a*) a homolog of *CULA*, controls internode length, floral organ identity and rachis development (Jost et al., 2016)); and *OFP8-like*, a negative regulator of BR signaling (S. Wang et al., 2011; C. Yang et al., 2016). In Arabidopsis, LOB and BR form a feedback loop to regulate BR accumulation in organ boundaries to reduce cell division and limit growth, thus promoting boundary formation (Bell et al., 2012).

The barley *hvra2* mutants display defects in organ boundary formation, producing a spike branching phenotype. We propose that in *hvra2* mutants, the boundary formation is disturbed due to the abundance of BRs within the boundary domain. In the present study, the overexpressing *HvRA2* transgenic lines showed stunted growth, upward leaf curling, and very short spikes with few spikelets and floral development defects in T0 plants (Figure 3.2.1.1). Similar phenotypes

were also observed in Arabidopsis overexpressing the *AtLOB* gene (Bell et al., 2012; Shuai et al., 2002). Such phenotypic defects in our transgenic lines overexpressing *RA2* suggested that the overexpression of *RA2* promoted premature organ boundary formation by lowering BR levels compared to WT conditions. Furthermore, *HvRA2* transcripts were detected at the spikelet primordia during early developmental stages and throughout the boundary region during the stamen primordia stage (Koppolu et al., 2013); this supports the hypothesis that *HvRA2* may regulate boundary-related genes non-autonomously from the spikelet boundary domain via a movable signal to the adjacent meristem (Whipple, 2017; Zwirek et al., 2019). Overall, these studies suggest that *RA2* achieves its function by regulating multiple sets of genes involved in organ boundary formation and hormone signaling.

5.0. Outlook

1- *HvRA2* encodes a LOB domain (LBD) Transcription factor that controls the activity of downstream genes by binding to specific upstream DNA sequences known as cis-elements. Therefore, understanding the regulatory interaction networks for *HvRA2* and identifying the direct or indirect targets of *HvRA2* will help us to understand the molecular mechanisms involved in shaping barley spike architecture. To achieve this, we would utilize DAP-seq (DNA Affinity Purification sequencing (Galli et al., 2020; O'Malley et al., 2016); technique in barley. Which will allow us to discover novel TFBS and target genes for *HvRA2* even if distally located.

2- Knocking out putative genes involved in organ boundary formation to understand their regulation with *HvRA2*. With the aim of better understanding the boundary formation, we would utilize the RNA-seq data generated by Thiel et al., (2021), and identify putative genes involved in

the regulation of boundary formation, and generate loss-of-function mutants for these genes either through TILLING or RGEN approaches.

3- Profiling of phytohormones, auxin, and BRs in the *hvra2* mutants, and transgenic lines overexpressing *HvRA2*. The lateral organ boundary formation is characterized by a low rate of cell division, and this is achieved by spatial organization and control of auxin and BR (Bell et al., 2012; Gendron et al., 2012; Heisler et al., 2005; Vernoux et al., 2011). In the current study, the *HvRA2* protein-protein interaction showed two interacting proteins that are involved in hormonal signaling, including Auxin signaling (ARF-14-like) and BR signaling (a transcription repressor OFP8-like).

4- Validate the result of gene interaction from the Y2H experiment by using other methods such as (BiFC) or Co-Immunoprecipitation (Co-IP) and then followed by knocking out the genes that will be confirmed to study their potential interactions with *HvRA2*.

6.0. Summary

Inflorescence architecture in grasses is considered one of the most important agronomic traits affecting crop yield. The inflorescence architecture is quite diverse, which includes branchless forms, such as the spike of barley and wheat, to more branched inflorescence, such as the panicle of sorghum. Identifying the genetic regulation of inflorescence developmental and molecular mechanisms behind the variation in inflorescence architecture is essential to increasing cereal crop yields. *RAMOSA2* (*RA2*) encodes a LATERAL ORGAN BOUNDARY (LOB) domain transcription factor and is one of the central regulators in controlling inflorescence development among numerous species (Bortiri et al., 2006). The spatial-temporal activity of *RA2* expression and its dosage variation among different species could be one of the reasons for the variation in inflorescence architecture among different species, such as barley, sorghum, and wheat (Koppolu & Schnurbusch, 2019).

In the present study, to examine the spatial-temporal activity of *RA2* and its dosage among barley, wheat, and sorghum, transgenic experiments were carried out by swapping *RA2* promoters of different species fused with *HvRA2* CDS and performing genetic complementation studies in branched barley *ra2* mutant background and then quantifying recovery of canonical spike phenotypes.

A transgene that includes endogenous native *HvRA2*, including upstream and downstream flanking sequences, recovered near-complete wild-type spike phenotypes in *ra2* mutant plants; similar results were obtained with transgenes transformed with *HvRA2* CDS fused with *RA2* regulatory sequences from wheat and sorghum.

Expression analyses of *HvRA2* transgenes revealed that it was ubiquitously expressed in all constructs but with a lower amount of expression using the upstream and downstream flanking region from sorghum *RA2*. Nevertheless, the *HvRA2* fused with sorghum *RA2* regulatory sequence recovered the normal inflorescence phenotype. This pattern of ectopic expression indicates that the used regulatory sequences from this study are incomplete and may miss the cis-acting elements required for spatial-temporal activity. However, these data suggest a conserved function of *RA2* at the initial step in lateral organ development, and a low amount of *RA2* protein is sufficient to trigger the downstream target genes for proper inflorescence formation.

7.0. Zusammenfassung

Die Blütenstandsarchitektur von Gräsern gilt als eines der wichtigsten agronomischen Merkmale, die den Ernteertrag beeinflussen. Die Blütenstandsarchitektur ist sehr vielfältig und umfasst verzweigte Formen wie die Ähre von Gerste und Weizen bis hin zu verzweigteren Blütenständen wie der Rispe von Sorghum. Die Identifizierung der genetischen Regulation der Blütenstandsentwicklung und der molekularen Mechanismen hinter der Variation in der Blütenstandsarchitektur ist für die Steigerung der Getreideerträge von wesentlicher Bedeutung. *RAMOSA2* (*RA2*) codiert einen Transkriptionsfaktor der LATERAL ORGAN BOUNDARY (*LOB*)-Domäne und ist einer der zentralen Regulatoren bei der Steuerung der Infloreszenzentwicklung bei zahlreichen Arten (Bortiri et al., 2006). Die räumlich-zeitliche Aktivität der *RA2*-Expression und ihre Dosisvariationen zwischen verschiedenen Arten könnten einer der Gründe für die Variation der Blütenstandsarchitektur zwischen verschiedenen Arten wie Gerste, Sorghum und Weizen sein (Koppolu & Schnurbusch, 2019).

In der vorliegenden Studie wurden zur Untersuchung der räumlich-zeitlichen Aktivität von RA2 und seiner Dosierung bei Gerste, Weizen und Sorghum transgene Experimente durchgeführt, indem RA2-Promotoren verschiedener Arten, die mit HvRA2-CDS fusioniert waren, ausgetauscht und genetische Komplementationsstudien in verzweigtem Gersten-ra2 durchgeführt wurden. Mutantenhintergrund und anschließende Quantifizierung der Wiederherstellung kanonischer Spike-Phänotypen.

Ein Transgen, das endogenes natives HvRA2 enthält, einschließlich stromaufwärts und stromabwärts gelegener flankierender Sequenzen, hat nahezu vollständige Wildtyp-Spike-Phänotypen in ra2-Mutantenpflanzen gewonnen; ähnliche Ergebnisse wurden mit Transgenen erhalten, die mit HvRA2-CDS transformiert waren, das mit regulatorischen RA2-Sequenzen aus Weizen und Sorghum fusioniert war.

Expressionsanalysen von HvRA2-Transgenen enthüllten, dass es in allen Konstrukten allgegenwärtig exprimiert wurde, jedoch mit einer geringeren Expressionsmenge unter Verwendung der stromaufwärts und stromabwärts gelegenen flankierenden Region von Sorghum RA2. Nichtsdestotrotz stellte das mit der regulatorischen Sequenz von Sorghum RA2 fusionierte HvRA2 den normalen Blütenstandsphänotyp wieder her. Dieses Muster der ektopischen Expression weist darauf hin, dass die verwendeten regulatorischen Sequenzen aus dieser Studie unvollständig sind und möglicherweise die cis-wirkenden Elemente vermissen, die für die räumlich-zeitliche Aktivität erforderlich sind. Diese Daten deuten jedoch auf eine konservierte Funktion von RA2 im Anfangsschritt der lateralen Organentwicklung hin, bei der eine geringe Menge an RA2-Protein ausreicht, um die nachgeschalteten Zielgene für eine ordnungsgemäße Blütenstandsbildung auszulösen.

8.0. References

- Abdeeva, I., Abdeev, R., Bruskin, S., & Piruzi, E. (2012). Transgenic Plants as a Tool for Plant Functional Genomics. In R. Abdeev (Ed.), *Transgenic Plants - Advances and Limitations* (p. Ch. 13). InTech. <https://doi.org/10.5772/33553>
- Aklilu, E. (2021). Review on forward and reverse genetics in plant breeding. *All Life*, *14*(1), 127–135. <https://doi.org/10.1080/26895293.2021.1888810>
- Aliaga-Franco, N., Zhang, C., Presa, S., Srivastava, A. K., Granell, A., Alabadí, D., Sadanandom, A., Blázquez, M. A., & Minguet, E. G. (2019). Identification of Transgene-Free CRISPR-Edited Plants of Rice, Tomato, and Arabidopsis by Monitoring DsRED Fluorescence in Dry Seeds. *Frontiers in Plant Science*, *10*(September), 1–9. <https://doi.org/10.3389/fpls.2019.01150>
- Alonso, J. M., & Ecker, J. R. (2006). Moving forward in reverse: Genetic technologies to enable genome-wide phenomic screens in Arabidopsis. *Nature Reviews Genetics*, *7*(7), 524–536. <https://doi.org/10.1038/nrg1893>
- Arndell, T., Sharma, N., Langridge, P., Baumann, U., Watson-Haigh, N. S., & Whitford, R. (2019). GRNA validation for wheat genome editing with the CRISPR-Cas9 system. *BMC Biotechnology*, *19*(1), 1–12. <https://doi.org/10.1186/s12896-019-0565-z>
- Badr, A., Müller, K., Schäfer-Pregl, R., El Rabey, H., Effgen, S., Ibrahim, H. H., Pozzi, C., Rohde, W., & Salamini, F. (2000). On the origin and domestication history of barley (*Hordeum vulgare*). *Molecular Biology and Evolution*, *17*(4), 499–510. <https://doi.org/10.1093/oxfordjournals.molbev.a026330>
- Bag, P., & Ryde, N. (1993). *Chromosomal Position Effects and the Modulation Transgene Expression*.
- Baik, B. K., & Ullrich, S. E. (2008). Barley for food: Characteristics, improvement, and renewed interest. *Journal of Cereal Science*, *48*(2), 233–242. <https://doi.org/10.1016/j.jcs.2008.02.002>
- Bailey, T. L., Boden, M., Buske, F. A., Frith, M., Grant, C. E., Clementi, L., Ren, J., Li, W. W., & Noble, W. S. (2009). MEME Suite: Tools for motif discovery and searching. *Nucleic Acids Research*, *37*(SUPPL. 2), 202–208. <https://doi.org/10.1093/nar/gkp335>

- Barg, R., Sobolev, I., Eilon, T., Gur, A., Chmelnitsky, I., Shabtai, S., Grotewold, E., & Salts, Y. (2005). The tomato early fruit specific gene *Lefsm1* defines a novel class of plant-specific SANT/MYB domain proteins. *Planta*, *221*(2), 197–211. <https://doi.org/10.1007/s00425-004-1433-0>
- Barone, P., Wu, E., Lenderts, B., Anand, A., Gordon-Kamm, W., Svitashv, S., & Kumar, S. (2020). Efficient Gene Targeting in Maize Using Inducible CRISPR-Cas9 and Marker-free Donor Template. *Molecular Plant*, *13*(8), 1219–1227. <https://doi.org/10.1016/j.molp.2020.06.008>
- Bélanger, S., Gauthier, M., Jean, M., Sato, K., & Belzile, F. (2014). Genomic characterization of the *Hordeum vulgare* DEP1 (*HvDEP1*) gene and its diversity in a collection of barley accessions. *Euphytica*, *198*(1), 29–41. <https://doi.org/10.1007/s10681-014-1089-1>
- Bell, E. M., Lin, W. -c., Husbands, A. Y., Yu, L., Jaganatha, V., Jablonska, B., Mangeon, A., Neff, M. M., Girke, T., & Springer, P. S. (2012). Arabidopsis LATERAL ORGAN BOUNDARIES negatively regulates brassinosteroid accumulation to limit growth in organ boundaries. *Proceedings of the National Academy of Sciences*, *109*(51), 21146–21151. <https://doi.org/10.1073/pnas.1210789109>
- Biłas, R., Szafran, K., Hnatuszko-Konka, K., & Kononowicz, A. K. (2016). Cis-regulatory elements used to control gene expression in plants. *Plant Cell, Tissue and Organ Culture*, *127*(2), 269–287. <https://doi.org/10.1007/s11240-016-1057-7>
- Boettcher, M., & McManus, M. T. (2015). Choosing the Right Tool for the Job: RNAi, TALEN, or CRISPR. *Molecular Cell*, *58*(4), 575–585. <https://doi.org/10.1016/j.molcel.2015.04.028>
- Bommert, P., Satoh-Nagasawa, N., Jackson, D., & Hirano, H. Y. (2005). Genetics and evolution of inflorescence and flower development in grasses. *Plant and Cell Physiology*, *46*(1), 69–78. <https://doi.org/10.1093/pcp/pci504>
- Bommert, P., & Whipple, C. (2018). Grass inflorescence architecture and meristem determinacy. *Seminars in Cell and Developmental Biology*, *79*, 37–47. <https://doi.org/10.1016/j.semcdb.2017.10.004>
- Bortiri, E., Chuck, G., Vollbrecht, E., Rocheford, T., Martienssen, R., & Hake, S. (2006). *ramosa2* Encodes a LATERAL ORGAN BOUNDARY Domain Protein That Determines

- the Fate of Stem Cells in Branch Meristems of Maize. *The Plant Cell*, 18(3), 574–585.
<https://doi.org/10.1105/tpc.105.039032>
- Bothmer, R. Von, Sato, K., Komatsuda, T., Yasuda, S., & Fischbeck, G. (2003). *The domestication of cultivated barley*. 9–27.
- Bouchez, D., & Ho, H. (1998). Update on Genomics Functional Genomics in Plants. *Plant Physiol.*, 118, 725–732.
- Briggs, D. E. (1978). Grain quality and germination. In *Barley*. https://doi.org/10.1007/978-94-009-5715-2_5
- Brooks, C., Nekrasov, V., Lippman, Z. B., & Eck, J. Van. (2014). *Efficient Gene Editing in Tomato in the First Generation Using the Clustered Regularly Interspaced Short Palindromic Repeats / CRISPR-Associated9 System 1*. 166(November), 1292–1297.
<https://doi.org/10.1104/pp.114.247577>
- Brown, P. J., Klein, P. E., Bortiri, E., Acharya, C. B., Rooney, W. L., & Kresovich, S. (2006). Inheritance of inflorescence architecture in sorghum. *Theoretical and Applied Genetics*, 113(5), 931–942. <https://doi.org/10.1007/s00122-006-0352-9>
- Brown, R. H., & Bregitzer, P. (2011). A Ds insertional mutant of a barley miR172 gene results in indeterminate spikelet development. *Crop Science*, 51(4), 1664–1672.
<https://doi.org/10.2135/cropsci2010.09.0532>
- Budhagatapalli, N., Schedel, S., Gurushidze, M., Pencs, S., Hiekel, S., Rutten, T., Kusch, S., Morbitzer, R., Lahaye, T., Panstruga, R., Kumlehn, J., & Hensel, G. (2016). A simple test for the cleavage activity of customized endonucleases in plants. *Plant Methods*, 12(1), 1–10.
<https://doi.org/10.1186/s13007-016-0118-6>
- Bull, H., Casao, M. C., Zwirek, M., Flavell, A. J., Thomas, W. T. B., Guo, W., Zhang, R., Rapazote-Flores, P., Kyriakidis, S., Russell, J., Druka, A., McKim, S. M., & Waugh, R. (2017). Barley SIX-ROWED SPIKE3 encodes a putative Jumonji C-type H3K9me2/me3 demethylase that represses lateral spikelet fertility. *Nature Communications*, 8(1), 1–9.
<https://doi.org/10.1038/s41467-017-00940-7>
- Caldwell, D. G., McCallum, N., Shaw, P., Muehlbauer, G. J., Marshall, D. F., & Waugh, R. (2004). A structured mutant population for forward and reverse genetics in Barley

- (*Hordeum vulgare* L.). *Plant Journal*, 40(1), 143–150. <https://doi.org/10.1111/j.1365-313X.2004.02190.x>
- Campus, S., & Road, B. J. (2009). *Analysis of promoter activity in transgenic plants by normalizing expression with a reference gene : anomalies due to the influence of the test promoter on the reference promoter*. 34(December), 953–962. <https://doi.org/10.1007/s12038-009-0109-0>
- Cao, X., & Jiao, Y. (2019). Control of cell fate during axillary meristem initiation. *Cellular and Molecular Life Sciences*, 0123456789. <https://doi.org/10.1007/s00018-019-03407-8>
- Capilla-Perez, L., Solier, V., Portemer, V., Chambon, A., Hurel, A., Guillebaux, A., Vezon, D., Cromer, L., Grelon, M., & Mercier, R. (2018). The hem lines: a new library of homozygous arabidopsis thaliana ems mutants and its potential to detect meiotic phenotypes. *Frontiers in Plant Science*, 9(September), 1–9. <https://doi.org/10.3389/fpls.2018.01339>
- Carroll, D. (2011). Genome engineering with zinc-finger nucleases. *Genetics*, 188(4), 773–782. <https://doi.org/10.1534/genetics.111.131433>
- Casson, S. A., & Lindsey, K. (2006). The turnip mutant of Arabidopsis reveals that LEAFY COTYLEDON1 expression mediates the effects of auxin and sugars to promote embryonic cell identity. *Plant Physiology*, 142(2), 526–541. <https://doi.org/10.1104/pp.106.080895>
- Čermák, V., & Fischer, L. (2018). Pervasive read-through transcription of T-DNAs is frequent in tobacco BY-2 cells and can effectively induce silencing. *BMC Plant Biology*, 18(1), 1–14. <https://doi.org/10.1186/s12870-018-1482-3>
- Chen, R., Xu, Q., Liu, Y., Zhang, J., Ren, D., Wang, G., & Liu, Y. (2018). Generation of transgene-free maize male sterile lines using the crispr/cas9 system. *Frontiers in Plant Science*, 9(September), 1–8. <https://doi.org/10.3389/fpls.2018.01180>
- Chen, W.-F., Wei, X.-B., Rety, S., Huang, L.-Y., Liu, N.-N., Dou, S.-X., & Xi, X.-G. (2018). Structural analysis reveals a “molecular calipers” mechanism for a LATERAL ORGAN BOUNDARIES DOMAIN transcription factor protein from wheat. *Journal of Biological Chemistry*, 1–30. <https://doi.org/10.1074/jbc.RA118.003956>
- Christian, M., Cermak, T., Doyle, E. L., Schmidt, C., Zhang, F., Hummel, A., Bogdanove, A. J., & Voytas, D. F. (2010). Targeting DNA double-strand breaks with TAL effector nucleases.

Genetics, 186(2), 756–761. <https://doi.org/10.1534/genetics.110.120717>

- Christian, M., Qi, Y., Zhang, Y., & Voytas, D. F. (2013). Targeted Mutagenesis of Arabidopsis thaliana Using Engineered TAL Effector Nucleases. *G3: Genes, Genomes, Genetics*, 3(9), 1697–1705. <https://doi.org/10.1534/g3.113.007104>
- Chuck, G., Muszynski, M., Kellogg, E., Hake, S., & Schmidt, R. J. (2002). The control of spikelet meristem identity by the branched silkless1 gene in maize. *Science*, 298(5596), 1238–1241. <https://doi.org/10.1126/science.1076920>
- Chung, Y., Maharjan, P. M., Lee, O., Fujioka, S., Jang, S., Kim, B., Takatsuto, S., Tsujimoto, M., Kim, H., Cho, S., Park, T., Cho, H., Hwang, I., & Choe, S. (2011). Auxin stimulates DWARF4 expression and brassinosteroid biosynthesis in Arabidopsis. *Plant Journal*, 66(4), 564–578. <https://doi.org/10.1111/j.1365-313X.2011.04513.x>
- Claeys, H., Vi, S. L., Xu, X., Satoh-Nagasawa, N., Eveland, A. L., Goldshmidt, A., Feil, R., Beggs, G. A., Sakai, H., Brennan, R. G., Lunn, J. E., & Jackson, D. (2019). Control of meristem determinacy by trehalose 6-phosphate phosphatases is uncoupled from enzymatic activity. *Nature Plants*, 5(4), 352–357. <https://doi.org/10.1038/s41477-019-0394-z>
- Cockram, J., White, J., Zuluaga, D. L., Smith, D., Comadran, J., MacAulay, M., Luo, Z., Kearsey, M. J., Werner, P., Harrap, D., Tapsell, C., Liu, H., Hedley, P. E., Stein, N., Schulte, D., Steuernagel, B., Marshall, D. F., Thomas, W. T. B., Ramsay, L., ... Wang, M. (2010). Genome-wide association mapping to candidate polymorphism resolution in the unsequenced barley genome. *Proceedings of the National Academy of Sciences of the United States of America*, 107(50), 21611–21616. <https://doi.org/10.1073/pnas.1010179107>
- Cooper, E. A., Brenton, Z. W., Flinn, B. S., Jenkins, J., Shu, S., Flowers, D., Luo, F., Wang, Y., Xia, P., Barry, K., Daum, C., Lipzen, A., Yoshinaga, Y., Schmutz, J., Saski, C., Vermerris, W., & Kresovich, S. (2019). A new reference genome for Sorghum bicolor reveals high levels of sequence similarity between sweet and grain genotypes: Implications for the genetics of sugar metabolism. *BMC Genomics*, 20(1), 1–13. <https://doi.org/10.1186/s12864-019-5734-x>
- Cui, X., Balcerzak, M., Scherthner, J., Babic, V., Datla, R., Brauer, E. K., Labbé, N., Subramaniam, R., & Ouellet, T. (2019). An optimised CRISPR / Cas9 protocol to create

- targeted mutations in homoeologous genes and an efficient genotyping protocol to identify edited events in wheat. *Plant Methods*, 1–12. <https://doi.org/10.1186/s13007-019-0500-2>
- Dahleen, L. S., & Manoharan, M. (2007). Recent advances in barley transformation. *In Vitro Cellular and Developmental Biology - Plant*, 43(6), 493–506. <https://doi.org/10.1007/s11627-007-9068-z>
- Daly, P., McClellan, C., Maluk, M., Oakey, H., Lapierre, C., Waugh, R., Stephens, J., Marshall, D., Barakate, A., Tsuji, Y., Goeminne, G., Vanholme, R., Boerjan, W., Ralph, J., & Halpin, C. (2019). RNAi-suppression of barley caffeic acid O -methyltransferase modifies lignin despite redundancy in the gene family. *Plant Biotechnology Journal*, 17(3), 594–607. <https://doi.org/10.1111/pbi.13001>
- de Souza Moraes, T., van Es, S. W., Hernández-Pinzón, I., Kirschner, G. K., van der Wal, F., da Silveira, S. R., Busscher-Lange, J., Angenent, G. C., Moscou, M., Immink, R. G. H., & van Esse, G. W. (2022). The TCP transcription factor HvTB2 heterodimerizes with VRS5 and controls spike architecture in barley. *Plant Reproduction*, 0123456789. <https://doi.org/10.1007/s00497-022-00441-8>
- Debernardi, J. M., Lin, H., Chuck, G., Faris, J. D., & Dubcovsky, J. (2017). microRNA172 plays a crucial role in wheat spike morphogenesis and grain threshability. *Development*, 144(11), 1966–1975. <https://doi.org/10.1242/dev.146399>
- Deng, W., Casao, M. C., Wang, P., Sato, K., Hayes, P. M., Finnegan, E. J., & Trevaskis, B. (2015). Direct links between the vernalization response and other key traits of cereal crops. *Nature Communications*, 6(May 2014). <https://doi.org/10.1038/ncomms6882>
- Dixon, L. E., Greenwood, J. R., Bencivenga, S., Zhang, P., Cockram, J., Mellers, G., Ramm, K., Cavanagh, C., Swain, S. M., & Boden, S. A. (2018). TEOSINTE BRANCHED1 regulates inflorescence architecture and development in bread wheat (*Triticum aestivum*). *Plant Cell*, 30(3), 563–581. <https://doi.org/10.1105/tpc.17.00961>
- Dobrovolskaya, O. B., Amagai, Y., Popova, K. I., Dresvyannikova, A. E., Martinek, P., Krasnikov, A. A., & Watanabe, N. (2017). Genes WHEAT FRIZZY PANICLE and SHAM RAMIFICATION 2 independently regulate differentiation of floral meristems in wheat. *BMC Plant Biology*, 17(Suppl 2). <https://doi.org/10.1017/S0950268808001623>

- Dobrovolskaya, O., Pont, C., Sibout, R., Martinek, P., Badaeva, E., Murat, F., Chosson, A., Watanabe, N., Prat, E., Gautier, N., Gautier, V., Poncet, C., Orlov, Y. L., Krasnikov, A. A., Bergès, H., Salina, E., Laikova, L., & Salse, J. (2015). Frizzy panicle drives supernumerary spikelets in bread wheat. *Plant Physiology*, *167*(1), 189–199. <https://doi.org/10.1104/pp.114.250043>
- Doench, J. G., Fusi, N., Sullender, M., Hegde, M., Vaimberg, E. W., Donovan, K. F., Smith, I., Tothova, Z., Wilen, C., Orchard, R., Virgin, H. W., Listgarten, J., & Root, D. E. (2016). Optimized sgRNA design to maximize activity and minimize off-target effects of CRISPR-Cas9. *Nature Biotechnology*, *November 2015*, 1–12. <https://doi.org/10.1038/nbt.3437>
- Dong, O. X., Yu, S., Jain, R., Zhang, N., Duong, P. Q., Butler, C., Li, Y., Lipzen, A., Martin, J. A., Barry, K. W., Schmutz, J., Tian, L., & Ronald, P. C. (2020). Marker-free carotenoid-enriched rice generated through targeted gene insertion using CRISPR-Cas9. *Nature Communications*, *11*(1), 1–10. <https://doi.org/10.1038/s41467-020-14981-y>
- Druka, A., Franckowiak, J., Lundqvist, U., Bonar, N., Alexander, J., Houston, K., Radovic, S., Shahinnia, F., Vendramin, V., Morgante, M., Stein, N., & Waugh, R. (2011). Genetic Dissection of Barley Morphology and Development. *Plant Physiology*, *155*(2), 617–627. <https://doi.org/10.1104/pp.110.166249>
- Du, D., Zhang, D., Yuan, J., Feng, M., Li, Z., Wang, Z., Zhang, Z., Li, X., Ke, W., Li, R., Chen, Z., Chai, L., Hu, Z., Guo, W., Xing, J., Su, Z., Peng, H., Xin, M., Yao, Y., ... Ni, Z. (2021). FRIZZY PANICLE defines a regulatory hub for simultaneously controlling spikelet formation and awn elongation in bread wheat. *New Phytologist*, *231*(2), 814–833. <https://doi.org/10.1111/nph.17388>
- Du, H., Yu, Y., Ma, Y., Gao, Q., Cao, Y., Chen, Z., Ma, B., Qi, M., Li, Y., Zhao, X., Wang, J., Liu, K., Qin, P., Yang, X., Zhu, L., Li, S., & Liang, C. (2017). Sequencing and de novo assembly of a near complete indica rice genome. *Nature Communications*, *8*(2), 1–12. <https://doi.org/10.1038/ncomms15324>
- El-Mounadi, K., Morales-Floriano, M. L., & Garcia-Ruiz, H. (2020). Principles, Applications, and Biosafety of Plant Genome Editing Using CRISPR-Cas9. *Frontiers in Plant Science*, *11*(February), 1–16. <https://doi.org/10.3389/fpls.2020.00056>

- Elliot, M. (1997). *Molecular Dissection of the AGAMOUS Control Region Shows That cis Elements for Spatial Regulation Are Located Intragenically*. 9(March), 355–365.
- Eveland, A. L., Goldshmidt, A., Pautler, M., Morohashi, K., Liseron-Monfils, C., Lewis, M. W., Kumari, S., Hiraga, S., Yang, F., Unger-Wallace, E., Olson, A., Hake, S., Vollbrecht, E., Grotewold, E., Ware, D., & Jackson, D. (2014). Regulatory modules controlling maize inflorescence architecture. *Genome Research*, 24(3), 431–443.
<https://doi.org/10.1101/gr.166397.113>
- Fan, M., Xu, C., Xu, K., & Hu, Y. (2012). LATERAL ORGAN BOUNDARIES DOMAIN transcription factors direct callus formation in Arabidopsis regeneration. *Cell Research*, 22(7), 1169–1180. <https://doi.org/10.1038/cr.2012.63>
- Feng, Z., Mao, Y., Xu, N., Zhang, B., Wei, P., Yang, D.-L., Wang, Z., Zhang, Z., Zheng, R., Yang, L., Zeng, L., Liu, X., & Zhu, J.-K. (2014). Multigeneration analysis reveals the inheritance, specificity, and patterns of CRISPR/Cas-induced gene modifications in Arabidopsis. *Proceedings of the National Academy of Sciences*, 111(12), 4632–4637.
<https://doi.org/10.1073/pnas.1400822111>
- Fischbeck, G. (2003). *Diversification through breeding*. 29–52.
- Forster, B. P., Franckowiak, J. D., Lundqvist, U., Lyon, J., Pitkethly, I., & Thomas, W. T. B. (2007). The barley phytomer. *Annals of Botany*, 100(4), 725–733.
<https://doi.org/10.1093/aob/mcm183>
- Franckowiak, J. D., & Lundqvist, U. (2012). Descriptions of Barley Genetic Stocks for 2012. *Barley Genetics Newsletter*, 42, 36–173.
<http://citeseerx.ist.psu.edu/viewdoc/download?doi=10.1.1.410.635&rep=rep1&type=pdf>
- Furtado, A., Henry, R. J., & Takaiwa, F. (2008). Comparison of promoters in transgenic rice. *Plant Biotechnology Journal*, 6(7), 679–693. <https://doi.org/10.1111/j.1467-7652.2008.00352.x>
- Gai, W.-X., Ma, X., Qiao, Y.-M., Shi, B.-H., ul Haq, S., Li, Q.-H., Wei, A.-M., Liu, K.-K., & Gong, Z.-H. (2020). Characterization of the bZIP Transcription Factor Family in Pepper (*Capsicum annuum* L.): CabZIP25 Positively Modulates the Salt Tolerance. *Frontiers in Plant Science*, 11. <https://doi.org/10.3389/fpls.2020.00139>

- Gallavotti, A., Long, J. A., Stanfield, S., Yang, X., Jackson, D., Vollbrecht, E., & Schmidt, R. J. (2010). The control of axillary meristem fate in the maize ramosa pathway. *Development*, *137*(17), 2849–2856. <https://doi.org/10.1242/dev.051748>
- Gallavotti, A., Yang, Y., Schmidt, R. J., & Jackson, D. (2008). The relationship between auxin transport and maize branching. *Plant Physiology*, *147*(4), 1913–1923. <https://doi.org/10.1104/pp.108.121541>
- Galli, M., Feng, F., & Gallavotti, A. (2020). Mapping Regulatory Determinants in Plants. *Frontiers in Genetics*, *11*(October). <https://doi.org/10.3389/fgene.2020.591194>
- Galli, M., Khakhar, A., Lu, Z., Chen, Z., Sen, S., Joshi, T., Nemhauser, J. L., Schmitz, R. J., & Gallavotti, A. (2018). The DNA binding landscape of the maize AUXIN RESPONSE FACTOR family. *Nature Communications*, *9*(1), 4526. <https://doi.org/10.1038/s41467-018-06977-6>
- Galli, M., Martiny, E., Imani, J., Kumar, N., Koch, A., Steinbrenner, J., & Kogel, K. H. (2022). CRISPR/SpCas9-mediated double knockout of barley Microrchidia MORC1 and MORC6a reveals their strong involvement in plant immunity, transcriptional gene silencing and plant growth. *Plant Biotechnology Journal*, *20*(1), 89–102. <https://doi.org/10.1111/pbi.13697>
- Gasparis, Przyborowski, Kała, & Nadolska-Orczyk. (2019a). Knockout of the HvCKX1 or HvCKX3 Gene in Barley (*Hordeum vulgare* L.) by RNA-Guided Cas9 Nuclease Affects the Regulation of Cytokinin Metabolism and Root Morphology. *Cells*, *8*(8), 782. <https://doi.org/10.3390/cells8080782>
- Gasparis, S., Kała, M., Przyborowski, M., Łyznik, L. A., Orczyk, W., & Nadolska-Orczyk, A. (2018). A simple and efficient CRISPR/Cas9 platform for induction of single and multiple, heritable mutations in barley (*Hordeum vulgare* L.). *Plant Methods*, *14*(1), 1–14. <https://doi.org/10.1186/s13007-018-0382-8>
- Gasparis, S., Przyborowski, M., Kała, M., & Nadolska-Orczyk, A. (2019b). Knockout of the HvCKX1 or HvCKX3 Gene in Barley (*Hordeum vulgare* L.) by RNA-Guided Cas9 Nuclease Root Morphology. *Cells*, *8*(782).
- Gendron, J. M., Liu, J.-S., Fan, M., Bai, M.-Y., Wenkel, S., Springer, P. S., Barton, M. K., & Wang, Z.-Y. (2012). Brassinosteroids regulate organ boundary formation in the shoot apical

- meristem of Arabidopsis. *Proceedings of the National Academy of Sciences*, 109(51), 21152–21157. <https://doi.org/10.1073/pnas.1210799110>
- Goff, S. A., Ricke, D., Lan, T. H., Presting, G., Wang, R., Dunn, M., Glazebrook, J., Sessions, A., Oeller, P., Varma, H., Hadley, D., Hutchison, D., Martin, C., Katagiri, F., Lange, B. M., Moughamer, T., Xia, Y., Budworth, P., Zhong, J., ... Briggs, S. (2002). A draft sequence of the rice genome (*Oryza sativa* L. ssp. japonica). *Science*, 296(5565), 92–100. <https://doi.org/10.1126/science.1068275>
- González-Grandío, E., & Cubas, P. (2016). TCP Transcription Factors: Evolution, Structure, and Biochemical Function. In D. H. B. T.-P. T. F. Gonzalez (Ed.), *Plant Transcription Factors* (pp. 139–151). Elsevier. <https://doi.org/10.1016/B978-0-12-800854-6.00009-9>
- Gottwald, S., Bauer, P., Komatsuda, T., Lundqvist, U., & Stein, N. (2009). TILLING in the two-rowed barley cultivar “Barke” reveals preferred sites of functional diversity in the gene HvHox1. *BMC Research Notes*, 2, 1–14. <https://doi.org/10.1186/1756-0500-2-258>
- Greenwood, J. R., Finnegan, E. J., Watanabe, N., Trevaskis, B., & Swain, S. M. (2017). *New alleles of the wheat domestication gene Q reveal multiple roles in growth and reproductive development*. 1959–1965. <https://doi.org/10.1242/dev.146407>
- Guilfoyle, T. J., & Hagen, G. (2012). Plant Science Getting a grasp on domain III / IV responsible for Auxin Response Factor – IAA protein interactions. *Plant Science*, 190, 82–88. <https://doi.org/10.1016/j.plantsci.2012.04.003>
- Gupta, M. Das, & Tsiantis, M. (2018). ScienceDirect Gene networks and the evolution of plant morphology GRN-A. *Current Opinion in Plant Biology*, 45(Figure 1), 82–87. <https://doi.org/10.1016/j.pbi.2018.05.011>
- Gurushidze, M., Hensel, G., Hiekel, S., Schedel, S., Valkov, V., & Kumlehn, J. (2014). True-breeding targeted gene knock-out in barley using designer TALE-nuclease in haploid cells. *PLoS ONE*, 9(3), 1–9. <https://doi.org/10.1371/journal.pone.0092046>
- Hagen, G., & Guilfoyle, T. (2002). *Auxin-responsive gene expression : genes , promoters and regulatory factors*. 373–385.
- Han, Y., Broughton, S., Liu, L., Zhang, X. Q., Zeng, J., He, X., & Li, C. (2021). Highly efficient and genotype-independent barley gene editing based on anther culture. *Plant*

- Communications*, 2(2), 100082. <https://doi.org/10.1016/j.xplc.2020.100082>
- Hardison, R. C., & Taylor, J. (2012). Genomic approaches towards finding cis-regulatory modules in animals. *Nature Reviews Genetics*, 13(7), 469–483. <https://doi.org/10.1038/nrg3242>
- Harwood, W. A. (2012). Advances and remaining challenges in the transformation of barley and wheat. *Journal of Experimental Botany*, 63(5), 1791–1798. <https://doi.org/10.1093/jxb/err380>
- Haun, W., Coffman, A., Clasen, B. M., Demorest, Z. L., Lowy, A., Ray, E., Retterath, A., Stoddard, T., Juillerat, A., Cedrone, F., Mathis, L., Voytas, D. F., & Zhang, F. (2014). Improved soybean oil quality by targeted mutagenesis of the fatty acid desaturase 2 gene family. *Plant Biotechnology Journal*, 12(7), 934–940. <https://doi.org/10.1111/pbi.12201>
- He, F., Chen, S., Ning, Y., & Wang, G. L. (2016). Rice (*Oryza sativa*) Protoplast Isolation and Its Application for Transient Expression Analysis. *Current Protocols in Plant Biology*, 1(2), 373–383. <https://doi.org/10.1002/cppb.20026>
- Heisler, M. G., Ohno, C., Das, P., Sieber, P., Reddy, G. V, Long, J. A., & Meyerowitz, E. M. (2005). *Patterns of Auxin Transport and Gene Expression during Primordium Development Revealed by Live Imaging of the Arabidopsis Inflorescence Meristem*. 15, 1899–1911. <https://doi.org/10.1016/j.cub.2005.09.052>
- Hensel, G., Himmelbach, A., Chen, W., Douchkov, D. K., & Kumlehn, J. (2011). Transgene expression systems in the Triticeae cereals. *Journal of Plant Physiology*, 168(1), 30–44. <https://doi.org/10.1016/j.jplph.2010.07.007>
- Hensel, G., Kastner, C., Oleszczuk, S., Riechen, J., & Kumlehn, J. (2009). Agrobacterium-mediated gene transfer to cereal crop plants: Current protocols for barley, wheat, triticale, and maize. *International Journal of Plant Genomics*, 2009. <https://doi.org/10.1155/2009/835608>
- Hensel, G., Valkov, V., Middlefell-Williams, J., & Kumlehn, J. (2008). Efficient generation of transgenic barley: The way forward to modulate plant–microbe interactions. *Journal of Plant Physiology*, 165(1), 71–82. <https://doi.org/10.1016/j.jplph.2007.06.015>
- Hernandez-Garcia, C. M., & Finer, J. J. (2014). Identification and validation of promoters and

- cis-acting regulatory elements. *Plant Science*, 217–218, 109–119.
<https://doi.org/10.1016/j.plantsci.2013.12.007>
- Hilscher, J., Bürstmayr, H., & Stoger, E. (2017). Targeted modification of plant genomes for precision crop breeding. *Biotechnology Journal*, 12(1).
<https://doi.org/10.1002/biot.201600173>
- Hisano, H., Meints, B., Moscou, M. J., Cistue, L., Echávarri, B., Sato, K., & Hayes, P. M. (2017). Selection of transformation-efficient barley genotypes based on TFA (transformation amenability) haplotype and higher resolution mapping of the TFA loci. *Plant Cell Reports*, 36(4), 611–620. <https://doi.org/10.1007/s00299-017-2107-2>
- Holme, I. B., Wendt, T., Gil-Humanes, J., Deleuran, L. C., Starker, C. G., Voytas, D. F., & Brinch-Pedersen, H. (2017). Evaluation of the mature grain phytase candidate HvPAPhy_a gene in barley (*Hordeum vulgare* L.) using CRISPR/Cas9 and TALENs. *Plant Molecular Biology*, 95(1–2), 111–121. <https://doi.org/10.1007/s11103-017-0640-6>
- Holubová, K., Hensel, G., Vojta, P., Tarkowski, P., Bergougnoux, V., & Galuszka, P. (2018). Modification of barley plant productivity through regulation of cytokinin content by reverse-genetics approaches. *Frontiers in Plant Science*, 871(November), 1–18.
<https://doi.org/10.3389/fpls.2018.01676>
- Hong, R. L., Hamaguchi, L., Busch, M. A., & Weigel, D. (2003). *Regulatory Elements of the Floral Homeotic Gene AGAMOUS Identified by Phylogenetic Footprinting and Shadowing*. 15(June), 1296–1309. <https://doi.org/10.1105/tpc.009548.throughout>
- Houston, K., McKim, S. M., Comadran, J., Bonar, N., Druka, I., Uzrek, N., Cirillo, E., Guzy-Wrobelska, J., Collins, N. C., Halpin, C., Hansson, M., Dockter, C., Druka, A., & Waugh, R. (2013). Variation in the interaction between alleles of HvAPETALA2 and microRNA172 determines the density of grains on the barley inflorescence. *Proceedings of the National Academy of Sciences of the United States of America*, 110(41), 16675–16680.
<https://doi.org/10.1073/pnas.1311681110>
- Hsu, P. D., Lander, E. S., & Zhang, F. (2014). Development and applications of CRISPR-Cas9 for genome engineering. *Cell*, 157(6), 1262–1278.
<https://doi.org/10.1016/j.cell.2014.05.010>

- Hu, G., Wang, K., Huang, B., Mila, I., Frasse, P., Maza, E., Djari, A., Hernould, M., Zouine, M., Li, Z., & Bouzayen, M. (2022). The auxin-responsive transcription factor SIDOF9 regulates inflorescence and flower development in tomato. *Nature Plants*, 8(4), 419–433.
<https://doi.org/10.1038/s41477-022-01121-1>
- Husbands, A., Bell, E. M., Shuai, B., Smith, H. M. S., & Springer, P. S. (2007). Lateral organ boundaries defines a new family of DNA-binding transcription factors and can interact with specific bHLH proteins. *Nucleic Acids Research*, 35(19), 6663–6671.
<https://doi.org/10.1093/nar/gkm775>
- Ijaz, U., Pervaiz, T., Ahmed, T., Seemab, R., Shahid, M., Noman, M., Nadeem, M., & Azeem, F. (2020). Plant Cis-regulatory elements: Methods of identification and applications. *Asian Journal of Agriculture and Biology*, 8(2), 207–222.
<https://doi.org/10.35495/ajab.2019.08.352>
- Jaganathan, D., Ramasamy, K., Sellamuthu, G., Jayabalan, S., & Venkataraman, G. (2018). CRISPR for crop improvement: An update review. *Frontiers in Plant Science*, 9(July), 1–17. <https://doi.org/10.3389/fpls.2018.00985>
- Jiang, C., Lei, M., Guo, Y., Gao, G., Shi, L., Jin, Y., Cai, Y., Himmelbach, A., Zhou, S., He, Q., Yao, X., Kan, J., Haberer, G., Duan, F., Li, L., Liu, J., Zhang, J., Spannagl, M., Liu, C., ... Yang, P. (2022). A reference-guided TILLING by amplicon-sequencing platform supports forward and reverse genetics in barley. *Plant Communications*, 3(4), 100317.
<https://doi.org/10.1016/j.xplc.2022.100317>
- Jiang, W., Sun, L., Yang, X., Wang, M., Esmaili, N., & Pehlivan, N. (2017). The Effects of Transcription Directions of Transgenes and the gypsy Insulators on the Transcript Levels of Transgenes in Transgenic Arabidopsis. *Scientific Reports*, October, 1–12.
<https://doi.org/10.1038/s41598-017-15284-x>
- Jiang, X., Lubini, G., Hernandez-Lopes, J., Rijnsburger, K., Veltkamp, V., De Maagd, R. A., Angenent, G. C., & Bemer, M. (2022). FRUITFULL-like genes regulate flowering time and inflorescence architecture in tomato. *Plant Cell*, 34(3), 1002–1019.
<https://doi.org/10.1093/plcell/koab298>
- Jinek, M., Chylinski, K., Fonfara, I., Hauer, M., Doudna, J. A., & Charpentier, E. (2012). A

- Programmable Dual-RNA–Guided DNA Endonuclease in Adaptive Bacterial Immunity. *Science*, 337(6096), 816–821. <https://doi.org/10.1126/science.1225829>
- Jost, M., Taketa, S., Mascher, M., Himmelbach, A., Yuo, T., Shahinnia, F., Rutten, T., Druka, A., Schmutzer, T., Steuernagel, B., Beier, S., Taudien, S., Scholz, U., Morgante, M., Waugh, R., & Stein, N. (2016). A homolog of blade-on-petiole 1 and 2 (BOP1/2) controls internode length and homeotic changes of the barley inflorescence. *Plant Physiology*, 171(2), 1113–1127. <https://doi.org/10.1104/pp.16.00124>
- Jung, J. H., & Altpeter, F. (2016). TALEN mediated targeted mutagenesis of the caffeic acid O-methyltransferase in highly polyploid sugarcane improves cell wall composition for production of bioethanol. *Plant Molecular Biology*, 92(1–2), 131–142. <https://doi.org/10.1007/s11103-016-0499-y>
- Kapusi, E., Corcuera-Gómez, M., Melnik, S., & Stoger, E. (2017). Heritable Genomic Fragment Deletions and Small Indels in the Putative ENGase Gene Induced by CRISPR/Cas9 in Barley. *Frontiers in Plant Science*, 8(April), 1–11. <https://doi.org/10.3389/fpls.2017.00540>
- Kawamoto, Y., Toda, H., Inoue, H., Kobayashi, K., & Yamaoka, N. (2020). *Fast and Inexpensive Phenotyping and Genotyping*.
- Kellogg, E. A. (2007). Floral displays: genetic control of grass inflorescences. *Current Opinion in Plant Biology*, 10(1), 26–31. <https://doi.org/10.1016/j.pbi.2006.11.009>
- Kellogg, E. A. (2022). Genetic control of branching patterns in grass inflorescences. *The Plant Cell*, 1–16. <https://doi.org/10.1093/plcell/koac080>
- Khan, Z., Khan, S. H., Mubarik, M. S., Sadia, B., & Ahmad, A. (2017). Use of TALEs and TALEN Technology for Genetic Improvement of Plants. *Plant Molecular Biology Reporter*, 35(1), 1–19. <https://doi.org/10.1007/s11105-016-0997-8>
- Kilian, B., Ozkan, H., Pozzi, C., & Salamini, F. (2009). *Domestication of the Triticeae in the Fertile Crescent*. <https://doi.org/10.1007/978-0-387-77489-3>
- Kirby, E. J. M., & Appleyard, M. (1987). *Cereal Development Guide*.
- Kishor, D. S., Seo, J., Chin, J. H., & Koh, H. J. (2020). Evaluation of Whole-Genome Sequence, Genetic Diversity, and Agronomic Traits of Basmati Rice (*Oryza sativa* L.). *Frontiers in Genetics*, 11(February), 1–12. <https://doi.org/10.3389/fgene.2020.00086>

- Kitchen, B. M., & Rasmusson, D. C. (1983). (1983) *Duration and Inheritance of Leaf Initiation, Spike Initiation, and Spike Growth in Barley*.
- Klein, H., Gallagher, J., Demesa-Arevalo, E., Abraham-Juarez, M. J., Heeney, M., Feil, R., Lunn, J. E., Xiao, Y., Chuck, G., Whipple, C., Jackson, D., & Bartlett, M. (2022). Recruitment of an ancient branching program to suppress carpel development in maize flowers. *Proceedings of the National Academy of Sciences of the United States of America*, 119(2). <https://doi.org/10.1073/pnas.2115871119>
- Knudsen, S., Wendt, T., Dockter, C., Thomsen, H. C., Rasmussen, M., Egevang Jørgensen, M., Lu, Q., Voss, C., Murozuka, E., Østerberg, J. T., Harholt, J., Braumann, I., Cuesta-Seijo, J. A., Kale, S. M., Bodevin, S., Tang Petersen, L., Carciofi, M., Pedas, P. R., Opstrup Husum, J., ... Skadhauge, B. (2022). FIND-IT: Accelerated trait development for a green evolution. *Science Advances*, 8(34), eabq2266. <https://doi.org/10.1126/sciadv.abq2266>
- Kochetov, A. V., & Shumny, V. K. (2017). Transgenic plants as genetic models for studying functions of plant genes. *Russian Journal of Genetics: Applied Research*, 7(4), 421–427. <https://doi.org/10.1134/S2079059717040050>
- Kolovos, P., Knoch, T. A., Grosveld, F. G., Cook, P. R., & Papantonis, A. (2012). Enhancers and silencers: An integrated and simple model for their function. *Epigenetics and Chromatin*, 5(1), 1–8. <https://doi.org/10.1186/1756-8935-5-1>
- Komatsu, M., Chujo, A., Nagato, Y., Shimamoto, K., & Kyojuka, J. (2003). Frizzy panicle is required to prevent the formation of axillary meristems and to establish floral meristem identity in rice spikelets. *Development*, 130(16), 3841–3850. <https://doi.org/10.1242/dev.00564>
- Komatsuda, T., Pourkheirandish, M., He, C., Azhaguvel, P., Kanamori, K., Perovic, D., Stein, N., Graner, A., Wicker, T., Tagiri, A., Lundqvist, U., Fujimura, T., Matsuoka, M., Matsumoto, T., & Yano, M. (2007). Six-rowed barley originated from a mutation in a homeodomain-leucine zipper I-class homeobox gene. *Proceedings of the National Academy of Sciences of the United States of America*, 104(4), 1424–1429. <https://doi.org/10.1073/pnas.0608580104>
- Komatsuda, T., Tanno, K., Salomon, B., Bryngelsson, T., & von Bothmer, R. (1998). Phylogeny

- in the genus *Hordeum* based on nucleotide sequences closely linked to the *vrs1* locus (row number of spikelets). *Genome*, *42*(5), 973–981. <https://doi.org/10.1139/g99-025>
- Koppolu, R., Anwar, N., Sakuma, S., Tagiri, A., Lundqvist, U., Pourkheirandish, M., Rutten, T., Seiler, C., Himmelbach, A., Ariyadasa, R., Youssef, H. M., Stein, N., Sreenivasulu, N., Komatsuda, T., & Schnurbusch, T. (2013). Six-rowed spike4 (*Vrs4*) controls spikelet determinacy and row-type in barley. *Proceedings of the National Academy of Sciences of the United States of America*, *110*(32), 13198–13203. <https://doi.org/10.1073/pnas.1221950110>
- Koppolu, R., Chen, S., & Schnurbusch, T. (2022). Evolution of inflorescence branch modifications in cereal crops. *Current Opinion in Plant Biology*, *65*, 102168. <https://doi.org/10.1016/j.pbi.2021.102168>
- Koppolu, R., & Schnurbusch, T. (2019). Developmental pathways for shaping spike inflorescence architecture in barley and wheat. *Journal of Integrative Plant Biology*, *61*(3), 278–295. <https://doi.org/10.1111/jipb.12771>
- Krasileva, K. V., Vasquez-Gross, H. A., Howell, T., Bailey, P., Paraiso, F., Clissold, L., Simmonds, J., Ramirez-Gonzalez, R. H., Wang, X., Borrill, P., Fosker, C., Ayling, S., Phillips, A. L., Uauy, C., & Dubcovsky, J. (2017). Uncovering hidden variation in polyploid wheat. *Proceedings of the National Academy of Sciences*, *114*(6), E913–E921. <https://doi.org/10.1073/pnas.1619268114>
- Křenek, P., Chubar, E., Vadovič, P., Ohnoutková, L., Vlčko, T., Bergougnoux, V., Cápál, P., Ovečka, M., & Šamaj, J. (2021). CRISPR/Cas9-Induced Loss-of-Function Mutation in the Barley Mitogen-Activated Protein Kinase 6 Gene Causes Abnormal Embryo Development Leading to Severely Reduced Grain Germination and Seedling Shootless Phenotype. *Frontiers in Plant Science*, *12*(July). <https://doi.org/10.3389/fpls.2021.670302>
- Krysan, P. J. (1999). T-DNA as an Insertional Mutagen in Arabidopsis. *The Plant Cell Online*, *11*(12), 2283–2290. <https://doi.org/10.1105/tpc.11.12.2283>
- Kumar, J., Kumar, A., Sen Gupta, D., Kumar, S., & DePauw, R. M. (2022). Reverse genetic approaches for breeding nutrient-rich and climate-resilient cereal and food legume crops. *Heredity*, *128*(6), 473–496. <https://doi.org/10.1038/s41437-022-00513-5>

- Kumlehn, J., & Hensel, G. (2009). Genetic transformation technology in the Triticeae. *Breeding Science*, 59(5), 553–560. <https://doi.org/10.1270/jsbbs.59.553>
- Kurbidaeva, A. (2021). *Insulators in Plants : Progress and Open Questions*.
- Kurowska, M., Daszkowska-Golec, A., Gruszka, D., Marzec, M., Szurman, M., Szarejko, I., & Maluszynski, M. (2011). TILLING - a shortcut in functional genomics. *Journal of Applied Genetics*, 52(4), 371–390. <https://doi.org/10.1007/s13353-011-0061-1>
- Kyrchanova, O., & Georgiev, P. (2014). Chromatin insulators and long-distance interactions in *Drosophila*. *FEBS Letters*, 588(1), 8–14. <https://doi.org/10.1016/j.febslet.2013.10.039>
- Lababidi, S., Mejlhede, N., Rasmussen, S. K., Backes, G., Al-Said, W., Baum, M., & Jahoor, A. (2009). Identification of barley mutants in the cultivar “lux” at the dhn loci through tilling. *Plant Breeding*, 128(4), 332–336. <https://doi.org/10.1111/j.1439-0523.2009.01640.x>
- Lawrenson, T., Hinchliffe, A., Clarke, M., Morgan, Y., & Harwood, W. (2021). *In-planta Gene Targeting in Barley Using Cas9 With and Without Geminiviral Replicons*. 3(June), 1–12. <https://doi.org/10.3389/fgeed.2021.663380>
- Lawrenson, T., Shorinola, O., Stacey, N., Li, C., Østergaard, L., Patron, N., Uauy, C., & Harwood, W. (2015). Induction of targeted, heritable mutations in barley and Brassica oleracea using RNA-guided Cas9 nuclease. *Genome Biology*, 16(1), 1–13. <https://doi.org/10.1186/s13059-015-0826-7>
- Li, J., Manghwar, H., Sun, L., Wang, P., Wang, G., Sheng, H., Zhang, J., Liu, H., Qin, L., Rui, H., Li, B., Lindsey, K., Daniell, H., & Jin, S. (2019). *Whole genome sequencing reveals rare off-target mutations and considerable inherent genetic or / and somaclonal variations in CRISPR / Cas9-edited cotton plants*. 858–868. <https://doi.org/10.1111/pbi.13020>
- Li, J., Meng, X., Zong, Y., Chen, K., Zhang, H., Liu, J., Li, J., & Gao, C. (2016). Gene replacements and insertions in rice by intron targeting using CRISPR-Cas9. *Nature Plants*, 2(10), 1–6. <https://doi.org/10.1038/nplants.2016.139>
- Li, J., Wang, K., Li, G., Li, Y., Zhang, Y., Liu, Z., Ye, X., Xia, X., He, Z., & Cao, S. (2019). Dissecting conserved cis-regulatory modules of Glu-1 promoters which confer the highly active endosperm-specific expression via stable wheat transformation. *Crop Journal*, 7(1), 8–18. <https://doi.org/10.1016/j.cj.2018.08.003>

- Li, T., Liu, B., Spalding, M. H., Weeks, D. P., & Yang, B. (2012). High-efficiency TALEN-based gene editing produces disease-resistant rice. *Nature Biotechnology*, *30*(5), 390–392. <https://doi.org/10.1038/nbt.2199>
- Li, Y., Guo, G., Xu, H., He, T., Zong, Y., Zhang, S., Faheem, M., Lu, R., Zhou, L., & Liu, C. (2021). Comparative transcriptome analysis reveals compatible and recalcitrant genotypic response of barley microspore-derived embryogenic callus toward *Agrobacterium* infection. *BMC Plant Biology*, 1–17. <https://doi.org/10.1186/s12870-021-03346-2>
- Li, Y., Li, L., Zhao, M., Guo, L., Guo, X., Zhao, D., Batool, A., Dong, B., Xu, H., Cui, S., Zhang, A., Fu, X., Li, J., Jing, R., & Liu, X. (2021). Wheat FRIZZY PANICLE activates VERNALIZATION1-A and HOMEBOX4-A to regulate spike development in wheat. *Plant Biotechnology Journal*, *19*(6), 1141–1154. <https://doi.org/10.1111/pbi.13535>
- Li, Z., Woo, H. R., & Guo, H. (2018). Genetic redundancy of senescence-associated transcription factors in *Arabidopsis*. *Journal of Experimental Botany*, *69*(4), 811–823. <https://doi.org/10.1093/jxb/erx345>
- Liang, Z., Chen, K., Li, T., Zhang, Y., Wang, Y., Zhao, Q., Liu, J., Zhang, H., Liu, C., Ran, Y., & Gao, C. (2017). Efficient DNA-free genome editing of bread wheat using CRISPR/Cas9 ribonucleoprotein complexes. *Nature Communications*, *8*, 6–10. <https://doi.org/10.1038/ncomms14261>
- Liang, Z., Zhang, K., Chen, K., & Gao, C. (2014). Targeted mutagenesis in *Zea mays* using TALENs and the CRISPR/Cas system. *Journal of Genetics and Genomics*, *41*(2), 63–68. <https://doi.org/10.1016/j.jgg.2013.12.001>
- Liller, C. B., Neuhaus, R., Von Korff, M., Koornneef, M., & Van Esse, W. (2015). Mutations in barley row type genes have pleiotropic effects on shoot branching. *PLoS ONE*, *10*(10), 1–20. <https://doi.org/10.1371/journal.pone.0140246>
- Liu, C., Xi, W., Shen, L., Tan, C., & Yu, H. (2009). Article Regulation of Floral Patterning by Flowering Time Genes. *Developmental Cell*, *16*(5), 711–722. <https://doi.org/10.1016/j.devcel.2009.03.011>
- Liu, G., Li, H., & Grierson, D. (2022). *NAC Transcription Factor Family Regulation of Fruit Ripening and Quality : A Review*. 1–29.

- Liu, R., Zou, X., Wang, Y., Long, Q., & Pei, Y. (2020). A 100 bp GAGA motif-containing sequence in *AGAMOUS* second intron is able to suppress the activity of *CaMV35S* enhancer in vegetative tissues. 1–16. <https://doi.org/10.1371/journal.pone.0230203>
- Livak, K. J., & Schmittgen, T. D. (2001). Analysis of relative gene expression data using real-time quantitative PCR and the 2- $\Delta\Delta$ CT method. *Methods*, 25(4), 402–408. <https://doi.org/10.1006/meth.2001.1262>
- Long, H. K., Prescott, S. L., & Wysocka, J. (2016). Ever-Changing Landscapes: Transcriptional Enhancers in Development and Evolution. *Cell*, 167(5), 1170–1187. <https://doi.org/10.1016/j.cell.2016.09.018>
- Lor, V. S., Starker, C. G., Voytas, D. F., Weiss, D., & Olszewski, N. E. (2014). Targeted mutagenesis of the tomato *procera* gene using transcription activator-like effector nucleases. *Plant Physiology*, 166(3), 1288–1291. <https://doi.org/10.1104/pp.114.247593>
- Lu, H., Dai, Z., Li, L., Wang, J., Miao, X., & Shi, Z. (2017). OsRAMOSA2 Shapes Panicle Architecture through Regulating Pedicel Length. *Frontiers in Plant Science*, 8(September), 1–11. <https://doi.org/10.3389/fpls.2017.01538>
- Lu, Z., Marand, A. P., Ricci, W. A., Ethridge, C. L., Zhang, X., & Schmitz, R. J. (2019). The prevalence, evolution and chromatin signatures of plant regulatory elements. *Nature Plants*, 5(12), 1250–1259. <https://doi.org/10.1038/s41477-019-0548-z>
- Lundquist, U. (2005). The Swedish Collection of Barley Mutants held at the Nordic Genebank. *Barley Genetics Newsletter*, 35, 150–154.
- Lundqvist, U., & Franckowiak, J. D. (2003). Chapter 5 - Diversity of barley mutants. In R. von Bothmer, T. van Hintum, H. Knüpfner, & K. B. T.-D. in P. G. and B. Sato (Eds.), *Diversity in Barley* (Vol. 7, pp. 77–96). Elsevier. [https://doi.org/https://doi.org/10.1016/S0168-7972\(03\)80007-5](https://doi.org/https://doi.org/10.1016/S0168-7972(03)80007-5)
- Lundqvist, U., Franckowiak, J. D., & Konishi, T. (1997). New and revised descriptions of barley genes. In *Barley genetics newsletter: Vol. v. 26*.
- Lundqvist, U., & Lundqvist, A. (1988). Induced intermedium mutants in barley: origin, morphology and inheritance. *Hereditas*, 108(1), 13–26. <https://doi.org/10.1111/j.1601-5223.1988.tb00677.x>

- Lyu, T., & Cao, J. (2018). *Cys 2 / His 2 Zinc-Finger Proteins in Transcriptional Regulation of Flower Development*. <https://doi.org/10.3390/ijms19092589>
- Ma, L., Zhu, F., Li, Z., Zhang, J., Li, X., Dong, J., & Wang, T. (2015). TALEN-Based mutagenesis of lipoxygenase LOX3 enhances the storage tolerance of rice (*Oryza sativa*) Seeds. *PLoS ONE*, *10*(12), 1–16. <https://doi.org/10.1371/journal.pone.0143877>
- Malzahn, A., Lowder, L., & Qi, Y. (2017). Plant genome editing with TALEN and CRISPR. *Cell & Bioscience*, *7*(1), 21. <https://doi.org/10.1186/s13578-017-0148-4>
- Mascher, M., Wicker, T., Jenkins, J., Plott, C., Lux, T., Koh, C. S., Ens, J., Gundlach, H., Boston, L. B., Tulpová, Z., Holden, S., Hernández-Pinzón, I., Scholz, U., Mayer, K. F. X., Spannagl, M., Pozniak, C. J., Sharpe, A. G., Simková, H., Moscou, M. J., ... Stein, N. (2021). Long-read sequence assembly: A technical evaluation in barley. *Plant Cell*, *33*(6), 1888–1906. <https://doi.org/10.1093/plcell/koab077>
- Matres, J. M., Hilscher, J., Datta, A., Armario-Nájera, V., Baysal, C., He, W., Huang, X., Zhu, C., Valizadeh-Kamran, R., Trijatmiko, K. R., Capell, T., Christou, P., Stoger, E., & Slamet-Loedin, I. H. (2021). Genome editing in cereal crops: an overview. In *Transgenic Research* (Vol. 30, Issue 4). <https://doi.org/10.1007/s11248-021-00259-6>
- Maul, R. S., Zhang, H., Iv, J. D. R., Pedigo, N. G., & Kaetzel, D. M. (1998). Identification of a Cell Type-specific Enhancer in the Distal 5' -Region of the Platelet-derived Growth Factor A-chain Gene *. *Journal of Biological Chemistry*, *273*(50), 33239–33246. <https://doi.org/10.1074/jbc.273.50.33239>
- McCallum, C. M., Comai, L., Greene, E. A., & Henikoff, S. (2000). Targeting Induced Local Lesions IN Genomes (TILLING) for Plant Functional Genomics. *Plant Physiology*, *123*(2), 439–442. <https://doi.org/10.1104/pp.123.2.439>
- McKim, S. M., Koppolu, R., & Schnurbusch, T. (2018). *Barley Inflorescence Architecture*. 171–208. https://doi.org/10.1007/978-3-319-92528-8_12
- McSteen, P. (2006). Branching Out: The ramosa Pathway and the Evolution of Grass Inflorescence Morphology. *The Plant Cell*, *18*(3), 518–522. <https://doi.org/10.1105/tpc.105.040196>
- Meissner, R. C., Jin, H., Cominelli, E., Denekamp, M., Fuertes, A., Greco, R., Kranz, H. D.,

- Penfield, S., Petroni, K., Urzainqui, A., Martin, C., Paz-Ares, J., Smeeckens, S., Tonelli, C., Weisshaar, B., Baumann, E., Klimyuk, V., Marillonnet, S., Patel, K., ... Bevan, M. (1999). Function search in a large transcription factor gene family in Arabidopsis: Assessing the potential of reverse genetics to identify insertional mutations in R2R3 MYB genes. *Plant Cell*, *11*(10), 1827–1840. <https://doi.org/10.1105/tpc.11.10.1827>
- Mithra, S. V. A., Kulkarni, K., & Srinivasan, R. (2017). *Plant Biotechnology: Principles and Applications* (M. Z. Abdin, U. Kiran, Kamaluddin, & A. Ali (eds.)). Springer Singapore. <https://doi.org/10.1007/978-981-10-2961-5>
- Miura, K., Ikeda, M., Matsubara, A., Song, X. J., Ito, M., Asano, K., Matsuoka, M., Kitano, H., & Ashikari, M. (2010). OsSPL14 promotes panicle branching and higher grain productivity in rice. *Nature Genetics*, *42*(6), 545–549. <https://doi.org/10.1038/ng.592>
- Nagaya, S., Kato, K., Ninomiya, Y., Horie, R., Sekine, M., Yoshida, K., & Shinmyo, A. (2005). Expression of randomly integrated single complete copy transgenes does not vary in Arabidopsis thaliana. *Plant and Cell Physiology*, *46*(3), 438–444. <https://doi.org/10.1093/pcp/pci039>
- Naito, T., Yamashino, T., Kiba, T., Koizumi, N., Kojima, M., Sakakibara, H., & Mizuno, T. (2007). A link between cytokinin and ASL9 (Asymmetric Leaves 2 Like 9) that belongs to the AS2/LOB (Lateral Organ Boundaries) family genes in Arabidopsis thaliana. *Bioscience, Biotechnology and Biochemistry*, *71*(5), 1269–1278. <https://doi.org/10.1271/bbb.60681>
- Nakano, T., Suzuki, K., Fujimura, T., & Shinshi, H. (2006). Genome-wide analysis of the ERF gene family in Arabidopsis and rice. *Plant Physiology*, *140*(2), 411–432. <https://doi.org/10.1104/pp.105.073783>
- Nevo, E., Ordentlich, A., Beiles, A., & Raskin, I. (1992). Genetic divergence of heat production within and between the wild progenitors of wheat and barley: evolutionary and agronomical implications. *Theoretical and Applied Genetics*, *84*(7–8), 958–962. <https://doi.org/10.1007/BF00227410>
- O'Malley, R. C., Huang, S. S. C., Song, L., Lewsey, M. G., Bartlett, A., Nery, J. R., Galli, M., Gallavotti, A., & Ecker, J. R. (2016). Cistrome and Epicistrome Features Shape the Regulatory DNA Landscape. *Cell*, *165*(5), 1280–1292.

<https://doi.org/10.1016/j.cell.2016.04.038>

- Okushima, Y., Overvoorde, P. J., Arima, K., Alonso, J. M., Chan, A., Chang, C., Ecker, J. R., Hughes, B., Lui, A., Nguyen, D., Onodera, C., Quach, H., & Smith, A. (2005). *Functional Genomic Analysis of the AUXIN RESPONSE FACTOR Gene Family Members in Arabidopsis thaliana : Unique and Overlapping Functions of ARF7 and ARF19*. 17(February), 444–463. <https://doi.org/10.1105/tpc.104.028316.2>
- Pandey, B., Prakash, P., Verma, P. C., & Srivastava, R. (2018). Regulated gene expression by synthetic modulation of the promoter architecture in plants. In *Current Developments in Biotechnology and Bioengineering: Synthetic Biology, Cell Engineering and Bioprocessing Technologies*. Elsevier B.V. <https://doi.org/10.1016/B978-0-444-64085-7.00010-1>
- Park, S. J., Jiang, K., Tal, L., Yichie, Y., Gar, O., Zamir, D., Eshed, Y., & Lippman, Z. B. (2014). *Optimization of crop productivity in tomato using induced mutations in the florigen pathway*. November. <https://doi.org/10.1038/ng.3131>
- Paterson, A. H., Bowers, J. E., Bruggmann, R., Dubchak, I., Grimwood, J., Gundlach, H., Haberler, G., Hellsten, U., Mitros, T., Poliakov, A., Schmutz, J., Spannagl, M., Tang, H., Wang, X., Wicker, T., Bharti, A. K., Chapman, J., Feltus, F. A., Gowik, U., ... Rokhsar, D. S. (2009). The Sorghum bicolor genome and the diversification of grasses. *Nature*, 457(7229), 551–556.
http://www.ncbi.nlm.nih.gov/sites/entrez?Db=pubmed&DbFrom=pubmed&Cmd=Link&LinkName=pubmed_pubmed&LinkReadableName=RelatedArticles&IdsFromResult=19189423&ordinalpos=3&itool=EntrezSystem2.PEntrez.Pubmed.Pubmed_ResultsPanel.Pubmed_RVDocSum
- Patil, V., McDermott, H. I., McAllister, T., Cummins, M., Silva, J. C., Mollison, E., Meikle, R., Morris, J., Hedley, P. E., Waugh, R., Dockter, C., Hansson, M., & McKim, S. M. (2019). APETALA2 control of barley internode elongation. In *Development*. <https://doi.org/10.1242/dev.170373>
- Pauwels, L., Clercq, R. De, Goossens, J., Iñigo, S., & Williams, C. (2018). *A Dual sgRNA Approach for Functional Genomics in Arabidopsis thaliana*. 8(August), 2603–2615. <https://doi.org/10.1534/g3.118.200046>

- Peach, C., & Velten, J. (1991). Transgene expression variability (position effect) of CAT and GUS reporter genes driven by linked divergent T-DNA promoters. *Plant Molecular Biology*, *17*(1), 49–60. <https://doi.org/10.1007/BF00036805>
- Peng, F. Y., Hu, Z., & Yang, R. C. (2016). Bioinformatic prediction of transcription factor binding sites at promoter regions of genes for photoperiod and vernalization responses in model and temperate cereal plants. *BMC Genomics*, *17*(1), 1–16. <https://doi.org/10.1186/s12864-016-2916-7>
- Peng, Y., Xiong, D., Zhao, L., Ouyang, W., Wang, S., Sun, J., Zhang, Q., Guan, P., Xie, L., Li, W., Li, G., Yan, J., & Li, X. (2019). Chromatin interaction maps reveal genetic regulation for quantitative traits in maize. *Nature Communications*, *10*(1), 1–11. <https://doi.org/10.1038/s41467-019-10602-5>
- Pérez-gonzález, A., & Caro, E. (2019). *Benefits of using genomic insulators flanking transgenes to increase expression and avoid positional effects*. May, 1–11. <https://doi.org/10.1038/s41598-019-44836-6>
- Pérrilleux, C., Bouché, F., Randoux, M., & Orman-Ligeza, B. (2019). Turning Meristems into Fortresses. *Trends in Plant Science*, *24*(5), 431–442. <https://doi.org/10.1016/j.tplants.2019.02.004>
- Perlot, T., & Alt, F. W. (2008). Cis-regulatory elements and epigenetic changes control genomic rearrangements of the IgH locus. *Advances in Immunology*, *99*, 1–32. [https://doi.org/10.1016/S0065-2776\(08\)00601-9](https://doi.org/10.1016/S0065-2776(08)00601-9)
- Perreta, M. G., Ramos, J. C., & Vegetti, A. C. (2009). Development and structure of the grass inflorescence. *Botanical Review*, *75*(4), 377–396. <https://doi.org/10.1007/s12229-009-9038-8>
- Peters, J. L., Cnudde, F., & Gerats, T. (2003). Forward genetics and map-based cloning approaches. *Trends in Plant Science*, *8*(10), 484–491. <https://doi.org/10.1016/j.tplants.2003.09.002>
- Pins, J. J., & Kaur, H. (2006). A review of the effects of barley beta-glucan on cardiovascular and diabetic risk. *Cereal Foods World*, *51* SRC-, 8–11.
- Pourabed, E., Ghane Golmohamadi, F., Soleymani Monfared, P., Razavi, S. M., & Shobbar, Z.

- S. (2015). Basic Leucine Zipper Family in Barley: Genome-Wide Characterization of Members and Expression Analysis. *Molecular Biotechnology*, 57(1), 12–26. <https://doi.org/10.1007/s12033-014-9797-2>
- Pourkheirandish, M., & Komatsuda, T. (2007). The importance of barley genetics and domestication in a global perspective. *Annals of Botany*, 100(5), 999–1008. <https://doi.org/10.1093/aob/mcm139>
- Poursarebani, N., Seidensticker, T., Koppolu, R., Trautewig, C., Gawroński, P., Bini, F., Govind, G., Rutten, T., Sakuma, S., Tagiri, A., Wolde, G. M., Youssef, H. M., Battal, A., Ciannamea, S., Fusca, T., Nussbaumer, T., Pozzi, C., Börner, A., Lundqvist, U., ... Schnurbusch, T. (2015). The genetic basis of composite spike form in barley and ‘miracle-wheat.’ *Genetics*, 201(1), 155–165. <https://doi.org/10.1534/genetics.115.176628>
- Poursarebani, N., Trautewig, C., Melzer, M., Nussbaumer, T., Lundqvist, U., Rutten, T., Schmutzer, T., Brandt, R., Himmelbach, A., Altschmied, L., Koppolu, R., Youssef, H. M., Sibout, R., Dalmais, M., Bendahmane, A., Stein, N., Xin, Z., & Schnurbusch, T. (2020). COMPOSITUM 1 contributes to the architectural simplification of barley inflorescence via meristem identity signals. *Nature Communications*, 11(1). <https://doi.org/10.1038/s41467-020-18890-y>
- Privalsky, M. L. (2004). *THE ROLE OF COREPRESSORS IN TRANSCRIPTIONAL REGULATION BY*. <https://doi.org/10.1146/annurev.physiol.66.032802.155556>
- Provart, N. J., Brady, S. M., Parry, G., Schmitz, R. J., Queitsch, C., Bonetta, D., Waese, J., Schneeberger, K., & Loraine, A. E. (2021). Anno genominis XX: 20 years of Arabidopsis genomics. *Plant Cell*, 33(4), 832–845. <https://doi.org/10.1093/plcell/koaa038>
- Quinde, Z., Ullrich, S., & Baik, B. (2004). variation in color and discoloration potential of barley-based food products. *Cereal Chemistry*, 81 SRC-, 752–758.
- Radhamony, R. N., Prasad, A. M., Srinivasan, R., & Elect, J. (2005). T-DNA insertional mutagenesis in Arabidopsis: a tool for functional genomics. *Of Biotech*, 8 SRC-B, 82–106.
- Rajeevkumar, S., Anunanthini, P., & Sathishkumar, R. (2015). Epigenetic silencing in transgenic plants. *Frontiers in Plant Science*, 6(September), 1–8. <https://doi.org/10.3389/fpls.2015.00693>

- Ramsay, L., Comadran, J., Druka, A., Marshall, D. F., Thomas, W. T. B., Macaulay, M., MacKenzie, K., Simpson, C., Fuller, J., Bonar, N., Hayes, P. M., Lundqvist, U., Franckowiak, J. D., Close, T. J., Muehlbauer, G. J., & Waugh, R. (2011). INTERMEDIUM-C, a modifier of lateral spikelet fertility in barley, is an ortholog of the maize domestication gene TEOSINTE BRANCHED 1. *Nature Genetics*, *43*(2), 169–172. <https://doi.org/10.1038/ng.745>
- Rasheed, A., Gill, R. A., Hassan, M. U., Mahmood, A., Qari, S., Zaman, Q. U., Ilyas, M., Aamer, M., Batool, M., Li, H., & Wu, Z. (2021). A critical review: Recent advancements in the use of crispr/cas9 technology to enhance crops and alleviate global food crises. *Current Issues in Molecular Biology*, *43*(3), 1950–1976. <https://doi.org/10.3390/cimb43030135>
- Rast, M. I., & Simon, R. (2008). The meristem-to-organ boundary: more than an extremity of anything. *Current Opinion in Genetics and Development*, *18*(4), 287–294. <https://doi.org/10.1016/j.gde.2008.05.005>
- Ricci, W. A., Lu, Z., Ji, L., Marand, A. P., Ethridge, C. L., Murphy, N. G., Noshay, J. M., Galli, M., Mejía-Guerra, M. K., Colomé-Tatché, M., Johannes, F., Rowley, M. J., Corces, V. G., Zhai, J., Scanlon, M. J., Buckler, E. S., Gallavotti, A., Springer, N. M., Schmitz, R. J., & Zhang, X. (2019). Widespread long-range cis-regulatory elements in the maize genome. *Nature Plants*, *5*(12), 1237–1249. <https://doi.org/10.1038/s41477-019-0547-0>
- Rogowsky, P. M., Guidet, F. L. Y., Langridge, P., Shepherd, K. W., & Koebner, R. M. D. (1991). Isolation and characterization of wheat-rye recombinants involving chromosome arm 1DS of wheat. *Theoretical and Applied Genetics*, *82*(5), 537–544. <https://doi.org/10.1007/BF00226788>
- Rojas-Gracia, P., Roque, E., Medina, M., López-Martín, M. J., Cañas, L. A., Beltrán, J. P., & Gómez-Mena, C. (2019). The DOF Transcription Factor SIDOF10 Regulates Vascular Tissue Formation During Ovary Development in Tomato . In *Frontiers in Plant Science* (Vol. 10). <https://www.frontiersin.org/article/10.3389/fpls.2019.00216>
- Rusche, L. N., Kirchmaier, A. L., & Rine, J. (2003). *inheritance, and function of silenced chromatin in Saccharomyces cerevisiae*. 481–516. <https://doi.org/10.1146/annurev.biochem.72.121801.161547>

- Sakkour, A., Mascher, M., Himmelbach, A., Haberer, G., Lux, T., Spannagl, M., Stein, N., Kawamoto, S., & Sato, K. (2022). Chromosome-scale assembly of barley cv. “Haruna Nijo” as a resource for barley genetics. *DNA Research*, 29(1), 1–8.
<https://doi.org/10.1093/dnares/dsac001>
- Sakuma, S., Lundqvist, U., Kakei, Y., Thirulogachandar, V., Suzuki, T., Hori, K., Wu, J., Tagiri, A., Rutten, T., Koppolu, R., Shimada, Y., Houston, K., Thomas, W. T. B., Waugh, R., Schnurbusch, T., & Komatsuda, T. (2017). Extreme suppression of lateral floret development by a single amino acid change in the VRS1 transcription factor. *Plant Physiology*, 175(4), 1720–1731. <https://doi.org/10.1104/pp.17.01149>
- Sakuma, S., Salomon, B., & Komatsuda, T. (2011). The domestication syndrome genes responsible for the major changes in plant form in the triticeae crops. *Plant and Cell Physiology*, 52(5), 738–749. <https://doi.org/10.1093/pcp/pcr025>
- Sakuma, S., & Schnurbusch, T. (2019). Of floral fortune: tinkering with the grain yield potential of cereal crops. *New Phytologist*, 225(5), 1873–1882. <https://doi.org/10.1111/nph.16189>
- Satoh-nagasawa, N., Nagasawa, N., Malcomber, S., Sakai, H., & Jackson, D. (2006). *LETTERS A trehalose metabolic enzyme controls inflorescence architecture in maize*. 441(May), 227–230. <https://doi.org/10.1038/nature04725>
- Schmitz, R. J., & Grotewold, E. (2022). *Cis-regulatory sequences in plants : Their importance , discovery , and future challenges*. 718–741.
- Schreiber, M., Barakate, A., Uzrek, N., Macaulay, M., Sourdille, A., Morris, J., Hedley, P. E., Ramsay, L., & Waugh, R. (2019). A highly mutagenised barley (cv. Golden Promise) TILLING population coupled with strategies for screening-by-sequencing. *Plant Methods*, 15(1), 1–14. <https://doi.org/10.1186/s13007-019-0486-9>
- Schubert, D., Lechtenberg, B., Forsbach, A., Gils, M., Bahadur, S., & Schmidt, R. (2004). Silencing in Arabidopsis T-DNA transformants: The predominant role of a gene-specific RNA sensing mechanism versus position effects. *Plant Cell*, 16(10), 2561–2572.
<https://doi.org/10.1105/tpc.104.024547>
- Shahmuradov, I. A., Gammerman, A. J., Hancock, J. M., Bramley, P. M., & Solovyev, V. V. (2003). *PlantProm : a database of plant promoter sequences*. 31(1), 114–117.

<https://doi.org/10.1093/nar/gkg041>

- Shan, Q., Wang, Y., Chen, K., Liang, Z., Li, J., Zhang, Y., Zhang, K., Liu, J., Voytas, D. F., Zheng, X., Zhang, Y., & Gao, C. (2013). Rapid and Efficient Gene Modification in Rice and Brachypodium Using TALENs. *Molecular Plant*, 6(4), 1365–1368. <https://doi.org/10.1093/mp/sss162>
- Shang, Y., Yuan, L., Di, Z., Jia, Y., Zhang, Z., Li, S., Xing, L., Qi, Z., Wang, X., Zhu, J., Hua, W., Wu, X., Zhu, M., Li, G., & Li, C. (2020). A CYC/TB1-type TCP transcription factor controls spikelet meristem identity in barley. *Journal of Experimental Botany*, 71(22), 7118–7131. <https://doi.org/10.1093/jxb/eraa416>
- Shen, L., Wang, C., Fu, Y., Wang, J., Liu, Q., Zhang, X., Yan, C., Qian, Q., & Wang, K. (2018). QTL editing confers opposing yield performance in different rice varieties. *Journal of Integrative Plant Biology*, 60(2), 89–93. <https://doi.org/10.1111/jipb.12501>
- Shuai, B., Reynaga-Peña, C. G., & Springer, P. S. (2002). The Lateral Organ Boundaries Gene Defines a Novel, Plant-Specific Gene Family. *Plant Physiology*, 129(2), 747–761. <https://doi.org/10.1104/pp.010926>
- Shukla, V. K., Doyon, Y., Miller, J. C., DeKolver, R. C., Moehle, E. A., Worden, S. E., Mitchell, J. C., Arnold, N. L., Gopalan, S., Meng, X., Choi, V. M., Rock, J. M., Wu, Y.-Y., Katibah, G. E., Zhifang, G., McCaskill, D., Simpson, M. A., Blakeslee, B., Greenwalt, S. A., ... Urnov, F. D. (2009). Precise genome modification in the crop species *Zea mays* using zinc-finger nucleases. *Nature*, 459(7245), 437–441. <https://doi.org/10.1038/nature07992>
- Signor, S. A., & Nuzhdin, S. V. (2018). The Evolution of Gene Expression in cis and trans. *Trends in Genetics*, 34(7), 532–544. <https://doi.org/10.1016/j.tig.2018.03.007>
- Singer, S. D., Cox, K. D., & Liu, Z. (2011). *Enhancer – promoter interference and its prevention in transgenic plants*. 723–731. <https://doi.org/10.1007/s00299-010-0977-7>
- Sobel, J. M., & Streisfeld, M. A. (2013). Flower color as a model system for studies of plant evo-devo. *Frontiers in Plant Science*, 4(AUG), 1–17. <https://doi.org/10.3389/fpls.2013.00321>
- Soyk, S., Lemmon, Z. H., Oved, M., Fisher, J., Liberatore, K. L., Park, S. J., Goren, A., Jiang, K., Ramos, A., van der Knaap, E., Van Eck, J., Zamir, D., Eshed, Y., & Lippman, Z. B. (2017). Bypassing Negative Epistasis on Yield in Tomato Imposed by a Domestication

- Gene. *Cell*, 169(6), 1142-1155.e12. <https://doi.org/10.1016/j.cell.2017.04.032>
- Sreenivasulu, N., & Schnurbusch, T. (2012). A genetic playground for enhancing grain number in cereals. *Trends in Plant Science*, 17(2), 91–101. <https://doi.org/10.1016/j.tplants.2011.11.003>
- Srivastava, R., Mohan, K., Srivastava, M., Kumar, V., & Pandey, B. (2014). Distinct Role of Core Promoter Architecture in Regulation of Light-Mediated Responses in Plant Genes. *Molecular Plant*, 7(4), 626–641. <https://doi.org/10.1093/mp/sst146>
- Stam, M., Belele, C., Dorweiler, J. E., & Chandler, V. L. (2002). Differential chromatin structure within a tandem array 100 kb upstream of the maize b1 locus is associated with paramutation. *Genes and Development*, 16(15), 1906–1918. <https://doi.org/10.1101/gad.1006702>
- Stam, M., Belele, C., Ramakrishna, W., Dorweiler, J. E., Bennetzen, J. L., & Chandler, V. L. (2002). The Regulatory Regions Required for B ' Paramutation and Expression Are Located Far Upstream of the Maize b1 Transcribed Sequences. *Genetics*, 162(2), 917–930. <https://doi.org/10.1093/genetics/162.2.917>
- Strable, J., Unger-wallace, E., Raygoza, A. A., Briggs, S., & Vollbrecht, E. (2022). *Interspecies transfer of syntenic RAMOSA1 orthologs and promoter cis sequences impacts maize inflorescence architecture*. 1–32.
- Sun, Z., Li, N., Huang, G., Xu, J., Pan, Y., Wang, Z., Tang, Q., Song, M., & Wang, X. (2013). Site-Specific Gene Targeting Using Transcription Activator-Like Effector (TALE)-Based Nuclease in Brassica oleracea. *Journal of Integrative Plant Biology*, 55(11), 1092–1103. <https://doi.org/10.1111/jipb.12091>
- Suzuki, C., Tanaka, W., & Hirano, H. (2019). *Transcriptional Corepressor ASP1 and CLV-Like Signaling Regulate Meristem Maintenance in Rice 1 [OPEN]*. 180(July), 1520–1534. <https://doi.org/10.1104/pp.19.00432>
- Szarejko, I., Szurman-Zubrzycka, M., Nawrot, M., Marzec, M., Gruszka, D., & Kurowska, M. (2017). Creation of a TILLING population in barley after chemical mutagenesis with sodium azide and MNU,” in *Biotechnologies for Plant Mutation Breeding. Protocols Eds J.*
- Talamè, V., Bovina, R., Sanguineti, M. C., Tuberosa, R., Lundqvist, U., & Salvi, S. (2008).

- TILLMore, a resource for the discovery of chemically induced mutants in barley. *Plant Biotechnology Journal*, 6(5), 477–485. <https://doi.org/10.1111/j.1467-7652.2008.00341.x>
- Tang, G., Xu, P., Li, P., Zhu, J., Chen, G., Shan, L., & Wan, S. (2021). Cloning and functional characterization of seed-specific LEC1A promoter from peanut (*Arachis hypogaea* L.). *PLOS ONE*, 16(3), e0242949. <https://doi.org/10.1371/journal.pone.0242949>
- Tang, X., Liu, G., Zhou, J., Ren, Q., You, Q., Tian, L., Xin, X., Zhong, Z., Liu, B., Zheng, X., Zhang, D., Malzahn, A., Gong, Z., Qi, Y., & Zhang, T. (2018). A large-scale whole-genome sequencing analysis reveals highly specific genome editing by both Cas9 and Cpf1 (Cas12a) nucleases in rice. 1–13.
- Tavakol, E., Okagaki, R., Verderio, G., Vahid, S. J., Hussien, A., Bilgic, H., Scanlon, M. J., Todt, N. R., Close, T. J., Druka, A., Waugh, R., Steuernagel, B., Ariyadasa, R., Himmelbach, A., Stein, N., Muehlbauer, G. J., & Rossini, L. (2015). The barley Uriculme4 gene encodes a BLADE-ON-PETIOLE-like protein that controls tillering and leaf patterning. *Plant Physiology*, 168(1), 164–174. <https://doi.org/10.1104/pp.114.252882>
- The Arabidopsis Genome Initiative. (2000). Analysis of the genome sequence of the flowering plant *Arabidopsis thaliana*. *Nature*, 408(6814), 796–815. <https://doi.org/10.1038/35048692>
- The International Barley Genome Sequencing Consortium. (2012). A physical, genetic and functional sequence assembly of the barley genome. *Nature*, 491(7426), 711–716. <https://doi.org/10.1038/nature11543>
- The International Brachypodium Initiative. (2010). Genome sequencing and analysis of the model grass *Brachypodium distachyon*. *Nature*, 463(7282), 763–768. <https://doi.org/10.1038/nature08747>
- Thiel, J., Koppolu, R., Trautewig, C., Hertig, C., Kale, S. M., Erbe, S., Mascher, M., Himmelbach, A., Rutten, T., Esteban, E., Pasha, A., Kumlehn, J., Provar, N. J., Froberg, C., Schnurbusch, T., & Vanderauwera, S. (2021). *Transcriptional landscapes of floral meristems in barley*. 6940(April), 0–3.
- Tingay, S., McElroy, D., Kalla, R., Fieg, S., Wang, M., Thornton, S., Brettell, R., & Plant, J. (1997). *Agrobacterium tumefaciens-mediated barley transformation*. 11 SRC-, 1369–1376.
- Ulker, B., & Weisshaar, B. (2011). Genetics and Genomics of the Brassicaceae. In *Genetics and*

- Genomics of the Brassicaceae*. <https://doi.org/10.1007/978-1-4419-7118-0>
- van Esse, G. W., Walla, A., Finke, A., Koornneef, M., Pecinka, A., & von Korff, M. (2017). Six-rowed spike3 (VRS3) is a histone demethylase that controls lateral spikelet development in Barley. *Plant Physiology*, *174*(4), 2397–2408. <https://doi.org/10.1104/pp.17.00108>
- Vatov, E., Ludewig, U., & Zentgraf, U. (2021). Disparate dynamics of gene body and cis-regulatory element evolution illustrated for the senescence-associated cysteine protease gene SAG12 of plants. *Plants*, *10*(7). <https://doi.org/10.3390/plants10071380>
- Vavilova, V., Konopatskaia, I., Kuznetsova, A. E., Blinov, A., & Goncharov, N. P. (2017). DEP1 gene in wheat species with normal, compactoid and compact spikes. *BMC Genetics*, *18*(Suppl 1). <https://doi.org/10.1186/s12863-017-0583-6>
- Verma, A. K., Mandal, S., Tiwari, A., Monachesi, C., Catassi, G. N., Srivastava, A., Gatti, S., Lionetti, E., & Catassi, C. (2021). Current status and perspectives on the application of crispr/cas9 gene-editing system to develop a low-gluten, non-transgenic wheat variety. *Foods*, *10*(10), 1–19. <https://doi.org/10.3390/foods10102351>
- Vernoux, T., Brunoud, G., Farcot, E., Morin, V., Van Den Daele, H., Legrand, J., Oliva, M., Das, P., Larrieu, A., Wells, D., Guédon, Y., Armitage, L., Picard, F., Guyomarc'H, S., Cellier, C., Parry, G., Koumproglou, R., Doonan, J. H., Estelle, M., ... Traas, J. (2011). The auxin signalling network translates dynamic input into robust patterning at the shoot apex. *Molecular Systems Biology*, *7*(508). <https://doi.org/10.1038/msb.2011.39>
- Verstegen, H., Köneke, O., Korzun, V., & von Broock, R. (2014). *The World Importance of Barley and Challenges to Further Improvements BT - Biotechnological Approaches to Barley Improvement* (J. Kumlehn & N. Stein (eds.); pp. 3–19). Springer Berlin Heidelberg. https://doi.org/10.1007/978-3-662-44406-1_1
- Vollbrecht, E., Springer, P. S., Goh, L., Buckler IV, E. S., & Martienssen, R. (2005). Architecture of floral branch systems in maize and related grasses. *Nature*, *436*(7054), 1119–1126. <https://doi.org/10.1038/nature03892>
- von Bothmer, R., & Jacobsen, N. (1986). Interspecific crosses in *Hordeum* (Poaceae). *Plant Systematics and Evolution*, *153*(1–2), 49–64. <https://doi.org/10.1007/BF00989417>
- Wada, N., Ueta, R., Osakabe, Y., & Osakabe, K. (2020). Precision genome editing in plants:

- State-of-the-art in CRISPR/Cas9-based genome engineering. *BMC Plant Biology*, 20(1), 1–12. <https://doi.org/10.1186/s12870-020-02385-5>
- Wahbi, A. (1989). Gregory, Differences in Root and Shoot Growth of Barley (*Hordeum vulgare*). I. Glasshouse Studies of Young Plants and Effects of Rooting Medium. *Experimental Agriculture*, 25 SRC-, 375–387.
- Wan, Y., & Lemaux, P. G. (1994). Generation of large numbers of independently transformed fertile barley plants. *Plant Physiology*, 104(1), 37–48. <https://doi.org/10.1104/pp.104.1.37>
- Wang, B., Yang, X., Jia, Y., Xu, Y., Jia, P., Dang, N., Wang, S., Xu, T., Zhao, X., Gao, S., Dong, Q., & Ye, K. (2021). High-quality *Arabidopsis thaliana* Genome Assembly with Nanopore and HiFi Long Reads. *Genomics, Proteomics & Bioinformatics*. <https://doi.org/10.1016/j.gpb.2021.08.003>
- Wang, C., Yang, X., & Li, G. (2021). Molecular Insights into Inflorescence Meristem Specification for Yield Potential in Cereal Crops. *International Journal of Molecular Sciences*, 22(7), 3508. <https://doi.org/10.3390/ijms22073508>
- Wang, J., Zhang, W., Cheng, Y., & Feng, L. (2021). Genome-Wide Identification of LATERAL ORGAN BOUNDARIES DOMAIN (LBD) Transcription Factors and Screening of Salt Stress Candidates of *Rosa rugosa* Thunb. *Biology*, 10(10), 992. <https://doi.org/10.3390/biology10100992>
- Wang, Q., Hasson, A., Rossmann, S., & Theres, K. (2016). Divide et impera: Boundaries shape the plant body and initiate new meristems. *New Phytologist*, 209(2), 485–498. <https://doi.org/10.1111/nph.13641>
- Wang, S., Chang, Y., Guo, J., Zeng, Q., Ellis, B. E., & Chen, J. (2011). *Arabidopsis Ovate Family Proteins* , a Novel Transcriptional Repressor Family , Control Multiple Aspects of Plant Growth and Development. 6(8). <https://doi.org/10.1371/journal.pone.0023896>
- Wang, W., Simmonds, J., Pan, Q., Davidson, D., He, F., Battal, A., Akhunova, A., Trick, H. N., Uauy, C., & Akhunov, E. (2018). Gene editing and mutagenesis reveal inter-cultivar differences and additivity in the contribution of TaGW2 homoeologues to grain size and weight in wheat. *Theoretical and Applied Genetics*, 131(11), 2463–2475. <https://doi.org/10.1007/s00122-018-3166-7>

- Wang, X., Aguirre, L., Rodríguez-Leal, D., Hendelman, A., Benoit, M., & Lippman, Z. B. (2021). Dissecting cis-regulatory control of quantitative trait variation in a plant stem cell circuit. *Nature Plants*, 7(4), 419–427. <https://doi.org/10.1038/s41477-021-00898-x>
- Wang, Y., Cheng, X., Shan, Q., Zhang, Y., Liu, J., Gao, C., & Qiu, J.-L. (2014). Simultaneous editing of three homoeoalleles in hexaploid bread wheat confers heritable resistance to powdery mildew. *Nature Biotechnology*, 32(9), 947–951. <https://doi.org/10.1038/nbt.2969>
- Watt, C., Zhou, G., Angessa, T. T., Moody, D., & Li, C. (2020). A novel polymorphism in the 5' UTR of HvDEP1 is associated with grain length and 1000-grain weight in barley (*Hordeum vulgare*). *Crop and Pasture Science*, 71(8), 752–759. <https://doi.org/10.1071/CP20169>
- Wei, Z., Teo, N., Zhou, W., & Shen, L. (2019). *Dissecting the Function of MADS-Box Transcription Factors in Orchid Reproductive Development*. 10(November), 1–17. <https://doi.org/10.3389/fpls.2019.01474>
- Wendt, T., Holm, P. B., Starker, C. G., Christian, M., Voytas, D. F., Brinch-Pedersen, H., & Holme, I. B. (2013). TAL effector nucleases induce mutations at a pre-selected location in the genome of primary barley transformants. *Plant Molecular Biology*, 83(3), 279–285. <https://doi.org/10.1007/s11103-013-0078-4>
- Wendt, T., Holme, I., Dockter, C., Preu, A., Thomas, W., Druka, A., Waugh, R., Hansson, M., & Braumann, I. (2016). HvDep1 Is a Positive regulator of culm elongation and grain size in barley and impacts yield in an environment-dependent manner. *PLoS ONE*, 11(12), 1–21. <https://doi.org/10.1371/journal.pone.0168924>
- Whipple, C. J. (2017). Grass inflorescence architecture and evolution: the origin of novel signaling centers. *New Phytologist*, 216(2), 367–372. <https://doi.org/10.1111/nph.14538>
- Witt Hmon, K. P., Shehzad, T., & Okuno, K. (2014). QTLs underlying inflorescence architecture in sorghum (*Sorghum bicolor* (L.) Moench) as detected by association analysis. *Genetic Resources and Crop Evolution*, 61(8), 1545–1564. <https://doi.org/10.1007/s10722-014-0129-y>
- Xiao, J., Jin, R., Yu, X., Shen, M., Wagner, J. D., Pai, A., Song, C., Klasfeld, S., He, C., Santos, A. M., Helliwell, C., Pruneda-paz, J. L., Kay, S. A., Lin, X., Cui, S., Garcia, M. F., Clarenz, O., Goodrich, J., Zhang, X., ... Wagner, D. (2017). *Cis and trans determinants of epigenetic*

silencing by Polycomb repressive complex 2 in Arabidopsis. August.

<https://doi.org/10.1038/ng.3937>

- Xu, C., Luo, F., & Hochholdinger, F. (2016). LOB Domain Proteins: Beyond Lateral Organ Boundaries. *Trends in Plant Science*, *21*(2), 159–167.
<https://doi.org/10.1016/j.tplants.2015.10.010>
- Yamagata, H., Yonesu, K., Hirata, A., & Aizono, Y. (2002). TGTCACA motif is a novel cis-regulatory enhancer element involved in fruit-specific expression of the cucumisin gene. *Journal of Biological Chemistry*, *277*(13), 11582–11590.
<https://doi.org/10.1074/jbc.M109946200>
- Yanagisawa, S. (2004). Dof domain proteins: Plant-specific transcription factors associated with diverse phenomena unique to plants. *Plant and Cell Physiology*, *45*(4), 386–391.
<https://doi.org/10.1093/pcp/pch055>
- Yang, C., Shen, W., He, Y., Tian, Z., & Li, J. (2016). OVATE Family Protein 8 Positively Mediates Brassinosteroid Signaling through Interacting with the GSK3-like Kinase in Rice. *PLoS Genetics*, *12*(6), 1–15. <https://doi.org/10.1371/journal.pgen.1006118>
- Yang, Q., Zhong, X., Li, Q., Lan, J., Tang, H., Qi, P., Ma, J., Wang, J., Chen, G., Pu, Z., Li, W., Lan, X., Deng, M., Harwood, W., Li, Z., Wei, Y., Zheng, Y., & Jiang, Q. (2020). Mutation of the D-hordein gene by RNA-guided Cas9 targeted editing reducing the grain size and changing grain compositions in barley. *Food Chemistry*, *311*, 125892.
<https://doi.org/10.1016/j.foodchem.2019.125892>
- Yang, X., Wang, J., Dai, Z., Zhao, X., Miao, X., & Shi, Z. (2019). miR156f integrates panicle architecture through genetic modulation of branch number and pedicel length pathways. *Rice*, *12*(1). <https://doi.org/10.1186/s12284-019-0299-5>
- Yang, Y., Singer, S. D., & Liu, Z. (2011). *Evaluation and comparison of the insulation efficiency of three enhancer-blocking insulators in plants.* 405–414. <https://doi.org/10.1007/s11240-010-9880-8>
- Yanofsky, M. F., Ma, H., Bowman, J. L., Drews, G. N., Feldmann, K. A., & Meyerowitz, E. M. (1990). The protein encoded by the Arabidopsis homeotic gene *agamous* resembles transcription factors. *Nature*, *346*(6279), 35–39. <https://doi.org/10.1038/346035a0>

- Youssef, H. M. (2015). Genotypic and phenotypic analysis of the spike row-type in barley (*Hordeum vulgare* L. *PhD Thesis MartinLutherUniversitt HalleWittenberg and LeibnizInstitute of Plant Genetics and Crop Plant Research IPK Gatersleben 140 Pp.*
- Youssef, H. M., Eggert, K., Koppolu, R., Alqudah, A. M., Poursarebani, N., Fazeli, A., Sakuma, S., Tagiri, A., Rutten, T., Govind, G., Lundqvist, U., Graner, A., Komatsuda, T., Sreenivasulu, N., & Schnurbusch, T. (2017). VRS2 regulates hormone-mediated inflorescence patterning in barley. *Nature Genetics*, *49*(1), 157–161.
<https://doi.org/10.1038/ng.3717>
- Youssef, H. M., Koppolu, R., Rutten, T., Korzun, V., Schweizer, P., & Schnurbusch, T. (2020). Correction to: Genetic mapping of the labile (lab) gene: a recessive locus causing irregular spikelet fertility in labile-barley (*Hordeum vulgare* convar. labile). *Theoretical and Applied Genetics*, *133*(9), 2759. <https://doi.org/10.1007/s00122-020-03646-5>
- Youssef, H. M., Koppolu, R., & Schnurbusch, T. (2012). Re-sequencing of vrs1 and int-c loci shows that labile barleys (*Hordeum vulgare* convar. labile) have a six-rowed genetic background. *Genetic Resources and Crop Evolution*, *59*(7), 1319–1328.
<https://doi.org/10.1007/s10722-011-9759-5>
- Youssef, H., Mascher, M., Ayoub, M., Stein, N., Kilian, B., & Schnurbusch, T. (2017). Natural diversity of inflorescence architecture traces cryptic domestication genes in barley (*Hordeum vulgare* L.). *Genetic Resources and Crop Evolution*, *64*(5), 843–853.
<https://doi.org/10.1007/s10722-017-0504-6>
- Yu, J., Hu, S., Wang, J., Wong, G. K. S., Li, S., Liu, B., Deng, Y., Dai, L., Zhou, Y., Zhang, X., Cao, M., Liu, J., Sun, J., Tang, J., Chen, Y., Huang, X., Lin, W., Ye, C., Tong, W., ... Yang, H. (2002). A draft sequence of the rice genome (*Oryza sativa* L. ssp. indica). *Science*, *296*(5565), 79–92. <https://doi.org/10.1126/science.1068037>
- Yuan, Z., Persson, S., & Zhang, D. (2020). Molecular and genetic pathways for optimizing spikelet development and grain yield. *ABIOTECH*, *1*(4), 276–292.
<https://doi.org/10.1007/s42994-020-00026-x>
- Zakhrabekova, S. M., Gough, S., Lundh, L., & Hansson, M. (2013). Functional genomics and forward and reverse genetics approaches for identification of important QTLs in plants.

Proc. Azerbaijan Natl. Acad. Sci, 68, 23–28.

<http://www.jbio.az/uploads/journal/222889591015b9d8e16469ac9cf9bacd.pdf>

- Zegeye, W. A., Tsegaw, M., Zhang, Y., & Cao, L. (2022). *CRISPR-Based Genome Editing : Advancements and Opportunities for Rice Improvement*.
- Zeng, Z., Han, N., Liu, C., Buerte, B., Zhou, C., Chen, J., Wang, M., Zhang, Y., Tang, Y., Zhu, M., Wang, J., Yang, Y., & Bian, H. (2020). Functional dissection of HGGT and HPT in barley vitamin E biosynthesis via CRISPR/Cas9-enabled genome editing. *Annals of Botany*, 126(5), 929–942. <https://doi.org/10.1093/aob/mcaa115>
- Zhang, D., & Yuan, Z. (2014). Molecular Control of Grass Inflorescence Development. *Annual Review of Plant Biology*, 65(1), 553–578. <https://doi.org/10.1146/annurev-arplant-050213-040104>
- Zhang, H., Zhang, J., Wei, P., Zhang, B., Gou, F., Feng, Z., Mao, Y., Yang, L., Zhang, H., Xu, N., & Zhu, J. (2014). *The CRISPR / Cas9 system produces specific and homozygous targeted gene editing in rice in one generation*. 797–807. <https://doi.org/10.1111/pbi.12200>
- Zhang, N., Roberts, H. M., Eck, J. Van, & Martin, G. B. (2020). *Generation and Molecular Characterization of CRISPR / Cas9- Induced Mutations in 63 Immunity- Associated Genes in Tomato Reveals Specificity and a Range of Gene Modifications*. 11(February), 1–13. <https://doi.org/10.3389/fpls.2020.00010>
- Zhang, Y., Li, Z., Ma, B., Hou, Q., & Wan, X. (2020). Phylogeny and functions of LOB domain proteins in plants. *International Journal of Molecular Sciences*, 21(7). <https://doi.org/10.3390/ijms21072278>
- Zhang, Y., Liang, Z., Zong, Y., Wang, Y., Liu, J., Chen, K., Qiu, J. L., & Gao, C. (2016). Efficient and transgene-free genome editing in wheat through transient expression of CRISPR/Cas9 DNA or RNA. *Nature Communications*, 7, 1–8. <https://doi.org/10.1038/ncomms12617>
- Zhang, Y., Zhang, F., Li, X., Baller, J. A., Qi, Y., Starker, C. G., Bogdanove, A. J., & Voytas, D. F. (2013). Transcription Activator-Like Effector Nucleases Enable Efficient Plant Genome Engineering. *Plant Physiology*, 161(1), 20–27. <https://doi.org/10.1104/pp.112.205179>
- Zhao, Y., Zheng, D., & Cvekl, A. (2019). Profiling of chromatin accessibility and identification

- of general cis - regulatory mechanisms that control two ocular lens differentiation pathways. *Epigenetics & Chromatin*, 1–23. <https://doi.org/10.1186/s13072-019-0272-y>
- Zheng, L., McMullen, M. D., Bauer, E., Schön, C. C., Gierl, A., & Frey, M. (2015). Prolonged expression of the BX1 signature enzyme is associated with a recombination hotspot in the benzoxazinoid gene cluster in *Zea mays*. *Journal of Experimental Botany*, 66(13), 3917–3930. <https://doi.org/10.1093/jxb/erv192>
- Zhou, J., Xin, X., He, Y., Chen, H., Li, Q., Tang, X., Zhong, Z., Deng, K., Zheng, X., Akher, S. A., Cai, G., Qi, Y., & Zhang, Y. (2019). Multiplex QTL editing of grain-related genes improves yield in elite rice varieties. *Plant Cell Reports*, 38(4), 475–485. <https://doi.org/10.1007/s00299-018-2340-3>
- Zhu, C., Yang, J., Box, M. S., Kellogg, E. A., & Eveland, A. L. (2018). A dynamic co-expression map of early inflorescence development in *setaria viridis* provides a resource for gene discovery and comparative genomics. *Frontiers in Plant Science*, 9(September), 1–17. <https://doi.org/10.3389/fpls.2018.01309>
- Zhu, Z., Tan, L., Fu, Y., Liu, F., Cai, H., Xie, D., Wu, F., Wu, J., Matsumoto, T., & Sun, C. (2013). Genetic control of inflorescence architecture during rice domestication. *Nature Communications*, 4, 1–8. <https://doi.org/10.1038/ncomms3200>
- Zwirek, M., Waugh, R., & McKim, S. M. (2019). Interaction between row-type genes in barley controls meristem determinacy and reveals novel routes to improved grain. *New Phytologist*, 221(4), 1950–1965. <https://doi.org/10.1111/nph.15548>

9.0. Appendix

Table 1. List of primers used in different parts of the current studies.

Primer name	Sequence (5' to 3')
Universal Primer for transgenic analysis	
GH-TE9-F1	TGCAAGCTGATCCACTAGAG
GH-NOS-F2	AAGATTGAATCCTGTTGCCG
35S-F2-Catrin	CATGGTGGAGCACGACTCTC
OE-HYG-F1	TATCGGCACTTTCATCGGC
OE- HYG-R1	TGCCGTCAACCAAGCTCTGA
Primers specific for overexpression constructs	
OE-UbiRA2-F1	CCAGCGTTGTTGTTGCTCCG
OE-UbiRA2-R1	GCTACGGGGGATTCCTTTCCC
OE-UbiRA2-F2	TGAGCAGCTTGGTACAGTT
OE-UbiRA2-R2	TTTAGCCCTGCCTTCATACG
OE-UbiRA2-F3	CAGACGGGATCGATCTAGGA
OE-UbiRA2-R3	GTTGAGCAGCTTGGTCACG
Primers specific for complementation constructs	
Aecom-F1	TACTCAAACGGGCCACTCAC
Aecom-R1	TTTCCCCATTTCTTGCGTCG
Aecom-F2	CGTAGACGGGGTCCTTGAC
Aecom-R2	GCTCCCAAACCCTAATCTCC
OE-F	GCATGCAAGCTGATCCACTA
OE-R	CCACCTCAGGATCAGAGAGC
BP-R	TCATGCAAAGGACAAAAGCA
SP-R	CCAATTTTCATGGCATTCTAA
Primers used for sequencing	
p6i-2x35S-TE9-F	AGAAGTACTCGCCGATAGTG
p6i-2x35S-TE9-R	GGTGGTTGAACAGAAGTCAT
P6i-F	GTGGCCTCTAATGACCGAAG
P6i-R	AAACGACAATCTGATCGGGTA
T7F	TAATACGACTCACTATAGGG
M13-F1	CAGGAAACAGCTATGACCATGATTACG
M13-R1	TGTA AAAACGACGGCCAGTGAATTGT
AD-F	GCCATGGAGTACCCATACGA

AD-R	TTGCGGGGTTTTTCAGTATC
BD-F	CCATCATGGAGGAGCAGAAG
BD-R	ACCCCTCAAGACCCGTTTAG
Primers used for RGEN constructs	
Bie475	TTAGCCCTGCCTTCATACG
GH-zCas9-R1	TTAATCATGTGGGCCAGAGC
GH-vrs4-PS1-F	GGCGGGAGTTGCCGGTGCTCGACG
GH-vrs4-PS2-F	GGCGTGACGCGGCCACGACACCGG
GH-OsU3T-R1	TCAGCGGGTCACCAGTGTG
Primers used for off-target analysis	
Off1-F1	GGCCTTGTTTAATTGGCTGA
Off1-R1	GGCATGCCCTTGCTATTATC
Off1-F2	AGTGTGACGTCAACATCCAAA
Off1-R2	TTCCATCCTTGGCACAGAC
Off1-F3	CGCGGTCATCTCTCCTC
Off1-R3	TTGGTGAGCCCAATAAAAC
Off2-F1	ACTGCATCCATCGTCATCG
Off2-R1	CAGCTGCGTTCAACTGCTAC
Off2-F2	ATGGAGTCACCGACCTCAAG
Off2-R2	GTCGTCCTGGCTGTCTTCAT
Primers used for GFP constructs	
SbGFP-F1	AAGTCGTGCTGCTTCATGTG
SbGFP-R1	CCTTCCCAGAACAATCCTCA
AeGFP-F1	AAGCGCATATCATCTCCAC
AeGFP-R1	ACGTAAACGGCCACAAGTTC
GH-GFP-F1	GGTCACGAACTCCAGCAGGA
GH-GFP-R2	TACGGCAAGCTGACCCTGAA
GFP-F	CGACCACTACCAGCAGAACA
GFP-R	ACCGGCAACAGGATTCAA
Primer for qRT-PCR	
Actin-F	AAGTACAGTGTCTGGATTGGAGGG
Actin-R	TCGCAACTTAGAAGCACTTCCG
Qgfp-F	CTGCTGCCCGACAACCAC
Qgfp-R	TCACGAACTCCAGCAGGAC
SbqpcrF1	GGGTCTTGGATGGCGTAGTA
SbqpcrR1	CTGTGGTTCCGCATGAAGTA
WBqpcrF1	GGCTTGTGGACGCGATAGTA
WBqpcrR1	TGTTGTTGCTCCGCATATTG
SbqpcrF2	AGACAGCAGCATGTGAAGTG
SbqpcrR2	TAAGGCCAAAGGGCTCAAAT

WBqperF2	CGACAGCAGCATGTGAACTG
WBqperR2	GGCCAAAGCGCATATCAT
qvrs4F	ATTACCACCACCTCAGGATCA
qvrs4R	GAGTAGGAGAGGTAATCCACA
qvrs1F	CCGAGATAGCTGCTGCCGCC
qvrs1R	TGCATCGCGGGCAATGGAGA
qhpt-in-F	CACGCCATGTAGTGTATTGACC
qhpt-in-R	GCCGATCTTAGCCAGACGAG
qhpt-F	ATAGGTCAGGCTCTCGCTGA
qhpt-R	GATGTAGGAGGGCGTGGATA
Primers used for Y2H constructs	
Y2HF1	ATATGGCCATGGAGGCCAGTGAATTCATGGACATGGGCTTCCAC GG
Y2HR1	CTACGATTCATCTGCAGCTCGAGCTCCTACTTGTACCCGAAGGTC T
Y2HF2	ATATGGCCATGGAGGCCAGTGAATTCATGGAATCCTCCACATCA C
Y2HR2	CTACGATTCATCTGCAGCTCGAGCTCTTACCAAAGAAGCTTGTC T
Y2HF3	ATATGGCCATGGAGGCCAGTGAATTCATGGGGATCGACCTCAAC AC
Y2HR3	CTACGATTCATCTGCAGCTCGAGCTCTCACATCCCAGAGGAGCA G
Y2HF4	ATATGGCCATGGAGGCCAGTGAATTCATGGAGCCGGGCGCCGAC GC
Y2HR4	CTACGATTCATCTGCAGCTCGAGCTCTCACGCTGATCCTTCTGCC G
Y2HF5	ATATGGCCATGGAGGCCAGTGAATTCATGGAAGCCGCACGGATC GC
Y2HR5	CTACGATTCATCTGCAGCTCGAGCTC CTACTGCGCGGGGCAAAGG
Y2HF6	ATATGGCCATGGAGGCCAGTGAATTCATGGGCGTGCTTTCTCGT G
Y2HR6	CTACGATTCATCTGCAGCTCGAGCTC TCATAAACTGATCAGTAGTC
Y2HF7	ATATGGCCATGGAGGCCAGTGAATTCATGCAGCAGCGCAAGGCC AA
Y2HR7	CTACGATTCATCTGCAGCTCGAGCTC CTACTGGGATCTTGAACGA
Y2HF8	ATATGGCCATGGAGGCCAGTGAATTCATGGACTACGAGCGCATC CA
Y2HR8	CTACGATTCATCTGCAGCTCGAGCTC TCATAGGCACCAGCACCAGC
Y2HF9	ATATGGCCATGGAGGCCAGTGAATTCATGTGAGCAAGCCGTCG TC
Y2HR9	CTACGATTCATCTGCAGCTCGAGCTC CTAGAACTGGCATGGCGAGG
Y2HF10	ATATGGCCATGGAGGCCAGTGAATTCATGTCAAGCCGCCGTGGC AG
Y2HR10	CTACGATTCATCTGCAGCTCGAGCTC CTAGCGGAGAAGGCTCCGGA

Y2HF11	ATATGGCCATGGAGGCCAGTGAATTCATGGACGACACCTTCAAG TC
Y2HR11	CTACGATTCATCTGCAGCTCGAGCTC TCATGGGAAGCCATGAGGGG
Y2HF12	ATATGGCCATGGAGGCCAGTGAATTCATGATGAAGGGGGCCGCT GC
Y2HR12	CTACGATTCATCTGCAGCTCGAGCTC TCACACGCGCAACGCGGGGC
Y2HF13	ATATGGCCATGGAGGCCAGTGAATTCATGGGGCGAACGAGCAGC AG
Y2HR13	CTACGATTCATCTGCAGCTCGAGCTCTCACGGCTTCTCCAGCTGG C
Y2HF14	ATATGGCCATGGAGGCCAGTGAATTCATGGGGGAGGGCGCGGTG GT
Y2HR14	CTACGATTCATCTGCAGCTCGAGCTCTCAACACAGGCACCCGCTA G
Y2HF15	ATATGGCCATGGAGGCCAGTGAATTCATGGGGCGTGCTCTTCTCGT G
Y2HR15	CTACGATTCATCTGCAGCTCGAGCTCTCATAAACTGATCAGTAGT C
Y2HF16	ATATGGCCATGGAGGCCAGTGAATTCATGCCAAGGAGACGCCGT GC
Y2HR16	CTACGATTCATCTGCAGCTCGAGCTC TCAGAAGATGTGGAGGATGT
Y2HF18	ATATGGCCATGGAGGCCAGTGAATTCATGGACAAGCATCAGCTC TT
Y2HR18	CTACGATTCATCTGCAGCTCGAGCTC TCAGGTCATCGTCCCGCCCC
Y2HF19	ATATGGCCATGGAGGCCAGTGAATTCATGGACAAGCAGCACCTC TT
Y2HR19	CTACGATTCATCTGCAGCTCGAGCTC TCAAATCAGCCCATACAGGC
GDSL-F	ATATGGCCATGGAGGCCAGTGAATTCATGGCGGCCTCCTCCACG GC
GDSL-R	CTACGATTCATCTGCAGCTCGAGCTCCTACGGGTGCCACGCGGC GA
HST -F	ATATGGCCATGGAGGCCAGTGAATTCATGAAGGTGGAGGTGGTG GA
HST -R	CTACGATTCATCTGCAGCTCGAGCTCTCACTCCCCGTAGAAGGCC T
Pep15-F	ATATGGCCATGGAGGCCAGTGAATTCATGGGATCAGAAGGGCCT TC
Pep15-R	CTACGATTCATCTGCAGCTCGAGCTCCTAGTTCAGGCTAGCGAGA G
BRUNO-F	ATATGGCCATGGAGGCCAGTGAATTCATGGCGGAGGACGGCGAG AA
BRUNO-R	CTACGATTCATCTGCAGCTCGAGCTCTCAAAAAGGTTTACTGTGC T
WD40-F	ATATGGCCATGGAGGCCAGTGAATTCATGTATTACGAATTCAGAA A
WD40-R	CTACGATTCATCTGCAGCTCGAGCTCCTACAGGTTGTTATTATGT A
SPL14-F	ATATGGCCATGGAGGCCAGTGAATTCATGGAGATTGGCAGCGGT GG

SPL14-R	CTACGATTCATCTGCAGCTCGAGCTCCTACAGGGACCAGTTGGAC G
LAX1-F	ATATGGCCATGGAGGCCAGTGAATTCATGGATCCATATCACTACG A
LAX1-R	CTACGATTCATCTGCAGCTCGAGCTC CTAATAAGATCCGTGAGCAT
LaXA-F	ATATGGCCATGGAGGCCAGTGAATTCATGAGCTCGGAGGACTCG
LaXA-R	CTACGATTCATCTGCAGCTCGAGCTCTCATGGGAAGCCATTGGG
Primers for transient expression assay for promoter activity	
Hvpluc-F	CACCgGATCCTATACTCTATCTTCA
Hvpluc-R	TGCCGGCGACCTGCGTATATA
Sbpluc-F	CACCGATCCGCTTTTTTTATATTAATAG
Sbpluc-R	TTCCTTCCTGGTCCTGGCC
Aepluc-F	CACCGGATCCGGAGGGAGTATCTA
Aepluc-R	CATTGCCAGCGACCTGTGTA

Table 2. Number of putative transcription factor binding sites (TFBSs) in the selected sequences as putative RA2 promoter of barley, wheat, and sorghum and their predicted biological function

TF-Type	No. TFBSs in RA2 promoter			Predicate biological function
	barley	wheat	sorghum	
At-HooK	24	26	27	Plant organ size development stress responses and regulation of growth and development
NAC; NAM	12	12	23	Shoot apical meristem and flower Development, and organ separation
MYB; ARR-B	5	3	4	Cellular morphogenesis, signal transduction in plant growth
Homeodomain; bZIP; HD-ZIP	10	12	11	Embryogenesis, flower development, and vascular development in plants, ABA response, and gibberellin biosynthesis
MYB-related	38	40	41	Cellular morphogenesis, signal transduction in plant growth, the MYB TFs are involved in different biological processes, such as circadian rhythm, defense and stress responses, cell fate and identity, seed and floral development, and regulation of primary and secondary metabolism in plants
AP2; ERF	32	32	9	Flower development, ethylene response, spikelet meristem determinacy, leaf epidermal cell identity, cell proliferation, secondary metabolism, abiotic and biotic stress responses, ABA response
B3; ARF	2	3	2	Auxin response factor and hormonal signaling, and response to light and environmental stress
Dof	54	52	62	Cell expansion, metabolism regulation, the control of flowering time, and abiotic stress responses
B3	17	18	16	Plant-specific superfamily transcription factors are involved in many aspects of plant development

bHLH	13	7	10	Plant developmental, photomorphogenesis, flowering induction, response to environmental
bZIP	45	32	55	Plant growth, development, and abiotic and biotic stress responses.
C2H2	34	34	30	Transcriptional regulation of flowering induction, floral organ morphogenesis, flowering time
EIN3 ; EIL;EIL	3	5	3	Key regulators of ethylene signaling/a crucial factor for plant growth and development under diverse environmental conditions.
GATA; tify	14	14	14	Plant development, flowering regulator, defenses and stress responses, phytohormones signaling
MADS-box; MIKC	4	8	4	inflorescence development, flowering time, and floral meristem identity
TALE; TALE	4	4	2	Regulation of secondary wall accumulation
MADF	19	17	9	Regulation of transcription, DNA-templated
Myb/SANT	123	135	101	Regulation of transcription and response to Abiotic stress
Myb/SANT; G2-like	14	15	10	Regulating chloroplast development, and flowering time
SBP	29	34	26	Play important roles in many growth and development processes including phase transition, leaf initiation, shoot and inflorescence branching, fruit development and ripening etc
Sox; YABBY	3	3	3	Lateral organ development and asymmetric growth of the ovule outer integument
TBP	4	2	7	Transcription initiation and formation of the transcription complex
WRKY	58	56	36	WRKY- Defense response HB (Homeodomain)- Development (leaf, root, internode, and ovule), stem cell identity, cell differentiation, growth responses, anthocyanin accumulation, and cell death

wox	6	6	6	Play a wide variety of roles in plant development and growth processes such as embryonic patterning, stem cell maintenance, and organ formation
TCP	4	4	16	Cell growth regulation, meristem identity, and the growth of lateral branches
Alpha-amylase	5	5	6	Important for the breakdown of endosperm starch during germination

Table.3 comparison analysis for motif function finding using tomtom tool analysis

Query_ID	Target_ID	Optimal_offset	p-value	E-value	q-value	Overlap	Query_consensus	Target_consensus	Orientation
3	C2C2dof_tnt.AT1G4765_5_colamp_a_m1	-18	1.34 E-05	0.01 1724	0.01 2818	15	GTATCTACATACATTTGTTTTTCATTATTT TTTTTCTGCGAGCTTATGTAA	TTTTTTCTTTTTTT	+
3	ABI3VP1_tnt.VRN1_col_a_m1	-9	1.75 E-05	0.01 5223	0.01 2818	29	GTATCTACATACATTTGTTTTTCATTATTT TTTTTCTGCGAGCTTATGTAA	TTTTTTTTTTTTTTTTTT TTTTTTTTTC	+
3	ABI3VP1_tnt.VRN1_colamp_a_m1	-16	2.25 E-05	0.01 9638	0.01 2818	19	GTATCTACATACATTTGTTTTTCATTATTT TTTTTCTGCGAGCTTATGTAA	CTGTTTTTTTTTTTTTTTT	+
3	REM_tnt.REM19_col_a_m1	-20	6.68 E-05	0.05 8218	0.02 85	15	GTATCTACATACATTTGTTTTTCATTATTT TTTTTCTGCGAGCTTATGTAA	TTTTTTTTTTTTTTTT	-
3	C2C2dof_tnt.AT1G6957_0_col_a_m1	-7	0.00 0101	0.08 8309	0.03 4585	27	GTATCTACATACATTTGTTTTTCATTATTT TTTTTCTGCGAGCTTATGTAA	TTTTCACTTTTTCTTTTT TTTTTTTTT	+
3	C2H2_tnt.SGR5_colamp_a_m1	-19	0.00 0134	0.11 7036	0.03 6063	15	GTATCTACATACATTTGTTTTTCATTATTT TTTTTCTGCGAGCTTATGTAA	TTTTGTCTTTTTTTTT	+
3	C2C2dof_tnt.OBP3_col_a_m1	-13	0.00 0148	0.12 8916	0.03 6063	21	GTATCTACATACATTTGTTTTTCATTATTT TTTTTCTGCGAGCTTATGTAA	TTTACTTTTTTTTTTTTT TT	+
3	C2H2_tnt.AtIDD11_col_a_m1	-14	0.00 0235	0.20 5047	0.04 7994	21	GTATCTACATACATTTGTTTTTCATTATTT TTTTTCTGCGAGCTTATGTAA	TTTTTTTTTTTGTCTTTTT CT	+
3	C2C2dof_tnt.OBP3_colamp_a_m1	-13	0.00 0262	0.22 8739	0.04 7994	19	GTATCTACATACATTTGTTTTTCATTATTT TTTTTCTGCGAGCTTATGTAA	TTTTTTTTTTTACTTTTT	+
3	C2C2dof_tnt.dof42_col_a_m1	-17	0.00 0281	0.24 5093	0.04 7994	19	GTATCTACATACATTTGTTTTTCATTATTT TTTTTCTGCGAGCTTATGTAA	TTTTTTGCCTTTTTTTTT	-
3	C2C2dof_tnt.AT5G0246_0_col_a_m1	-11	0.00 0369	0.32 2148	0.05 5499	21	GTATCTACATACATTTGTTTTTCATTATTT TTTTTCTGCGAGCTTATGTAA	TTTTTTTTTTTTTACTTTT TT	-
3	REM_tnt.REM19_colamp_a_m1	-19	0.00 0394	0.34 3288	0.05 5499	21	GTATCTACATACATTTGTTTTTCATTATTT TTTTTCTGCGAGCTTATGTAA	TTTTTTTTTTTTTTTTTTC AT	-
3	C2H2_tnt.SGR5_col_a_m1	-18	0.00 0423	0.36 8446	0.05 5499	15	GTATCTACATACATTTGTTTTTCATTATTT TTTTTCTGCGAGCTTATGTAA	TTTTGTCTTTTTTT	-
3	C2C2dof_tnt.At4g38000_col_a_m1	-16	0.00 0562	0.49 007	0.06 5117	28	GTATCTACATACATTTGTTTTTCATTATTT TTTTTCTGCGAGCTTATGTAA	TTTTTTTTTTTTTTTTTTT TACTTTTTT	+
3	C2C2dof_tnt.AT5G6694_0_colamp_a_m1	-13	0.00 0574	0.50 0131	0.06 5117	21	GTATCTACATACATTTGTTTTTCATTATTT TTTTTCTGCGAGCTTATGTAA	TTTTTTTACTTTTTCTTTT TT	+
3	NAC_tnt.NTM1_colamp_a_m1	-12	0.00 061	0.53 206	0.06 5117	21	GTATCTACATACATTTGTTTTTCATTATTT TTTTTCTGCGAGCTTATGTAA	TTTTACTTTTTCTTTTTT TT	-
3	C2C2dof_tnt.AT2G2881_0_col_a_m1	-12	0.00 0649	0.56 5894	0.06 5184	21	GTATCTACATACATTTGTTTTTCATTATTT TTTTTCTGCGAGCTTATGTAA	TTTTTTTTTTTTTACTTTT TT	+
3	C2C2dof_tnt.AT1G6957_0_colamp_a_m1	-11	0.00 069	0.60 1739	0.06 5462	21	GTATCTACATACATTTGTTTTTCATTATTT TTTTTCTGCGAGCTTATGTAA	CACTTTTTCTTTTTTTTT TTT	-

3	C2C2dof_tnt.AT5G6694_0_col_a_m1	-7	0.00 079	0.68 8842	0.07 0994	29	GTATCTACATACATTTGTTTTCAATTATTT TTTTTCTGCGAGCTTATGTAA	TTTTTTTTTTTTTTACTT TTTTTTTTTT	+
3	C2C2dof_tnt.Adof1_colamp_a_m1	-13	0.00 1054	0.91 8996	0.08 5715	21	GTATCTACATACATTTGTTTTCAATTATTT TTTTTCTGCGAGCTTATGTAA	TTTTTTTACTTTTTCTTTT TT	-
3	C2C2dof_tnt.At1g64620_100ng20cy_b_m1	-15	0.00 1054	0.91 9229	0.08 5715	19	GTATCTACATACATTTGTTTTCAATTATTT TTTTTCTGCGAGCTTATGTAA	TTTTTACTTTTTTTTTTTTT	-
3	C2C2dof_tnt.AT5G0246_0_colamp_a_m1	-17	0.00 1123	0.97 9243	0.08 7161	19	GTATCTACATACATTTGTTTTCAATTATTT TTTTTCTGCGAGCTTATGTAA	TTTTTACTTTTTTTTTTTTT	+
3	C2C2dof_tnt.OBP1_col_a_m1	-11	0.00 1259	1.09 811	0.09 3492	21	GTATCTACATACATTTGTTTTCAATTATTT TTTTTCTGCGAGCTTATGTAA	TTTTTTTTTTTTTTACTTT TT	+
3	C2H2_tnt.At5g66730_col_m1	-17	0.00 1582	1.37 956	0.11 256	17	GTATCTACATACATTTGTTTTCAATTATTT TTTTTCTGCGAGCTTATGTAA	TTTTTTGTCGTTTTCTT	-
3	C2H2_tnt.At5g66730_colamp_a_m1	-17	0.00 1691	1.47 416	0.11 4776	17	GTATCTACATACATTTGTTTTCAATTATTT TTTTTCTGCGAGCTTATGTAA	TTTTTTGTCGTTTTCTG	+
3	C2C2dof_tnt.COG1_col_a_m1	-17	0.00 1787	1.55 848	0.11 4776	21	GTATCTACATACATTTGTTTTCAATTATTT TTTTTCTGCGAGCTTATGTAA	TTTTCACTTTTTCTTTTT TTT	-
3	G2like_tnt.At3g13040_col_b_m1	-15	0.00 1846	1.60 953	0.11 4776	9	GTATCTACATACATTTGTTTTCAATTATTT TTTTTCTGCGAGCTTATGTAA	TGTTTTCTT	-
3	Orphan_tnt.BBX31_col_a_m1	-17	0.00 1882	1.64 118	0.11 4776	15	GTATCTACATACATTTGTTTTCAATTATTT TTTTTCTGCGAGCTTATGTAA	TTTTTTTTACTTTTT	-
3	C2C2dof_tnt.Adof1_col_a_m1	-16	0.00 2005	1.74 831	0.11 8052	21	GTATCTACATACATTTGTTTTCAATTATTT TTTTTCTGCGAGCTTATGTAA	TTTTTTTTACTTTTTCTTT TT	-
3	C2C2dof_tnt.At5g62940_col_a_m1	-15	0.00 2247	1.95 957	0.12 7907	21	GTATCTACATACATTTGTTTTCAATTATTT TTTTTCTGCGAGCTTATGTAA	TTTTTACTTTTTCTTTTT TT	-
3	C2C2dof_tnt.dof24_col_a_m1	-18	0.00 2324	2.02 627	0.12 7994	15	GTATCTACATACATTTGTTTTCAATTATTT TTTTTCTGCGAGCTTATGTAA	TTTTTTACTTTTTG	+
3	ABI3VP1_tnt.FUS3_col_a_m1	-1	0.00 2491	2.17 216	0.13 2411	15	GTATCTACATACATTTGTTTTCAATTATTT TTTTTCTGCGAGCTTATGTAA	TGCATGCATGTATAT	-
3	C2H2_tnt.MGP_col_a_m1	-14	0.00 2559	2.23 143	0.13 2411	20	GTATCTACATACATTTGTTTTCAATTATTT TTTTTCTGCGAGCTTATGTAA	TTTTTTTTIGTCGTTTTC TG	-
3	C2H2_tnt.IDD4_col_a_m1	-17	0.00 2666	2.32 502	0.13 3907	17	GTATCTACATACATTTGTTTTCAATTATTT TTTTTCTGCGAGCTTATGTAA	TTTTTTGTCGTTTTGTG	-
3	C2C2dof_tnt.OBP4_colamp_a_m1	-15	0.00 2983	2.60 153	0.14 0407	19	GTATCTACATACATTTGTTTTCAATTATTT TTTTTCTGCGAGCTTATGTAA	TTTTTACTTTTTGTTTT T	-
3	C2H2_tnt.IDD5_colamp_a_m1	-17	0.00 3029	2.64 111	0.14 0407	17	GTATCTACATACATTTGTTTTCAATTATTT TTTTTCTGCGAGCTTATGTAA	TTTTTTGTCGTTTTGTG	+
3	C2H2_tnt.NUC_col_a_m1	-14	0.00 3042	2.65 3	0.14 0407	20	GTATCTACATACATTTGTTTTCAATTATTT TTTTTCTGCGAGCTTATGTAA	TTTTTTTTIGTCGTTTTG TG	+
3	C2C2dof_tnt.At3g45610_colamp_a_m1	-18	0.00 3278	2.85 833	0.14 7293	15	GTATCTACATACATTTGTTTTCAATTATTT TTTTTCTGCGAGCTTATGTAA	TTTTTTTTACTTTTTG	+
3	C2H2_tnt.JKD_col_a_m1	-14	0.00 361	3.14 771	0.15 8046	20	GTATCTACATACATTTGTTTTCAATTATTT TTTTTCTGCGAGCTTATGTAA	TTTTTTTTIGTCGTTTTC TG	+
3	ABI3VP1_tnt.AT5G6013_0_colamp_a_m1	-20	0.00 4376	3.81 583	0.18 1313	21	GTATCTACATACATTTGTTTTCAATTATTT TTTTTCTGCGAGCTTATGTAA	TTTTTGCTTATTTTTTGC TTA	+

3	ABI3VP1_tnt.AT5G6013_0_col_a_m1	-21	0.00 4484	3.91 017	0.18 1313	19	GTATCTACATACATTTGTTTTTCATTATTT TTTTTCTGCGAGCTTATGTAA	TTTTGCTTATTTTTTGCT T	-
3	C2C2dof_tnt.AT3G5244_0_colamp_a_m1	-14	0.00 462	4.02 82	0.18 1313	21	GTATCTACATACATTTGTTTTTCATTATTT TTTTTCTGCGAGCTTATGTAA	AATTTTACTTTTTGTTTT TTT	+
3	C2H2_tnt.At1g14580_colamp_a_m1	-17	0.00 4688	4.08 816	0.18 1313	17	GTATCTACATACATTTGTTTTTCATTATTT TTTTTCTGCGAGCTTATGTAA	TTTTTTGTCGTTTTGTG	-
3	C2H2_tnt.At1g14580_col_a_m1	-19	0.00 4778	4.16 666	0.18 1313	20	GTATCTACATACATTTGTTTTTCATTATTT TTTTTCTGCGAGCTTATGTAA	TTTTTTTTTGTCGTTTTG TG	+
3	C2C2dof_tnt.CDF3_col_a_m1	-17	0.00 5027	4.38 343	0.18 66	19	GTATCTACATACATTTGTTTTTCATTATTT TTTTTCTGCGAGCTTATGTAA	TTTTCACTTTTTCTTTTT T	-
3	C2C2dof_tnt.COG1_colamp_a_m1	-18	0.00 5228	4.55 901	0.18 9944	15	GTATCTACATACATTTGTTTTTCATTATTT TTTTTCTGCGAGCTTATGTAA	TTTTTTCACTTTTTT	+
3	C2H2_tnt.IDD2_colamp_a_m1	-18	0.00 6023	5.25 215	0.21 4264	18	GTATCTACATACATTTGTTTTTCATTATTT TTTTTCTGCGAGCTTATGTAA	TTTTTTTGTCGTTTTCTT	+
3	C3H_tnt.EMB1789_col_a_m1	-23	0.00 6354	5.54 035	0.22 1409	15	GTATCTACATACATTTGTTTTTCATTATTT TTTTTCTGCGAGCTTATGTAA	TTTTTTTTTTACCGT	+
3	C2H2_tnt.NUC_colamp_a_m1	-17	0.00 6742	5.87 881	0.22 2494	17	GTATCTACATACATTTGTTTTTCATTATTT TTTTTCTGCGAGCTTATGTAA	TTTTTTTGTCGTTTTGTG	+
3	C2C2dof_tnt.CDF3_colamp_a_m1	-17	0.00 6761	5.89 57	0.22 2494	18	GTATCTACATACATTTGTTTTTCATTATTT TTTTTCTGCGAGCTTATGTAA	TTCACTTTTTCTTTTTT	+
3	Trihelix_tnt.AT5G47660_col_a_m1	-23	0.00 6776	5.90 837	0.22 2494	15	GTATCTACATACATTTGTTTTTCATTATTT TTTTTCTGCGAGCTTATGTAA	TTTTTTTTTTACCGT	+
3	HB_tnt.PHV_col_a_m1	-16	0.00 8734	7.61 632	0.28 14	15	GTATCTACATACATTTGTTTTTCATTATTT TTTTTCTGCGAGCTTATGTAA	GTAATCATTACTTTT	+
3	ND_tnt.FRS9_colamp_a_m1	-20	0.00 9135	7.96 595	0.28 8867	30	GTATCTACATACATTTGTTTTTCATTATTT TTTTTCTGCGAGCTTATGTAA	TTTTTATAATTCTAAACC AATAATATTCAA	-
# Tomtom (Motif Comparison Tool): Version 5.3.3 compiled on Feb 21 2021 at 14:52:43									
# The format of this file is described at https://meme-suite.org/meme/doc/tomtom-output-format.html .									
# tomtom -no-ssc -oc . -verbosity 1 -min-overlap 5 -mi 1 -dist pearson -evalue -thresh 10.0 -time 300 query_motifs db/ARABD/ArabidopsisDAPv1.meme									

10.0. Curriculum vitae

Personal Information

Name: Omar Heliel
Nationality: Egyptian
Date and place of Birth: 1/2/1983-Giza Egypt
Gender: Male
Marital status: Married

Education

2018 –now Ph.D. candidate Martin-Luther-University Halle-Wittenberg, Halle, Germany, the thesis work has been carried out at the Leibniz Institute of Plant Genetics and Crop Plant Research (IPK.)

2007 – 2009 M.Sc. Horticulture Genetics and Biotechnology. Mediterranean Agronomic Institute of Chania, Crete, Greece.

2000 – 2004 B. Sc. Biotechnology . Cairo University, Giza, Egypt. Faculty of Agriculture and Life Science

Work Experience

2017 –2022 Researcher Associate-Plant Architecture Research Goup, Leibniz Institute of Plant Genetics and Crop Plant Research (IPK) Gatersleben, 06466 Seeland Germany
Project: “Functional evaluation of RA2 cis-regulatory regions from different grass species for shaping inflorescence architecture in barley”

2012-2016 Researcher Assistant, Desert Research Center, Egypt.
Project work: ”Improving Soybean for salt Stress”.

2010-2011 Graduate Assistant, Mediterranean Agronomic Institute of Chania, Greece.
Project work: “Studies on the expression of ethylene biosynthetic genes in knockout p4h9 mutants and plants over-expressing p4h9 gene in Arabidopsis”

2005-2006 Researcher Assistant, Desert Research Center, Egypt.
Project work” Improving tomato tolerance for heat Stress”

Molecular biology Skills

•Nucleic acid isolation(DNA, RNA), quantification, and hybridization techniques• Bacterial Transformation, Cloning, Subcloning Techniques, gateway cloning strategies • Genome editing and gene knockout using CRISPR/Cas9-mediated targeted mutagenesis • Molecular characterization of putative transgenics/mutants• Gene expression analysis: Genevestigator, promoter analysis •PCR analysis-Real-time quantitative PCR (qPCR) •SDS Gel Electrophoresis and protein purification techniques. • Experience with Plant genetic transformation, Protoplast isolation, and transgenic analysis, (Barley, Tomato, Soybean, Arabidopsis) • Phenotyping for the trait in the field and glasshouse • Bacterial and yeast competent cell preparation • E.coli, Agrobacterium, and yeast transformation• Sanger sequencing and data analysis • Experience with plant management in controlled conditions and tissue culture

Publications and poster presentations based on the Ph.D. work

Heliel O., Koppolu R.,Hensel G Rutten T., Kumlehn J., Schnurbusch T. (2022).Toward understanding the spatial-temporal regulation of *HvRA2* in grass inflorescence(Manuscript under preparation)

Heliel O., Koppolu R.,Hensel G .,Kumlehn J., Schnurbusch T. Functional Evaluation of RAMOSA2 (RA2) Cis-Regulatory Regions from Different Grass Species for Shaping Inflorescence Architecture in Barley. Plant and Animal Genome conference XXIX, 8-12 January 2022, San Diego, USA (Poster presentation.)

Heliel O., Koppolu R.,Hensel G ., Schnurbusch T. Characterizing of VRS4 gene function in barley by using CRISPR/Cas9 genomic editing technology. Plant Genomics and Gene Editing Congress, 8-21, Jun, 15th Plant Science Student Conference (PSSC), Halle (Saale), Germany. (Poster presentation.)

Heliel O., Koppolu R.,Hensel G ., Schnurbusch T. Characterizing of VRS4 gene function in barley by using CRISPR/Cas9 genomic editing technology. Plant Genomics and Gene Editing Congress,21-22 May 2019, Rotterdam, Netherland (Poster presentation.)

I hereby declare that all information stated above is true

[]
Omar Heliel

11.0. Eidesstattliche Erklärung / Declaration under Oath

Ich erkläre an Eides statt, dass ich die Arbeit selbstständig und ohne fremde Hilfe verfasst, keine anderen als die von mir angegebenen Quellen und Hilfsmittel benutzt und die den benutzten Werken wörtlich oder inhaltlich entnommenen Stellen als solche kenntlich gemacht habe. I declare under penalty of perjury that this thesis is my own work entirely and has been written without any help from other people. I used only the sources mentioned and included all the citations correctly both in word or content.

_____ Datum /

Date Unterschrift des Antragstellers / Signature of the applicant

[_____]
Omar Heliel